Biomarkers in prosthetic joint infection

&

The molecular role of antibiotics in soft tissue repair

Caroline Margaret Atherton

BSc, MBChB, MRCS

Submitted in fulfilment of the requirements for the degree of Doctor of Medicine

Institute of Infection, Immunity and Inflammation

College of Medicine, Veterinary and Life Sciences

University of Glasgow

July 2021

Abstract

Background: In Orthopaedic surgery the diagnosis, treatment and prevention of infection are key to successful patient outcomes, this has led to the increased use of antibiotics. Infection following implant or graft surgery has high levels of patient morbidity and associated costs of treatment. Antibiotic prophylaxis coupled with early accurate diagnosis can improve outcomes. Currently, implant related infection is diagnosed using diagnostic algorithms which combine numerous blood and tissue investigations, however, there is no single test available to rule infection in or out and reliance on clinical judgement is still at the forefront. Novel gene sequencing techniques are coming to the forefront of diagnostics across all medical specialties and here I present a pilot study of the use of a new sequencing method and diagnostic rationale - looking at the patient's own immune response to identify the presence of implant infection. Antibiotic prophylaxis, usually given intravenously at the time of surgery has led to a significant reduction in implant infection. Developing more localised ways to administer this prophylaxis led to the introduction of an antibiotic 'wrap' - whereby tissue graft is wrapped in antibiotic solution prior to insertion. This method has significantly reduced infection rates following graft surgery however, it remains unknown if this antibiotic has any adverse molecular or biomechanical effect on the graft tissue, an issue this work aims to address.

Key Findings: Tissue and blood from patients undergoing orthopaedic implant related revision surgery was sequenced on a novel immune gene panel. From this, patterns of gene expression were identified in tissue which defined the infected from the aseptic control cohort. Furthermore, the immune gene response was able to characterise different time points of infection, identifying signatures for acute infection and chronic infection. Sequencing blood samples from the same cohort I was able to establish a gene signature which provided genus level bacterial identification, previously only provided following microbiology culture. Vancomycin antibiotic treatment of tendon graft tissue, used in anterior cruciate ligament reconstruction, was not associated with an increase in apoptotic gene or protein expression. Furthermore, no consistent changes were seen in tendon matrix gene or protein expression. I did identify a consistent trend of reduced levels of inflammatory cytokines following vancomycin compared with control conditions.

Conclusions: Novel gene sequencing techniques and a ‘switched’ diagnostic strategy have shown promise in diagnosing and categorising infection in orthopaedic implant surgery. Antibiotic ‘wrap’ of the hamstring graft in ACL surgery may induce a beneficial homeostatic molecular environment, via a reduction in inflammatory cytokines.

Table of Contents

List of Tables

List of Figures

Acknowledgement

First and foremost, I would like to thank my supervisors, Professor Iain B McInnes and Mr Neal Millar. Without your enthusiasm, support and guidance I would not have completed this MD. Your depth of knowledge and time management skills are something I can only ever aspire to.

My special thanks go to Katy McCall and Moeed Akbar. Katy, I am eternally grateful for your endless patience, teaching me *everything* I know about lab work. You have given me so much of your time over the last three years, when you had your own PhD to complete, I will never be able to repay this. Moeed, the 'leader' of TBG, there was no question you couldn't answer, no spurious result you couldn't explain, no problem you couldn't solve, even if it meant "do it again!…."

Being new to lab work I feel everyone on level 4 at SDGB helped me at one stage or another and although I can't list everyone here, my thanks also go to Susan Kitson, Donna McIntyre, Lyndsay Crowe and Emma Garcia-Melchor.

Taking 'time out' to complete an MD wasn't always plain sailing, especially when the 'time out' also included full time clinical work. I would like to say thank you to Richard and my Mum and Dad, Margaret and Frank, who like they have done throughout my medical career so far, steadied the ship when sometimes things got a bit too much. I'm very grateful for your unwavering encouragement and support.

Author's declaration

The work described in this thesis represents original work which has been generated through my own efforts and does not consist of work forming part of a thesis to be submitted elsewhere. Furthermore, no data has been given to me by anybody else to be submitted as part of my thesis. Where practical support has been provided by others appropriate acknowledgements have been made.

……

Caroline M Atherton

Definitions

ACL – Anterior cruciate ligament

ACLR – Anterior cruciate ligament replacement

AD – Alpha defensin

ASA – American Society of Anaesthesia

BMI – Body mass index

CRP – C-reactive protein

DAIR – Debridement antibiotics implant retention

DNA – Deoxyribonucleic acid

EBJIS – European Bone and Joint Infection Society

ECM – Extracellular matrix

eDNA – Extracellular deoxyribonucleic acid

ELISA – Enzyme linked immunosorbent assay

ESR – Erythrocyte sedimentation rate

FFPE – Formalin fixed paraffin embedded

GAG - Glycosaminoglycan

HPF – High powered field

ICM – International consensus meeting

IL – Interleukin

IV – Intravenous

LE - Leucocyte esterase

MDSC – Myeloid derived suppressor cell

MRSA – Methicillin resistant staphylococcus aureus

MSCRAM's - Microbial surface components recognising adhesive matrix molecules

MSIS – Musculoskeletal infection society

NGS – Next generation sequencing

NJR – National joint registry

OA – Osteoarthritis

PBS – Phosphate buffered saline

PCR – Polymerase chain reaction

PJI – Prosthetic joint infection

PROMs – Patient reported outcome measures

QC – Quality control

RNA – Ribonucleic acid

RPMI – Rosewell park memorial institute

SCV's – Small colony variants

SERAM's - Secretable expanded repertoire adhesive molecules

SLRP's – Small leucine rich proteoglycans

THR – Total hip replacement

TKR – Total knee replacement

UHMPE – Ultra high molecular weight polyethelyene

WCC – White cell count

1 Chapter 1: Introduction

1.1 Synovial Joint anatomy

A joint is formed in the human body where two bones meet. Synovial joints (e.g: hip, knee, shoulder) are the most common type of joint allowing for movement of the skeleton. Although adapted to their specific roles throughout the body based on their location and range of movement required, they share common characteristics. At the point where two bones meet or articulate, hyaline cartilage covers the articulating surface. The joint is encased in a fibrous capsule that on its inner surface forms the synovial membrane. This membrane acts to filter blood plasma and contains synoviocyte cells that secrete proteins, the combination of these proteins and filtered plasma forms synovial fluid (Ramachandran, 2006). Synovial joints are stabilised by ligaments and tendons. The key features of a synovial joint are illustrated in Figure 1-1. Articular hyaline cartilage creates a smooth lubricated surface for joint movement, thereby reducing friction and distributing load across the joint (Ramachandran, 2006). It is composed of chondrocyte cells and extracellular matrix (ECM) comprising type II collagen, water and proteins e.g. proteoglycans. The arrangement of these cells and ECM are akin to its functions: at the joint surface chondrocytes and collagen fibres lie parallel to the joint to resist shear forces, while more proximally the cells are rounder and the fibres perpendicular to the joint to resist compression Figure 1-2 (Sophia Fox et al., 2009).

Tendons and ligaments are both examples of dense connective tissue that are crucial for the structure and function of joints. Tendons attach muscle to bone to permit movement of the skeleton at joints; ligaments attach bone to bone providing structural support to the joints of the body. Tendons and ligaments are composed of fibroblast cells and ECM. Fibroblasts make up 95% of the cellular component of the tissues and produce the ECM, comprising collagen, water, glycoproteins and elastic fibres.

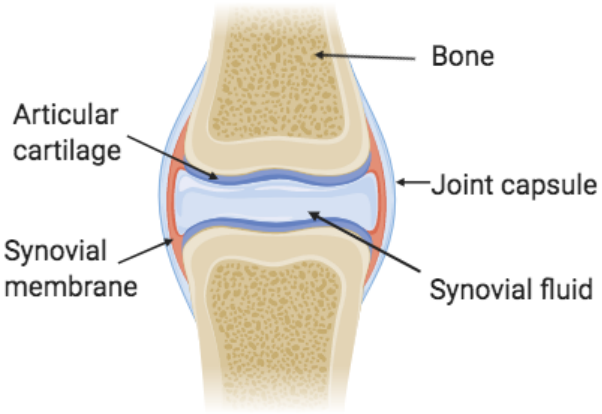

Figure 1-1 Schematic diagram of a synovial joint
A diagram representing the key features of a synovial joint. The articulating ends of the bones are covered with articular cartilage. A thick fibrous capsule surrounds the joint and provides stability. The synovial membrane acts to filter larger molecules from blood and also secrete key proteins to form synovial fluid. Image created in BioRender.

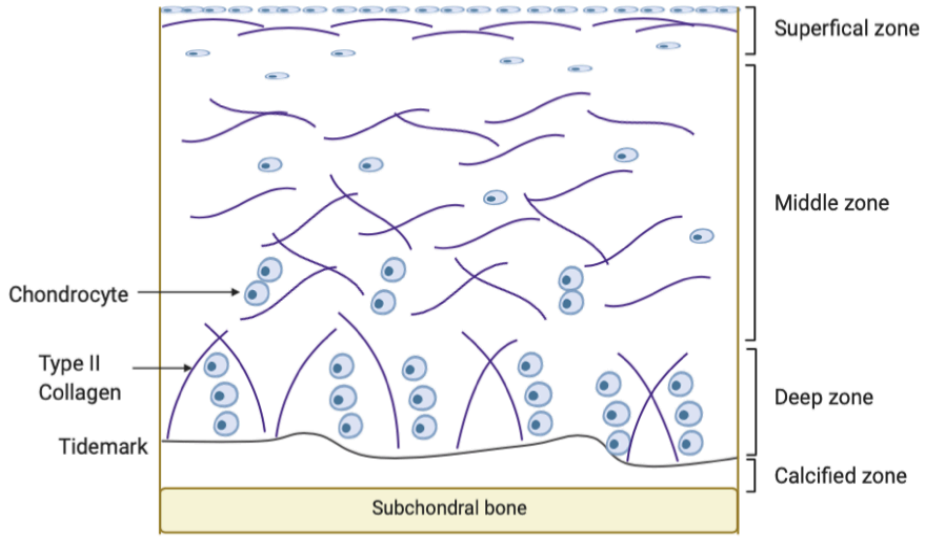

Figure 1-2 Schematic diagram of articular cartilage
A diagram showing the transition from subchondral bone to articular cartilage. In the deep zone chondrocytes are rounder and the type II collagen fibres are tangential to the joint line to resist compression. In the superficial zone cells are flat and collagen fibres parallel to the joint line to resist shear. Above the tidemark, articular cartilage is avascular. Images created in BioRender, adapted from (Sophia Fox et al., 2009).

Collagen: the most abundant protein in the human body is composed of three polypeptide alpha (α) chains, in a triple helix structure, forming tropocollagen. In tendon and ligament 85-90% is heterotrimetric Type I collagen, with two-α1 and one-α2 polypeptide chains. Tropocollagen synthesis by fibroblasts is then assembled into organised fibrils, fibres and fascicles that group together to form the whole ligament or tendon. The orientation of the collagen fibres is dictated by the direction of force; in tendons these are uniaxial resulting in parallel collagen fibres, in ligaments, there are multi-axial forces resulting in more varied cross-connections (Ramachandran, 2006).

Water: comprises two thirds of the weight of a tendon or ligament and is usually bound to negatively charged proteoglycans in the ECM. It is important for lubrication and gliding.

Glycoproteins: consist of a protein core covalently linked to a carbohydrate substrate. Proteoglycans are the most abundant glycoprotein in tendon and ligaments, formed of a core protein with a heavily glycosylated glycosaminoglycan (GAG) side chain. They can be divided into small leucine rich proteoglycans (SLRPs), of which the most abundant is decorin which has a critical role in collagen fibrillogensis and large aggregating proteoglycans, of which the most abundant is aggrecan, which has many negatively charged GAG side chains creating a hydrophilic environment important for binding water molecules (Thorpe et al., 2013).

Elastic fibres: formed of a central core of elastin linked to fibrillin type 1 and 2 polymers. Elastic fibres have important mechanical functions in energy storage and elastic recoil and are aligned with collagen fibres. The amount of elastic fibres varies in tendon and ligament depending on function (Thorpe et al., 2013).

1.2 The knee joint and anterior cruciate ligament

The knee joint is a complex modified synovial hinge joint composed of patellofemoral and medial and lateral tibiofemoral articulations. It predominantly allows movement in the sagittal plane (flexion and extension), but also permits small movements in the coronal plane(varus and valgus) and in

the axial plane (internal rotation in flexion and external rotation in extension) (Miller et al., 2016).

The stability of the knee joint is multifactorial and maintained by the shape of the tibial and femoral condyles, fibrocartilagenous menisci, extracapsular tendoligamentous structures: medial collateral ligament, lateral collateral ligament, patella ligament, quadriceps tendon, arcuate and oblique popliteal ligaments and intracapsular extra-articular ligaments: anterior and posterior cruciate ligament Figure 1-3. The anterior cruciate ligament (ACL) originates from the lateral border of the medial femoral condyle and runs obliquely through the intercondylar fossa to a broad insertion at the medial tibial eminence (Miller et al., 2016). Transition from ligament to bone is via a 4 zone direct fibrocartilagenous enthesis; ligament, cartilage, mineralised cartilage and finally cortical bone (Gulotta & Rodeo, 2007). The ACL primarily resists anterior displacement of the tibia relative to the femur and is a secondary stabiliser to internal rotation when the knee is extended. It has two distinct fibre bundles, an anterior medial bundle that resists anterior tibial translation and posterior lateral bundle that resists internal rotation. The blood supply to the ACL comes from two primary sources which anastomose; the endoligamentous supply formed of small vessels from the medial and lateral geniculate arteries and a synovial sheath of periligamentous vessels.

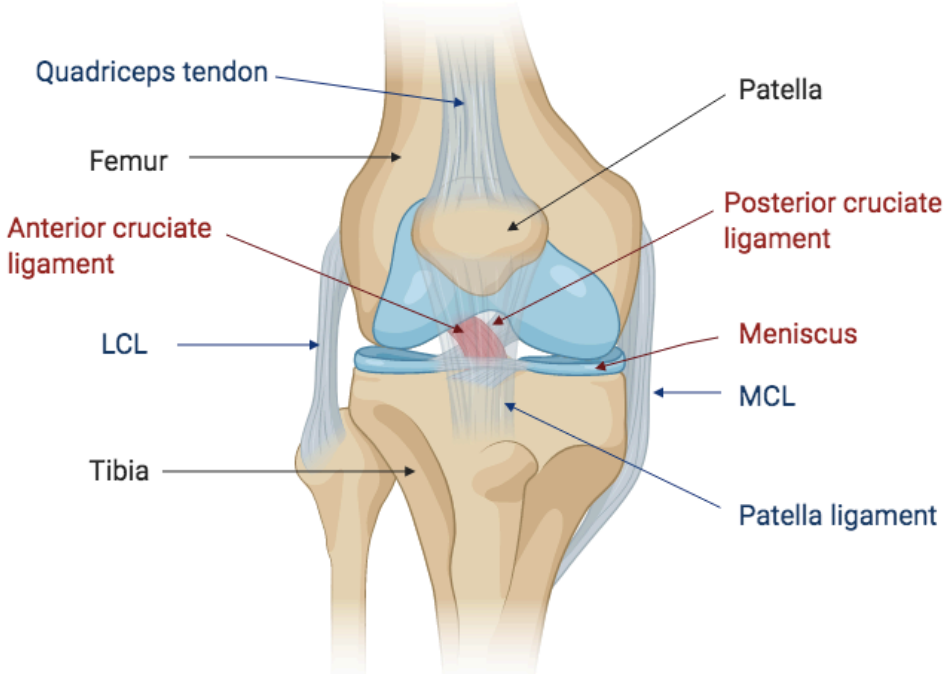

Figure 1-3 Knee joint anatomy
A diagram showing the bones and tendoligamentous anatomy of the knee joint. Three articulations between the femur, tibia and patella form the knee joint: medial and lateral tibiofemoral and patella joints. Medial and lateral fibrocartilagenous menisci increase the congruity of the tibiofemoral articulations. Extra articular tenodoligamentous structures are shown in blue and include: MCL= medical collateral ligament, LCL= lateral collateral ligament, quadriceps tendon and patella ligament. Intracapsular ligaments shown in red are the anterior and posterior cruciate ligaments. Image created in BioRender, adapted from (Miller et al., 2016).

1.3 ACL injury and reconstruction

The ACL is one of the most frequently injured ligaments, as a result national registries have been set up to analyse trends in ACL rupture and repair; they estimate the incidence of ACL rupture to be 34 per 100,000 population (Renstrom et al., 2008). Injury can lead to knee joint instability, pain, reduced functional performance in athletes and can accelerate degenerative changes to the soft tissues in the knee leading to osteoarthritis. ACL injuries are caused by acute contact knee trauma and increasingly, non-contact pivot/twisting knee injuries. The latter group can be affected by age, gender, genetics and body weight. ACL injury rate is reported to be higher in female athletes compared with male athletes; differences in elastin and protein content (Little et al., 2014), size of the ACL and the intercondylar notch it passes through, lower limb alignment and hormone differences are all believed to play a part (Renstrom et al., 2008). Age associated degeneration of the ACL shows disordered collagen fibres and increases in cell number and GAG protein accumulation, changes that are understood to play a role in non-contact pathogenesis of ACL rupture (Hasegawa et al., 2013). Following rupture, ligament healing occurs via a 3-phase pathway of inflammation, proliferation & repair and remodelling.

Inflammation: immune cells including platelets, monocytes, macrophages and neutrophils, migrate to the site of injury forming a haemostatic clot and begin to remove tissue debris by phagocytosis. There is an increase in water, GAG content and Type III collagen in the ligament tissue (Lin et al., 2004).

Proliferation & Repair: ligament tissue has a scar like appearance with a dense network of blood vessels. There remains a high level of Type III collagen, water and GAG proteins (Lin et al., 2004).

Remodelling: begins around 6-8 weeks after injury. There is a reduction in cellularity of the tissue, along with water and GAG content. Type III collagen is replaced with Type I collagen, which begins to align along the axis of force. The repaired tissue does not regain the mechanical properties pre-rupture due to residual increased cellularity and more disorganised collagen fibre arrangement (Lin et al., 2004).

Repair of the intra-articular ACL is poor, limited by its avascular nature which reduces inflammatory cell migration, and, the presence of synovial fluid (Murray et al., 2000). Studies have shown that the torn ligament ends retract and are covered by synovial membrane preventing repair(Murray et al., 2000).

Ligament reconstruction is the current gold standard of surgical treatment following ACL rupture. Tissue is taken from the patient's hamstring or patella tendon, or donor tissue is used and implanted through bone tunnels in the femur and tibia, to replicate the normal anatomical position of the ACL. Surgical reconstruction has superior results compared with conservative management in active patients with regards to return of pre-injury sporting activity (Monk et al., 2016); Using the patient's own tissue – 'autograft' compared with donor tissue 'allograft' is also associated with a lower re-rupture and revision rate, a zero risk of disease transmission and no immune mediated reaction to foreign tissue (Gulotta & Rodeo, 2007; Maletis et al., 2013; Marrale et al., 2007). Previous research has evaluated many aspects of the surgery, anatomical graft placement is now accepted as good practice, but other aspects of surgery including graft choice and fixation device show no superiority, with a trend now towards a more personalised surgery (Haddad, 2014). The limiting factor in reconstruction is the biology of graft healing which describes the process of graft integration into the bone tunnels in the femur and tibia. This process occurs with hamstring and patella tendon grafts, the latter of which has bone blocks at either end of the tendon graft, however, a portion of the tendon will remain in the tunnel. The tendon graft heals to bone initially with fibrocartilaginous scar tissue. The collagen fibres in this scar then align perpendicular to bone, in a similar way to Sharpey's fibres present at indirect tendon-bone attachments (Gulotta & Rodeo, 2007). The body of the tendon graft undergoes 'ligamentisation' – a process that can take up to 3 years, comprising avascular necrosis, cellular re-population, revascularisation and fibroblast metaplasia, resulting in a graft that is histologically similar to a native ACL (Deehan & Cawston, 2005; Gulotta & Rodeo, 2007).

1.4 Infection following ACL reconstruction

Post-operative infection following anterior cruciate ligament reconstruction (ACLR) is an uncommon but serious complication. Is has the potential to damage

the ACL graft and destroy articular cartilage leading to septic arthritis. The prevalence ranges from 0.14-1.8% (Burks et al., 2003a; Indelli et al., 2002; Torres-Claramunt et al., 2013). A large systematic review evaluated 14 studies assessing infection following ACLR; reporting a rate of 0.5%, based on 121 cases of infection out of 22,836 ACL surgery's. Increased risk of infection following ACLR is seen when additional procedures are performed, for example, meniscal repair, or in revision surgery (Kim et al., 2014). This may be due to increased operating times, larger surgical incisions or more 'foreign' suture material in the knee joint. As the condition is less common, there have been varying opinions and protocols for treatment. Synovial fluid aspiration to confirm the diagnosis along with administration of intravenous antibiotics and joint lavage are key. Choice and duration of antibiotics are guided by microbiology culture results, with the majority of infections caused by a *Staphylococcal* organism (Kim et al., 2014). The issue lies with how to treat the graft, either to retain it or remove it at first wash out. Published literature is available supporting both arguments (Burks et al., 2003b; Michael E. Hantes et al., 2017; Matava et al., 1998). Retention or removal of the graft may ultimately depend on patient, graft and microbial factors, with higher virulent organisms and allograft reconstruction associated with poorer outcomes (Michael E. Hantes et al., 2017; Matava et al., 1998).

1.5 Vancomycin wrap and ACL surgery

Current research in the field of ACL surgery is directed towards the use of biological agents to improve graft integration, reduce re-rupture rates and crucially, reduce post-operative infection rates (Hexter, Thangarajah, et al., 2018; Vertullo et al., 2012). In 2012 the vancomycin wrap was introduced; this involves wrapping the ACL graft in a sterile swab pre-soaked in 5mg/ml of vancomycin antibiotic solution whilst the graft bed and bone tunnels are prepared. The data from this initial study showed a significant reduction in post-operative infection rates in the vancomycin wrap treated group, N=870, infection rate 0% *vs* pre-operative antibiotics alone N=285, infection rate 1.4% (Vertullo et al., 2012). Results from this study have been replicated by other research groups, showing that vancomycin treatment of the ACL graft significantly reduces infection rates (Naendrup et al., 2019; Offerhaus et al., 2019; Pérez-Prieto et al., 2016; Phegan et al., 2016). Vancomycin is a

glycopeptide antibiotic initially developed to treat Methicillin resistant staphylococcus aureus (MRSA) and coagulase negative staphylococcus aureus. It is used in a number of specialities, including urology, cardiothoracic and orthopaedic surgery, either topically on wounds on in solution to immerse or wrap implants prior to surgery, reporting significant reductions in infection (Dhabuwala, 2010; Tarakji et al., 2016; Vander Salm et al., 1989). In cardiothoracic surgery, topical vancomycin powder is applied to sternotomy wounds following a seminal paper in 1989 and more recently implantable cardiac electronic devices are enveloped in a degradable antimicrobial sleeve (Tarakji et al., 2016; Vander Salm et al., 1989). In orthopaedic surgery, vancomycin powder is reconstituted in bone cement for routine arthroplasty and used as intravenous solution to treated prosthetic joint infection (Nowinski et al., 2012). A recent paper has shown that topical vancomycin powder significantly reduces both superficial and deep surgical site infection rates when applied to spinal surgery wounds, compared with a control group with no intrawound treatment (Lemans et al., 2019). The molecular effects of vancomycin on human and animal peri-articular tissues, including tendon has a limited evidence base. Porcine chondrocyte death was significantly increased after exposure to vancomycin at doses of 5mg/ml or higher (Shaw et al., 2018). Human *in vitro* studies have shown vancomycin toxicity to chondrocyte and osteoblast like cells, via a reduction in cell DNA, at doses of 250µg/ml and 125µg/ml for osteoblast and chondrocytes respectively, following 48hours of treatment (Antoci et al., 2007). Two further studies have concluded that vancomycin is not toxic at doses up to 16µg/ml for 36 hours in an *ex vivo* chondrocyte model (Dogan et al., 2016) and up to 1000µg/ml for 72 hours in an *in vitro* osteoblast model (Edin et al., 1996). Porcine tendon models show that vancomycin is effective at eliminating bacterial contamination at 5mg/ml after 20 minutes of soaking, and has no effect on the biomechanical properties at doses up to 10mg/ml(Schüttler et al., 2019). Bovine studies have demonstrated that tendon can act as a reservoir for vancomycin, releasing the antibiotic for up to 24 hours into the joint, changing a source of infection, into an intra-articular prophylactic vehicle (Grayson et al., 2011).

1.6 Tendon work aims

The clinical data shows that vancomycin, when used topically to treat the ACL graft, significantly reduces post-operative infection rates. This has been shown in animal studies (Schüttler et al., 2019) and in a number of human clinical trials (Offerhaus et al., 2019; Pérez-Prieto et al., 2016; Vertullo et al., 2012). Based on these results, the vancomycin wrap is currently employed in many clinical settings. However, studies looking at vancomycin toxicity in periarticular tissue give varying ranges for a safe dose regime and do not include human tendon tissue. It remains unclear if pre-treatment with vancomycin has any detrimental molecular or structural effects on the tendon graft, a gap in the current literature which this study aims to address.

1.7 Osteoarthritis and Total Joint Replacement

Osteoarthritis (OA) is the most common form of degenerative joint disease. It can be classified as primary OA, with risk factors including increasing age, female gender, obesity, and repetitive joint loading or secondary OA, which occurs due to an identifiable cause e.g.: trauma, joint surgery or developmental abnormality. The pathophysiology of OA involves the whole joint but begins with damage or fibrillations in the articular cartilage. This exposes the underlying subchondral bone, disrupts the osteochondral junction allowing pathological vascular and neural invasion. The ECM, chondrocyte and collagen network of the cartilage, shown as normal in Figure 1-2, is disrupted; proteinases – enzymes that break down collagen and ECM are increased, and there is accelerated chondrocyte cell death. Subsequent changes to subchondral bone, including reduced bone mineral density alters the mechanical properties of the joint further increasing the cartilage damage and leads to bone cyst formation. Finally, the proteinases released by damaged chondrocytes interact with the synovium, releasing further inflammatory cytokines including IL-1, IL-6 and IL-15. Treatment options include supportive measures: pain relief, activity modification and weight loss, or surgery, either to re-align and re-stabilise the joint in the younger candidate or replace the joint with an arthroplasty procedure.

National joint registry (NJR) data in England show that total hip replacements (THR's) and total knee replacements (TKR's) are the most common arthroplasty surgeries performed (NJR Editorial Board, 2019). The goal of arthroplasty surgery is to relieve the pain caused by 'bone on bone' articulation at the joint, and replace this with a biomaterial implant, restoring joint function and quality of life. Using THR as an example, the modern low friction design of which is accredited to Sir John Charnley in 1962, consists of a femoral stem, head and acetabular cup Figure 1-4 (Knight et al., 2011). The femoral stem is made from a metal alloy, commonly stainless steel. It can be implanted with or without bone cement, known as polymethymethacrylate that acts as a grout between bone and implant. Uncemented implants are coated with hydroxyapatite, the mineral form of bone, which promotes bone in growth into pores in the implant to create a stable construct (Knight et al., 2011; Ramachandran, 2006). The head of the femur is replaced with a cobalt chromium or ceramic ball, with its size corresponding to the implanted acetabular cup. The hip socket or acetabulum is formed from the fusion of three bones of the pelvis, the ilium, ischium and pubis, and is lined by articular cartilage. Any remaining cartilage is removed by reaming during surgery and a new cup implanted, either with bone cement or coated with hydroxyapatite to allow for bone in growth as with the femoral stem. Uncemented cups are made from metal alloys and require a liner to articular with the femoral head, which is either ultra-high molecular weight polyethylene (UHMWPE) or ceramic. Cemented cups are UHMPE and can articulate directly with the femoral head (Knight et al., 2011). Whilst the basics of hip replacement surgery have remained similar since their introduction, there have been vast advances in biomaterial engineering to improve the function and longevity of the implants. Implants are available for ankle, knee, shoulder, elbow, wrist and hand joint replacements and utilise the principles described here for THR. With advances in surgical technique and implant development, NJR data shows that 15 years following surgery, approximately 92% of THRs and 93% of TKR's are still functional (NJR Editorial Board, 2019). Through a series of questionnaires assessing function, pain and quality of life, patients are able to report their outcomes following arthroplasty surgery, known as Patient Reported Outcome Measures (PROMS) data, which has been collected by NHS England since 2009. For the 2018-2019 period, 97% of patients who underwent a THR and 94% of those undergoing a TKR reported improvements in their overall heath

following surgery (NHS Digital & Analytical Team PROMS, 2020). Despite the documented success of arthroplasty surgery, there are complications that can occur including fracture around the implant, loosening and prosthetic joint infection (PJI).

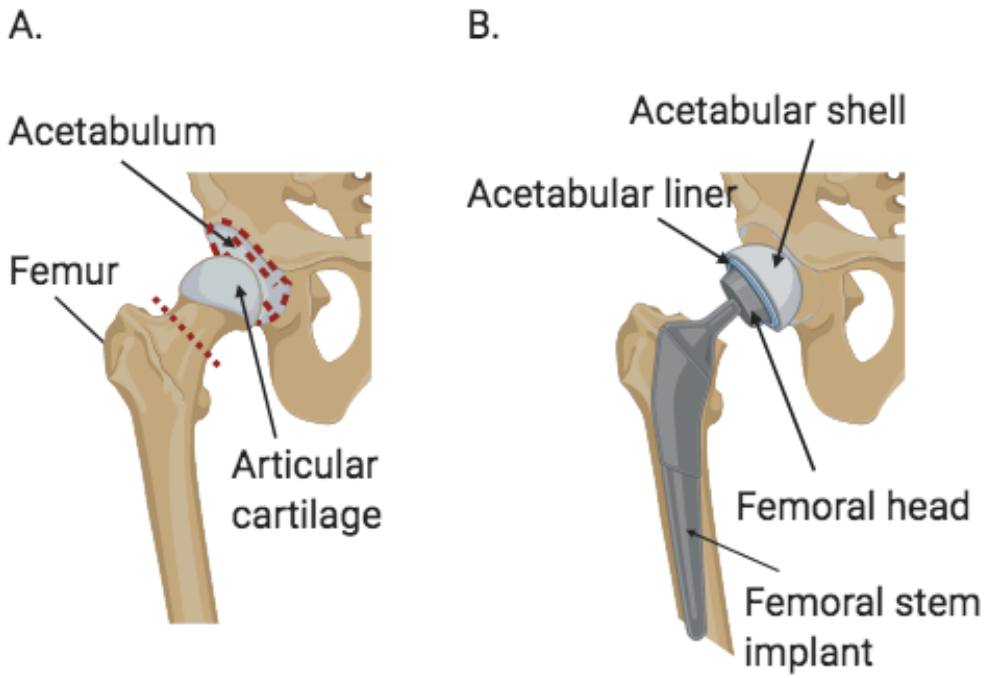

Figure 1-4 A schematic diagram of a total hip replacement
(A) Normal anatomy of the hip joint, a synovial joint, formed by the head of the femur articulating with the acetabulum. The femoral head and the acetabulum are covered with articular cartilage, shown in grey. The red lines indicate the bone cuts and areas of reaming to remove any remaining articular cartilage. (B) Implants used in a total hip replacement. The femoral stem is placed down the femur and is stabilised with bone cement or has a coating of Hydroxyapatite to stimulate bone growth onto the stem. The acetabular implant shown here is metal, coated with hydroxyapatite to stimulate bone growth to fix the implant in the acetabulum, with a liner, shown in blue, to articulate with the femoral head. Image created in BioRender.

1.8 Prosthetic Joint Infection and Biofilm

A surgical prosthesis or implant is susceptible to infection from three primary sources. The primary pathway is understood to be contamination of the implant or seeding of microorganisms onto the implant at the time of surgery, as data shows that nearly 50% of infections occur within the first year (Tande & Patel, 2014). Animal models have shown that when a prosthesis is implanted, a significantly smaller amount of bacteria is needed to establish infection versus a model with no implant, suggesting the implant reduces the immune response to bacteria thereby allowing immune evasion and survival (Southwood et al., 1985). Secondly, contiguous spread from a local source, including superficial surgical wound infection to involve the implant. Later, this can include disruption to local tissues cases by trauma, surgery or superficial infection such as cellulitis. Thirdly, a prosthesis can become infected at any point during its lifetime via haematogenous spread and seeding of bacteria onto the implant from a distant site (Tande & Patel, 2014).Therefore a complex underlying interaction between the immune response, invading microorganism and implant; results in a unique environment and the subsequent development of a biofilm on the implant. Biofilm consists of microorganisms, either monomicrobial or polymicrobial, embedded in an ECM which consists of proteins, polysaccharides and extracellular DNA (eDNA). The formation and development of biofilm can be described in four stages:

Attachment: bacterial attachment can occur via two routes, reversible electrostatic forces and irreversible binding via bacterial cell wall proteins (Gbejuade et al., 2015). Immediately following implantation, the prosthesis is coated with blood and interstitial fluid that contains host proteins including fibrinogen, collagen and fibronectin. *Staphylococcus aureus* (*S.aureus*) is the most common causative organism is PJI and is therefore the bacteria most extensively studied. *S.aureus* has several microbial surface components recognising adhesive matrix molecules (MSCRAMs) and secretable expanded repertoire adhesive molecules (SERAMs) that facilitate adhesion to host proteins including collagen-binding adhesins that bind collagen and fibronectin binding proteins that bind to fibronectin (Arciola et al., 2018). The concept of ‘race to the surface’ describes the competition between bacteria and host cells, as to which occupies the implant surface first. If the bacteria is first, integration of

the implant with bone may not occur and biofilm infection may form (Arciola et al., 2018)

Proliferation: once the bacteria are attached to the implant surface they can begin proliferation, production of ECM and formation of cell to cell adhesion bonds (Gbejuade et al., 2015).

Maturation: growth and regulation of the biofilm is coordinated by a unique bacterial signalling pathway of quorum sensing, controlled by the *agrBDCA* genes. This pathway regulates bacterial growth and response to stress signals, including hypoxia and cell density (Arciola et al., 2018; Gbejuade et al., 2015). A number of bacteria in the biofilm undergo programmed cell death or apoptosis in order to release eDNA into the ECM which allows resistance genes to be transferred to other bacteria within the biofilm.

Detachment: bacteria can disperse from the biofilm and spread via the bloodstream which may lead to systemic infection. This process is coordinated by the *agr* quorum sensing genes that signal the production of enzymes to break down bonds within the biofilm ECM, allowing bacteria to disperse (Arciola et al., 2018; Gbejuade et al., 2015).

The initial immune response treats the implant as a foreign body. As noted earlier, on contact with blood and interstitial fluid, it is coated with host proteins, also known as provisional matrix, which can act as attachments for bacteria but also initiate the complement and coagulation cascades. This triggers a release of cytokines and chemo-attractants for cells involved in the innate immune response Table 1-1. Neutrophils are the first cells to respond. These are polymorphonuclear leukocytes, also known as granulocytes that have numerous roles: phagocytosis of mirco-organisms and cell debris, release of antimicrobial peptides known as defensins, the production of neutrophil extracellular traps and NETosis – whereby a neutrophil releases a web of histones and granules to trap microorganisms, and the production of chemokine's to recruit other immune cells (Selders et al., 2017). The inflammatory response evolves from acute to chronic with the arrival of monocytes and their maturation to macrophages, which promote proliferation of fibroblasts and endothelial cells leading to granulation, fibrous tissue and the formation of multinucleated giant

Table 1-1 Components of the innate immune system

Innate Immune system	
Physical barrier	Skin, mucosal epithelium
Circulating proteins	Complement Acute phase proteins Cytokines Chemokines
Immune Cells Phagocytes	Dendritic cell, Macrophage, Neutrophil
Non-Phagocytes	Natural Killer cell, mast cell, eosinophil, basophil

cells (Anderson, 2001). The pathway of immune response to the implant is affected by a number of factors including the bearing surfaces of the implant and the volume of wear particles produced overtime, with a lower immune repose noted when the foreign material remains in 'bulk' form (Gibon et al., 2017). Despite this, a common pathway of granulocyte activation, chronic inflammation and giant cell formation is summarised in Figure 1-5.

The purpose of immune cell migration is to promote phagocytosis to clear micro-organisms from the tissue implant interface, however, due to the size and properties of orthopaedic implants, this is not possible. This leads to a phenomenon called 'frustrated phagocytosis' characterised by partial degranulation of immune cells, increased oxygen free radial production leading to cell apoptosis and degradation of defensins (neutrophil antimicrobial peptides) (Zimmerli & Sendi, 2011).

Furthermore, biofilm microorganisms have multiple methods by which they can evade the host immune response. Phagocytes can be physically excluded due to their size from micropores on the surface of the implant, which can instead be colonised by bacteria (Arciola et al., 2018). *S.aureus* has an array of defence mechanisms against the immune response, including inhibiting opsonisation, producing enzymes to breakdown neutrophil extracellular traps and releasing leucocyte toxins (Arciola et al., 2018). Small colony variants (SCV's) are a subpopulation of biofilm bacteria that can invade host cells, including osteoblasts and non-immune cells, evading detection and elimination by the immune system and antimicrobial therapies. They are able to re-initiate infection following completion of antibiotic therapy (Arciola et al., 2018; Zimmerli & Sendi, 2011).

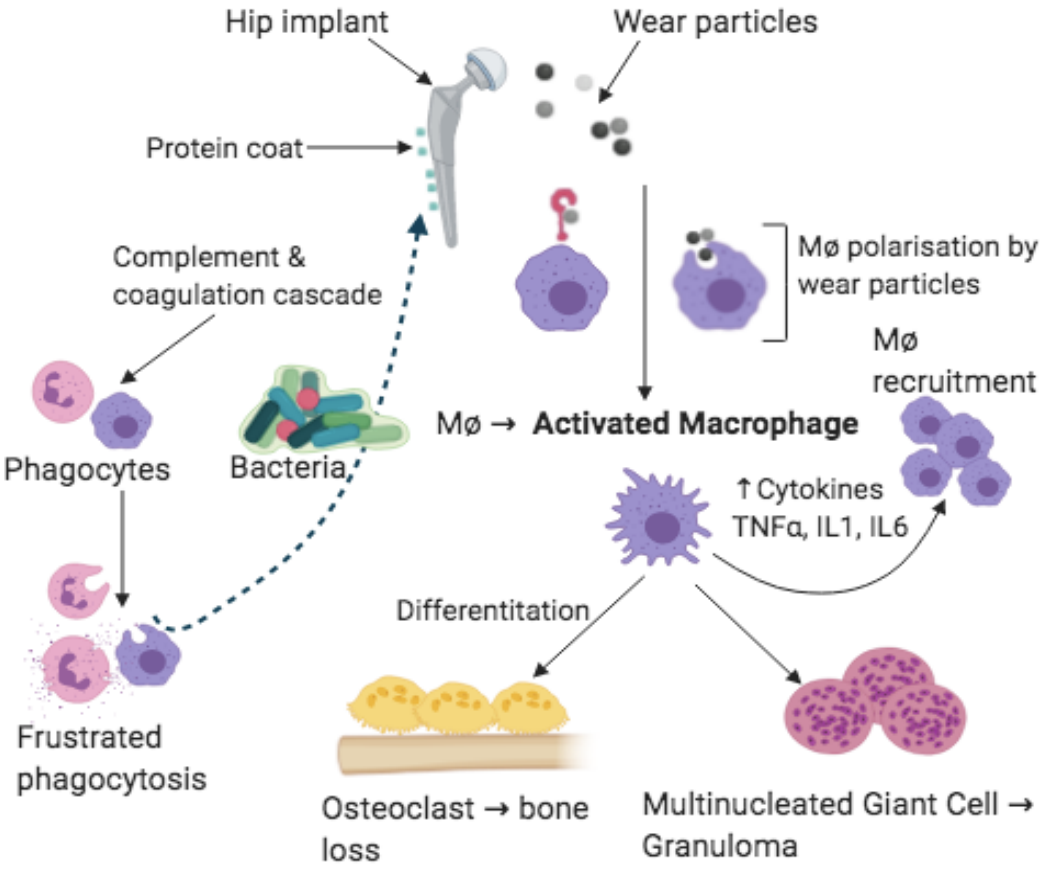

Figure 1-5 Biological response to an orthopaedic implant
The implant is coated with host proteins, 'provisional matrix' which activates the coagulation and complement cascades, attracting phagocytes. The cells are unable to phagocytose the implant and undergo partial degranulation and increased free radial production leading to frustrated phagocytosis. Bacteria have specific receptors that bind to host proteins in the provisional matrix on the implant, coupled with inefficient phagocytosis, this can lead to biofilm formation. Wear particles are produced by the implant which activate macrophages either by phagocytosis or through surface toll-like receptors. Activated macrophages assume a pro-inflammatory phenotype, increase the release of cytokines to recruit more macrophages, differentiated into osteoclasts to resorb bone or fuse to generate multi-nucleated giant cells. Osteoclasts can lead to bone resorption and subsequent loosening of the implant; MGC's lead to granuloma formation. MΦ= macrophage, TNFα = tumour necrosis factor alpha, IL = interleukin, MCG's – Multinucleated Giant Cells. Image created in BioRender, adapted from (Anderson, 2001; Gibon et al., 2017)

Recent work investigating biofilms has suggested an alternative pathway describing chronic infection of implants. These studies report an alternative activation pathway involving macrophages; instead of pro-inflammatory cytokines (IL-1, IL-6, IFNγ), anti-inflammatory cytokines (IL-10 ,IL-4) weaken the microbicidal response leading to pro-fibrotic changes and chronic infection (Gries & Kielian, 2017). Utilising mouse models of PJI and human PJI tissue samples, an altered immune cell environment was described, with an increased number of immature monocyte and macrophage pre-cursor cells namely myeloid derived suppresser cells and a reduction in T cell number (C. E. Heim et al., 2014; Cortney E. Heim et al., 2018; Cortney E. Heim, Vidlak, & Kielian, 2015). Through a more detailed understanding of the immune cell reaction and cytokines involved in the development and persistence of biofilm, it is hoped that molecular targets can be developed to aid with clinical diagnosis and management of PJI (Gries & Kielian, 2017).

1.9 Epidemiology of prosthetic joint infection

The NJR has been collecting data on all arthroplasty surgeries in England and Wales since 2003. Its database estimates the prevalence of prosthetic joint infection (PJI) to be between 0.8-2%, based on a recording of over 2,500,000 surgeries (NJR Editorial Board, 2019). The Scottish arthroplasty project, founded in 2001, produces an annual report looking at arthroplasty surgery in Scotland, it includes infection rates occurring within 1 year of surgery. In 2018 these figures were 0.9% for THR and 0.8% for TKR (Scottish arthroplasty project steering group, 2020). Available registry data suggests that approximately half of PJI's occur within 2 years of the primary surgery (NJR Editorial Board, 2019; Ong et al., 2009). However, up to 25% of patients can develop symptoms of primary infection up to 10 years following initial surgery (Lamagni, 2014; Ong et al., 2009). This can lead to a time lag and an under appreciation of the burden of PJI, given the large increase in arthroplasty in the last 5-10 years (NJR Editorial Board, 2019). Conflicting reports suggest that the absolute incidence of PJI is increasing. Data from the Nordic Arthroplasty register, a consolidation of data from 4 Nordic countries', investigated 432,168 THR's, including 2778 revision surgeries for infection. They reported an increase in the incidence of PJI in the years 2005-2009 calculated at 0.71% compared with 0.46% in 1995-1999. This increase was exclusively within the 1st year post primary surgery and was

not associated with an increase in incidence of known PJI risk factors (Dale et al., 2012). This finding is not supported by data from America, where a smaller sample size of 7367 arthroplasty surgeries reported static rates in PJI incidence over a 10-year follow up (Tsaras et al., 2012). Reasons for this may be an inter play between increased co-morbidities within the operative population, improved infection prevention measures and implant design (Tsaras et al., 2012). Furthermore, national joint registries may underestimate the prevalence of PJI, as microbiology results to stratify a case as infected are not available at the time of data entry on to the register. A study investigating this underreporting evaluated the Danish Hip Arthroplasty register, capturing 32,896 THR's, of which 1546 required revision. They found that relying on the registry to document a case as infected gave 1- and 5-year cumulative infection rates of 0.5% and 0.64% respectively. Utilising their algorithm, which drew on national clinical patient data including blood and microbiology results and pharmacy prescriptions up scaled this estimate to 1 and 5 year cumulative infection rates of 0.86% and 1.03% respectively, 40% higher than the registry data alone (Gundtoft et al., 2015).

The volume of arthroplasty surgery has increased over the last few years. The UK NJR shows that 25% of the total database entries were recorded in the years 2016 to 2018 (NJR Editorial Board, 2019). Despite the conflicts regarding increased incidence, and the balance of patient co-morbidities, surgical technique and implant design, we can predict that the absolute number of PJI cases will rise.

1.10 Risk factors for Prosthetic joint infection

Factors known to increase the risk of PJI include; multiple underlying co-morbidities, particularly diabetes, liver or renal disease, increased BMI >30kg/m^2, increased surgical operating time, revision surgery and male gender (Alamanda & Springer, 2019; Namba et al., 2013; NJR Editorial Board, 2019; Ong et al., 2009). Large registry data sets can stratify these risks further, for example, liver disease as a risk factor reaches significance >24 months after primary surgery whereas diabetes is a risk factor for early infection (NJR Editorial Board, 2019). Infection is the 4th most common reason for primary THR revision in UK joint registry data however, it becomes the leading cause for re-

revision surgery (NJR Editorial Board, 2019) which is believed to be due to poorer quality soft tissues, longer operating times and potentially undiagnosed low-grade infection at the time of revision. Male gender has been identified in a number of studies as being a factor of increased infection risk, although the biological reason for this is unexplained (Dale et al., 2012; Ong et al., 2009). Evidence suggests that implant bearing surface may play a role in infection rates, with ceramic surfaces associated with lower rates (Madanat et al., 2018). However, ceramics are used in younger patients, therefore this may be a confounding factor in these results. On the other hand, a large meta-analysis comparing ceramic, metal and UHMPWE identified no difference in infection rates (Hexter, Hislop, et al., 2018). Increasing age has not consistently been shown to be associated with increasing infection. One study, using UK NJR data looked at 623,253 THR's and reported an increased risk of infection with age >70 (NJR Editorial Board, 2019). However, a report of 39,929 patients found age to be non-significant in the overall cohort for developing infection (Ong et al., 2009). A large meta-analysis reviewed 104 studies encompassing over 640,000 total elbow and total shoulder replacements and found that age >75 years was associated with a lower risk of infection vs <75 years. One study in this meta-analysis reported high levels of *cutibabterium acnes (C.acnes)* in younger males which may have affected these results (Kunutsor et al., 2020).

1.11 Diagnosis of PJI and Consensus definition

Prior to 2011, the diagnosis of PJI was based on clinical history, blood inflammatory markers, tissue and synovial fluid culture, and histology. Without a standardised definition, the interpretation of these results was clinician based. The predominate pathogen seen on culture is *S.aureus*, however, there is a high number of poly-microbial infections and organisms of lower virulence such as *Proteus species* or *C.acnes* (Lamagni, 2014). This in part could account for the varying clinical picture from an acutely hot swollen painful joint to indolent increase in pain and stiffness, making diagnosis challenging. Furthermore, although the majority of infections occur acutely following surgery, a significant proportion present between 2-10 years post-operatively (Lamagni, 2014), see section 1.9. The varying clinical picture and lack of standardised definitions can lead to wide variation in clinical outcomes, making clinical research in this area inconsistent and therefore difficult to interpret.

In 2011 a standardised definition of PJI was formulated by the musculoskeletal infection society (MSIS), based on consensus opinion and review of the available literature, as summarised in Table 1-2. An international consensus group (International Consensus on Musculoskeletal Infection, ICM) updated the definition in 2013, modifying the minor diagnostic criteria to include leucocyte esterase, Table 1-3, and a sub-classification of acute and chronic infection Table 1-4. With the introduction of debridement, antibiotics with implant retention surgery (DAIR) and single staged revisions, separating this infected cohort became relevant to treatment decisions.

A standardised definition of PJI has allowed research in the field to expand resulting in several new biomarkers for infection being proposed. A number of these biomarkers are included in the 2018 ICM consensus update to the definition of PJI, which has adopted an algorithm approach Table 1-5. Aiding pre-operative surgical decision-making, a scoring system assesses the likelihood of an implant being infected. More recently, the European Bone and Joint Infection Society (EBJIS) supported by the MSIS have developed a 3-step guideline to diagnose PJI based on clinical history, examination findings and available diagnostic tests. If results from all tests come back negative then it is deemed ‘infection unlikely’. If two of the chosen parameters are positive, then ‘Infection Likely’ is concluded. Key diagnostic tests with the highest reported sensitivities from published literature diagnose ‘Infection confirmed’ if one alone is positive (McNally et al., 2020).

Table 1-2 2011 MSIS PJI criteria
The criteria proposed to diagnose PJI. ESR = Erythrocyte sedimentation rate, CRP = C reactive protein, WCC = white cell count, HPF = High powered field. CRP, WCC and synovial WCC values are included in the definition based on previous research. Table adapted from (Javad Parvizi et al., 2011).

Definite PJI exists when	
1.	A sinus tract communicates with the prosthesis **OR**
2.	The same pathogen is isolated by culture from two separate tissue or fluid samples from the prosthesis **OR**
3.	Four of the following six criteria are met:
a	Raised ESR (>30mm/hour) and CRP (>10mg/L)
b	Elevated synovial WCC (>3000 cells/μL)
c	Elevated synovial neutrophil % (>80%)
d	Pathogen isolated by culture from one tissue or fluid sample
e	Presence of pus in the joint
f	Histology tissue analysis reveals >5 neutrophils per HPF in 5 HPF's

Table 1-3 2013 update to MSIS PJI criteria
The updated diagnostic criteria included Leucocyte esterase. Table adapted from (Javad Parvizi & Gehrke, 2014).

Definite PJI exists when	
Major criteria	A sinus tract communicates with the prosthesis **OR**
	The same pathogen is isolated by culture from two separate tissue or fluid samples from the prosthesis
Minor criteria 3 out of 5	Raised ESR (>30mm/hour) and CRP (>10mg/L)
	Elevated synovial WCC or Leucocyte esterase strip (++)
	Elevated synovial neutrophil % (>80%)
	Pathogen isolated by culture from one tissue or fluid sample
	Histology tissue analysis reveals >5 neutrophils per HPF in 5 HPF's

Table 1-4 Acute and Chronic PJI criteria
Minor criteria thresholds for defining acute and chronic PJI. Table adapted from (Javad Parvizi & Gehrke, 2014).

Criteria	Acute <90 days	Chronic >90 days
ESR (mm/hr)	N/A	30
CRP (mg/L)	100	10
Synovial WCC (cells/ul)	10,000	3000
Synovial polymorphonuclear (%)	90	80
Leucocyte esterase	+ or ++	+ or ++
Histology (neutrophils /HPW)	>5	>5

Table 1-5 2018 PJI diagnostic algorithm
Most recent update to the PJI diagnostic criteria including new biomarkers. Table adapted from (Javad Parvizi et al., 2018).

	Sample	Test	Score	Decision
Major Criteria	Two Positive cultures same organism			Infected
	Sinus tract with communication to joint			
Minor Criteria, Preoperative	Serum	Elevated CRP >10mg/L, D-dimer >860	2	≥6 Infected 2-5 Possibly infected 0-1 not infected
		Elevated ESR >30mm/H	1	
	Synovial	Elevated WCC >3000cells/μL or LE (++)	3	
		Positive alpha-defensin	3	
		Elevated synovial PMN >80%	2	
		Elevated synovial CRP >6.9 mg/L	1	
Intraoperative diagnosis	Preoperative score		-	≥6 Infected 4-5 Inconclusive ≤3 Not infected
	Positive histology		3	
	Positive Purulence		3	
	Single positive culture		2	

1.11.1 Microbiology and histology analysis

Microbiological analysis of tissue from a suspected infected prosthesis forms the backbone of previous and current guidelines for diagnosing PJI. Two identical organisms cultured from intra-operative tissue samples confirm that an implant is infected (McNally et al., 2020; Javad Parvizi et al., 2018). To optimise microbiological diagnosis, current research suggests that multiple samples are taken from different areas of the joint using separate instruments for each sample. Recommendations are for five tissue samples, however, a more recent study has suggested four samples, utilising three different culture media's is sufficient, has high levels of concordance (up to 99.7%) and can reduce costs (Atkins et al., 1998; Bémer et al., 2016). Multiple samples increase sensitivity and specificity by distinguishing contaminants from infecting organisms. Microbiological cultures are incubated for a minimum of 5 to 14 days (Bémer et al., 2016; Drago & De Vecchi Elena, 2017) . The location of the tissue samples can also affect the culture outcome, suggesting that there is a spatial aspect to bacterial clusters (Walker et al., 2020). The other major criteria is the formation of a sinus between skin and implant, however, swabs or samples from the sinus are often contaminated with skin organisms and are not utilised for diagnosis.

Culture of synovial fluid can be performed pre-operatively to aid PJI diagnosis. Evaluated in a series of 145 revision TKR's, 40 of which were classified as PJI, synovial fluid culture had a sensitivity and specificity of 72.5% and 95.2% respectively (Fink et al., 2008). In this study, synovial fluid culture was found to be inferior to tissue culture. A large meta-analysis of 34 studies that evaluated pre-operative synovial fluid culture reported pooled sensitivity and specificity values of 76% and 95% respectively (Qu et al., 2013). Aspiration form TKR's was found to have higher diagnostic accuracy that THR, this may reflect the technical challenges and potential for contamination with hip aspiration. In more recent studies synovial fluid culture has been used as a comparison for more modern molecular techniques. In these studies sensitivity and specificity results concur with the values above, 66.3-72.2% and 96-96.9% respectively (Cazanave et al., 2013; Ryu et al., 2014). Synovial fluid, if it can be obtained, remains a useful test given its specificity and versatility Table 1-5.

Synovial fluid and tissues samples can be analysed by histology techniques to give pre, intra and post-operative results regarding PJI. Synovial fluid aspirated pre-operatively can be assessed under high-powered microscope for the presence of white cells (WCC) and the percentage of polymorphonuclear cells (%PMN). The current recommended cut off values are >3000 WCC and >80% PMN (Bori, 2018; McNally et al., 2020). Tissues may be analysed by frozen section to give intra-operative and by paraffin section to give definitive post-operative number of neutrophils per high powered field in 5 separate fields, with the current cut off being >5. Histology techniques can also be limited in coagulase negative staphylococcus infections (Bori, 2018).

The formation of biofilm on an implant can give rise to issues not only with eradication but also detection of the pathogen on tissues culture. Sonication, a method that uses sound energy to disrupt this biofilm membrane on the implant is now increasingly used. In a comparative study of 331 patients, 79 with confirmed PJI, sonicated fluid had a sensitivity of 78% and specificity of 98.9%, compared with standard tissue culture 60.8% and 99.2% (Trampuz et al., 2007). These finding have been replicated in a number of further studies showing that sonicate fluid culture had increased sensitivity compared with tissue and synovial fluid culture (Cazanave et al., 2013) with equivocal specificity (Cazanave et al., 2013; Portillo et al., 2012). Sonication is a potential method to improve standard microbiological culture and molecular techniques, particularly in a culture negative or chronic infection scenario and the technique is included in the EBJIS diagnostic guideline (McNally et al., 2020).

1.11.2 Molecular methods

The clinical challenge of receiving a negative culture result in suspected PJI, where other diagnostic markers point towards infection but no organism can be identified, has demanded the use of more advanced molecular methods. Although not included in the 2018 PJI definition update, or 2020 EBJIS guidelines, in clinical practice if traditional and extended tissue culture methods report no bacterial growth, samples are sent for analysis using molecular techniques. The results can therefore be considered as an extension of microbiology culture. Molecular polymerase chain reaction (PCR) techniques can be used in a number of ways to diagnose PJI. Specific PCR, whereby primers

for specific microorganisms or genes are used to detect their presence, or Broad PCR, which identifies a highly conserved region of ribosomal RNA common to almost all bacterial species and amplifies it to detect the presence of microorganisms (Drago and De Vecchi Elena, 2017). Current clinical practice utilises 16s rRNA PCR, the studies that have evaluated this technique and compared it with conventional tissue and synovial fluid culture techniques are summarised in Table 1-6. The reported sensitivity from the 13 studies ranged from 64.3% - 100%, similarly with specificity 74%-100%. This method has been evaluated on a range of biological samples: tissue, synovial fluid aspirate and sonicate fluid, and it allows bacterial RNA detection in samples even if prior antibiotics have been administered. Despite these advantages it is not a first line investigation for PJI due to limitations of cost, laboratory technique and the possibility of false positive results due to contamination from dead bacteria.

Table 1-6 Studies evaluating broad 16s rRNA PCR in PJI

Author year	Number of patients	Sample	Method	Sensitivity	Specificity
Panousis 2005	PJI 12 Aseptic 80	Synovial fluid PCR	RT-qPCR 16s rRNA, culture & histology	PCR: 92% Culture: 75% Histology: 92%	PCR: 74% Culture: 96% Histology: 100%
Dempsey 2007	PJI 5 Aseptic 5	Sonicate fluid	RT-qPCR 16s rRNA	Not reported	Not reported
Fenollar 2009	525 samples	Tissues/bone/ synovial fluid	RT-PCR 16s rRNA, culture	PCR: 92.5% Culture: 86.7%	PCR: 95.7% Culture: 89%
Kobayashi 2009	PJI Aseptic	Sonicate Tissue	16s rRNA universal RT-PCR + specific MRSA RT- PCR	87% (combined)	80% (combined)
Bergin 2010	PJI 14 Aseptic 50	Synovial fluid	16s rRNA RT qPCR	64.3%	100%
Marin 2012	PJI 40 Aseptic 82	Tissue	RT-qPCR 16s rRNA	67.1%	97.8%
Rak 2013	PJI 16 Aseptic 51	Tissue	Broad 16s rRNA RT qPCR	75%	94.1%
Bemer 2014	PJI 264 Aseptic 35	Tissue	RT qPCR 16s rRNA	73.3%	95.5%
Rak 2015	PJI 24 Aseptic 76	Tissue	Broad RT qPCR 16s rRNA	1 bacteria: 87.5% 2 bacteria: 83.3%	1 bacteria: 92.1% 2 bacteria: 100%
Rak 2016	PJI 29 Aseptic 58	Sonicate fluid & Tissue	Broad RT-qPCR 16s rRNA	Sonicate fluid: 93% Tissue: 76%	Sonicate fluid: 93% (83-98%) Tissue: 93% (83-98%)
An 2016	PJI 23 Aseptic 44	Tissue	RT qPCR 16s rRNA	76%	95%
Kuo 2018	PJI 25 Aseptic 189	Synovial fluid	RT qPCR 16s/28s rRNA	100%	99.5%
Fink 2018	PJI 27 Aseptic 89	Synovial fluid	RT qPCR 16sRNA	55.6%	82%

1.1.1 Biomarker literature search

The use of culture methods in diagnosing infection has long been established, however, the ear of 'biomarkers' is evolving in many disease entities including infection and cancer. To identify current and proposed biomarkers for PJI, a literature search was carried out. Databases Pubmed and Web of Science were searched using terms "Prosthetic joint infection" AND/OR "alpha defensin", "leucocyte esterase" as these are biomarkers currently known and detailed in the diagnostic criteria and "biomarker". Inclusion Criteria: All clinical trials, all prospective and retrospective data reviews, human studies, prosthetic joint. Exclusion criteria: studies not in humans, review or meta-analysis articles, native joints. It was deemed appropriate to include retrospective clinical data reviews in this report as high quality RCT's are often challenging to initiate in orthopaedics, and this would allow for studies with large data series. Searches retrieved a total of 96 articles which were screened by title and abstract for their relevance, with duplicate articles removed. The following review focuses on discussing the papers and biomarkers which are include in the updated PJI MSIS 2018 and EBJS 2020 guidelines, other biomarkers and references are noted in section 1.12.

1.11.3 C-reactive protein

C-reactive protein (CRP) is an acute phase protein synthesised in hepatocytes in response to any tissue damage including inflammation and infection. In the healthy adult population normal CRP levels are <10mg/L and they rapidly increases after stimulus, reaching a peak at 48hrs. CRP has a short half-life and is a readily available widely utilised blood test (Pepys, 1981). In the setting of PJI diagnosis, both serum and synovial CRP tests are utilized. In a study evaluating pre-operative serum CRP in diagnosing PJI, a value >5mg/L was found to correlate with a subsequent diagnosis of PJI (Windisch et al., 2017). A number of publications have questioned the reliability of serum CRP as a biomarker for PJI diagnosis. In one retrospective study, which looked at 73 patients with culture positive PJI, CRP was normal in 23/73 cases, missing nearly 32% of PJI's (Pérez-Prieto et al., 2017). A second similar retrospective study found CRP to be normal (cut off value <10mg/L) in 77 of 215 (35.8%) of patients who again had a culture positive PJI (Akgün et al., 2018). In both of these studies, it was noted a number of the cultures grew low virulence organisms including *C.acnes*, *coagulase negative S.aureus* and *Corynebacterum*. Furthermore, CRP monitoring post operatively following PJI treatment in the form of debridement, antibiotics, and implant retention surgery (DAIR) or two stage revision surgery found that values did not correlate well with infection relapse (Bejon et al., 2011). These studies were assessing CRP as a lone marker for PJI, in normal clinical practice and the updated guidelines it is evaluated in the context of the whole clinical picture and diagnostic algorithm. Measuring synovial CRP is a more recent development. A study evaluating its use prospectively in revision hip and knee surgery, using the 2013 ICM definition of PJI to classify patients as aseptic or infected, found synovial CRP to be significantly higher in those with PJI vs aseptic revision 31.7mg/dL vs 1.02mg/dL P<0.001(Sousa et al., 2017). This study proposed a synovial CRP cut off value of 6.7mg/dL giving sensitivity and specificity values of 78.3% and 93.8% respectively. Its diagnostic accuracy increased when it was used in combination with current synovial investigations - synovial WCC, resulting in 100% specificity (Sousa et al., 2017). A further study evaluating synovial fluid from 89 patients; 21 classified as PJI and 59 as aseptic as per microbiology results, 9 were excluded due to the inability to analyse the viscous fluid. Sensitivity and specificity of synovial CRP were reported as 95.5% and 93.3% respectively (M.

Omar et al., 2015). In the 2018 PJI diagnostic algorithm, markers were evaluated in a stepwise fashion in 1504 cases (684 PJI), beginning with the least invasive serum markers and using random forest analysis to calculate how important each variable was in predicting infection. Of the three serum markers, CRP (>1mg/dL) carried the highest weight and was the most predictive of PJI (Javad Parvizi et al., 2018), however, synovial CRP was found to carry the lowest weight in random forest analysis for predicting PJI compared with other synovial investigations including WCC, % PMN, Leucocytes esterase and alpha defensin Serum CRP is included in the 2020 EBJIS guidelines as the only blood 'biomarker', but the authors caution against its use as a sole marker for PJI, synovial CRP is not included as a diagnostic marker (McNally et al., 2020). To this author's knowledge, synovial CRP is not routinely available in all clinical settings.

1.11.4 Alpha Defensin

Alpha defensins (AD) are a family of 6 antimicrobial peptides. AD 1-4 are found in neutrophils, they are released in response to pathogen invasion and are able to disrupt the bacterial cell wall, therefore having bactericidal activity (Wang, 2014). AD has been an extensively studied biomarker in PJI and is credit to the field of translational medicine, from bench to clinically available bed-side test. The sensitivity and specificity of AD in diagnosing PJI is summarised in Table 1-7. Initially, AD was tested using a laboratory based ELISA method. These studies reported the highest sensitivity (50%-100%) and specificity (95%-100%) values for AD. Two studies reported lower values for sensitivity (50%, 78.6%) than the remaining five (94%-100%) studies and seem as outliers in their results, both of these studies included cases of chronic PJI and cultured low virulence organisms in a number of patients (Kleiss et al., 2019; Sigmund et al., 2018). A number of these studies using the ELISA method included patients who had been treated with antibiotics showing that this biomarker has the potential to work in routine clinical practice (Bingham et al., 2014; Deirmengian et al., 2014a, 2014b, 2015). With the clinical limitations of a laboratory-based assay in providing a rapid diagnosis for PJI, it has since been developed into a bedside lateral flow test. Evaluation of this point of care test, Synovasure®, show sensitivity and specificity values from 20%-97% and 90%-100% respectively Table 1-7. Studies that reported lower sensitivity values suggested possible interference with the

assay from blood or metal ions in the synovial fluid aliquot (Kasparek et al., 2016), the presence of a draining sinus, which would lead to a lower concentration of defensins in the fluid (Gehrke et al., 2018) or a diagnosis of chronic infection. In the random forest analysis for the 2018 MSIS update, AD performed as the second-best synovial marker for PJI.

Table 1-7 Studies evaluating Alpha defensin in PJI
Details of the 15 studies that assessed the utility of Alpha Defensin as a biomarker for PJI. There were 5 studies that looked at the ELISA based laboratory method, 8 that used the lateral flow test and 2 studies that assessed both methods.

Author/Year	Number. of Patients	Cut off value	Method	Sensitivity	Specificity
Bingham 2014	61	7.72mg/L	ELISA	100%	95%
Deirmengian C 2014 (a)	149	5.2mg/L	ELISA	97%	96%
Deirmengian C 2014 (b)	95	4.8mg/L	ELISA	100%	100%
Deirmengian C 2015	46	5.3mg/L	ELISA	100%	100%
Kleiss 2019	202	5.2mg/L	ELISA	78.2%	96.6%
Sigmund 2018	71	Standardised signal Aseptic <0.9 Infected >1.0	ELSIA & Lateral flow	ELISA: 50% Lateral flow: 46%	ELISA: 98% Lateral flow: 98%
Gehrke T 2018	195	Not documented	ELISA & Lateral flow	ELISA: 94% Lateral Flow: 92%	ELISA: 99% Lateral Flow: 100%
Sigmund I 2016	19	N/A	Lateral flow	43%	94%
Kasparek 2016	40	N/A	Lateral flow	67%	93%
Berger P 2017	121	N/A	Lateral flow	97%	97%
Balato G 2017	51	N/A	Lateral flow	88%	97%
Suda 2017	30	N/A	Lateral flow	77%	97%
Scholton R 2018	37	N/A	Lateral flow	20%	Not reported
de Saint Vincent B 2018	42	N/A	Lateral flow	88.9%	90.6%
Renz N 2018	212	N/A	Lateral flow	54%-85%	96%-99%

1.11.5 Leucocyte Esterase

Leucocyte esterase (LE) is an enzyme release by activated neutrophils at the site of infection and is in regular clinical use in the diagnosis of urinary tract infections. The urine sample is applied to a test strip, a reagent on the strip lyses any neutrophils present in the sample, LE is released leading to a colour change. A positive (++) result is indicated by dark purple. In recent years its use in detecting PJI has been investigated by a number of studies. Initially, synovial fluid aspirates taken pre-operatively in cases of PJI in TKR were compared with TKR revision control cases. Using only ++ as a positive result, they recorded a sensitivity of 80.6% and specificity of 100% for LE (J Parvizi et al., 2011). Following on from this, subsequent studies have compared LE in synovial fluid in cases of aseptic revision and PJI as per guidelines which were the gold standard at the time of their publication. Using ++ to indicate a positive result, reported sensitivities range from 66%-100% and specificities from 97%-100% (Wetters et al., 2012; Tischler, Cavanaugh and Parvizi, 2014; Colvin et al., 2015; Deirmengian et al., 2015). Given the clear advantages of a result in 2 minutes at the bedside and readily affordable test kit, this would indicate LE should be added to the armoury of tests to investigate for PJI. As with other synovial markers, interference with results has been noted from blood or metal ions (Shafafy et al., 2015; Wetters et al., 2012). Identifying the level of colour change by eye may also introduce bias to this result. To overcome this a more recent study used colourimetric analysis of the test strip rather than naked eye evaluation. At a setting of 125 WBC on the test strip reader, the sensitivity and specificity were 81.8% and 92.9% respectively and the results correlated with known synovial WCC cut off values >1600ul/L (Shafafy et al., 2015). In the updated 2018 diagnostic algorithm, LE is combined with synovial WCC.

1.11.6 D-Dimer

D-dimer is a fibrin degradation product, a marker of turnover of the coagulation system. It has previously been used as a marker of venous thromboembolism and more recently as a marker of sepsis with its relation to disseminated intravascular coagulation seen in severe cases. The rationale for testing D-dimer in the setting of PJI comes from two theories: Severely inflamed synovium in rheumatoid patients secretes high levels of fibrin, therefore, severely inflamed

peri-articular tissue in infection may also secrete high levels of fibrin, which is subsequently degraded to release d-dimer (Shahi et al., 2017). Secondly, animal models of septic arthritis have shown significantly raised synovial D-Dimer (Ribera et al., 2011). There has been one prospective study that has assessed D-Dimer as a potential marker of PJI. Blood samples were collected from 5 different groups of patients: Primary arthroplasty, revision for PJI, revision for asepsis as per MSIS guidelines, 2nd stage re-implantation and patients with infection at any other site not including a joint. The results showed that D-Dimer was significantly higher in revision for PJI group (median value 1110ng/mL) vs revision for asepsis (median value 299ng/ml) $p<0.001$ and it was more sensitive and specific than pre-operative CRP or ESR (Shahi et al., 2017). D-Dimer is included 2018 update to the PJI diagnostic algorithm grouped with CRP as a pre-operative blood test Table 1-5 (Javad Parvizi et al., 2018).

1.12 Biomarker

Biological markers or 'biomarkers' are used to aid diagnosis, drug response and prognosis in many diseases, including infection and cancer. A number of biomarkers for PJI have been studied, some are discussed above (see section 1.11.3, 1.11.4, 1.11.5) as they are included in current PJI diagnostic algorithms. With an increased understanding of PJI biofilm biology, potential new biomarkers are being studied, including:

- Calprotectin – A protein in found in the cytoplasm of neutrophils and released upon neutrophil activation. Currently used in the diagnosis of inflammatory bowel disease (Wouthuyzen-Bakker et al., 2018).

- Procalcitonin – A peptide released into the bloodstream following bacterial infection (Bottner et al., 2007; Randau et al., 2014; Saeed et al., 2013; Sousa et al., 2017)

- Adenosine deaminase – A protein involved in the purine metabolism pathway. Its measurement can indicate immune cell activation in response to infection (Sousa et al., 2017).

- Presepsin - The soluble subtype of CD14, present of the surface of monocytes. It is involved in pathogen recognition and shed into the bloodstream during activation of MMP-9, with downstream activation of the inflammatory response via IL6, TNFα and IL1β (Marazzi et al., 2018).

- Interleukin -6 - A cytokine released by macrophages in response to infection and involved upstream in CRP production (Deirmengian et al., 2014a; Ettinger et al., 2015; Majors & Jagadale, 2019; Sakamoto et al., 1994; Wimmer et al., 2016), see Appendix A Table 6-1.

However, the studies evaluating these markers report limitations, including challenges in establishing a reference range to define a positive result and evaluating the results in the context of known inflammatory diseases such as rheumatoid arthritis (Ettinger et al., 2015; Majors & Jagadale, 2019; Wouthuyzen-Bakker et al., 2018). An ideal biomarker will be specific to PJI, therefore likely to be released from tissues in the joint, e.g. bone or synovium, in response to infection. It would be advantageous if the biomarker test was non-invasive, easily accessible from tissue such as blood to allow the test to be used if synovial fluid is not available. For the test to be robust and usable in clinical practice, it will require high levels of sensitivity and specificity and be cost effective. The current cost of revision orthopaedic surgery to treat PJI can be up to 3-times more than for non-infective causes (£30011 vs £9655) (Kallala et al., 2015) and is associated with a high 5-year all-cause mortality rate, up to 21.65% (Lum et al., 2018). Therefore, identifying a novel biomarker or indeed a panel of novel markers to improve the diagnosis and subsequent treatment of this condition should be balanced against these known costs but would be attractive to reduce the significant burden of disease associated with PJI.

1.13 Prosthetic joint infection work aims

The literature now provides a detailed understanding of implant related infection from initiation of bacterial attachment, maturation and subsequently chronicity of biofilm infection. This also includes how the immune response both reacts to and is excluded from this unique bacterial environment. Targeting the immune response to a pathogen as the diagnostic test is gaining in popularity, particularly as we enter the phase of personalised medicine. The

first step in this process is to identify a consistent immune gene transcriptional signature in PJI cases. To do this, this work will utilise next generation sequencing techniques and investigate the immune signature in biological tissue both local to (peri-articular tissue) and distant from (peripheral blood) the implant infection site. Once an immune gene signature has been identified, larger cohorts can be used to validate it and investigate personalised prognostic information it may convey.

2 Chapter 2: Materials and Methods

This chapter outlines the general materials, methods and equipment used for the duration of the current research. Methods that were adapted at specific stages of the research are described in the appropriate later chapters.

2.1 Patient data collection

Retrospective patient data was collected to assess the outcomes of the vancomycin wrap during ACLR surgery. Patient data collection was in accordance with procedures and protocols approved by the NHS West of Scotland Ethics Committee (REC14/WS/1035) and informed consent was obtained from all patients according to local procedures. Data Search Criteria: Electronic operation note system (Bluespier®) was used to identify all anterior cruciate ligament reconstructions (ACLR) carried out between 1st July 2018 and 30th June 2019, in a single hospital trust, working across two clinical sites; Queen Elizabeth University Hospital and The New Victoria Hospital, Glasgow. All ACLR both primary and revision were included between the search dates above. Those operations incorrectly coded as ACLR were excluded. The operation notes along with electronic patient clinical notes were used to abstract the following information:

- Age
- Sex
- Surgery:
    - Type of graft used
    - Primary or revision
- Prophylactic IV antibiotics
- Use of vancomycin wrap
- 6 month follow up for infection
    - Bacterial species cultured
    - Treatment of infection: Antibiotic duration, further surgery

Metadata was also collected retrospectively from those patients whom blood and synovial tissue were taken during orthopaedic revision arthroplasty surgery. Data was collected from electronic case notes and included age, sex, co-

morbidities, clinical biochemistry and microbiology results pertaining to the time of surgery. Patient data collection was in accordance with procedures and protocols approved by the NHS West of Scotland Ethics Committee (REC14/WS/1035) and informed consent was obtained from all patients according to local procedures

2.2 Ethics and Human tissue collection

Human tendon tissue was obtained during surgery for anterior cruciate ligament hamstring reconstruction. Patients were screened and the tissue discarded if there was a prior history of surgery to that joint – excluding previous ACL reconstruction, infection or malignancy. Human synovial tissue and peripheral blood were obtained from patients undergoing Orthopaedic revision arthroplasty surgery. Patients were excluded if there was a history of malignancy. All tissue was collected in sterile containers containing RPMI. Tissue was stored at 4^{o}C in hospital until collection and delivery to the University Laboratory. All samples were obtained from the New Victoria Hospital and Queen Elizabeth University Hospital Glasgow and used on the day of collection. All patients gave prior written and informed consent in line with NHS Greater Glasgow and Clyde consent procedures and Glasgow University Ethics. Surplus tissues samples, including synovial tissue and hamstring tissue, were collected as part of the NHSGG&C Bio-repository and Pathology Tissue Resource II [16/WS/0207], approval letter in Appendix C. Blood samples were collected as additional tissue in line with NHSGG&C Additional Sample Tissue Resource to Support I3I Research [14/WS/1035] & [19/WS/0111], approval letter Appendix D. All samples were taken by qualified medical practitioners.

2.3 Human tissue culture

2.3.1 Tendon tissue

Human tendon tissue was collected following surgery for ACLR and transported in sterile RPMI from the hospital site to the research laboratory. For *in vitro* cell culture experiments, tenocytes were isolated and grown from the tendon tissue. The tendon tissue was cut into <0.5cm pieces using a scalpel and transferred to

a 25cm^2 culture flask with 5ml of RPMI supplemented with 10% (v/v) faetal calf serum, 100U/mL penicillin, 100µg/mL streptomycin (Gibco, Scotland, UK), at 37ºC humidified atmosphere of 5% CO_2. Cell culture was maintained for 28 days. Cells were passaged with trypsin at subconfluency and used at second or third passage for in vitro experiments. For *ex vivo* explant experiments, tendon tissue was cut into 1cm sections using a scalpel Figure 2-1. These sections were transferred to a 24 well flat bottom cell culture plate and treated with experimental conditions for 1 hour at 37ºC humidified atmosphere of 5% CO2. Supernatants were aspirated and stored for future protein quantitation analysis and replaced with RPMI for 16 hours at 37ºC humidified atmosphere of 5% CO_2. Following the 16-hour incubation, supernatants were aspirated and stored for future protein quantitation analysis. The tissue was transferred to RNALater (Invitrogen) or 4% buffered formalin (ThermoFischer Scientific) for qPCR and immunohistochemistry analysis, respectively. Tissue in RNALater was stored at 4ºC for 24 hours to allow the storage agent to penetrate the tissue, this was then stored at -20ºC or proceeded directly to RNA extraction section 2.7.1. For tendon biomechanical analysis, tendon tissue was cut into 3cm sections using a scalpel Figure 2-2. The tissue was transferred to a 6 well flat bottom cell culture plate and treated with experimental conditions for 1 hour at 37ºC humidified atmosphere of 5% CO_2. Supernatants were aspirated and stored at -20ºC, tissue was stored at -20ºC for future biomechanical analysis. Due to restrictions in place during the COVID 19 outbreak, biomechanical analysis was not completed within the time frame of this project.

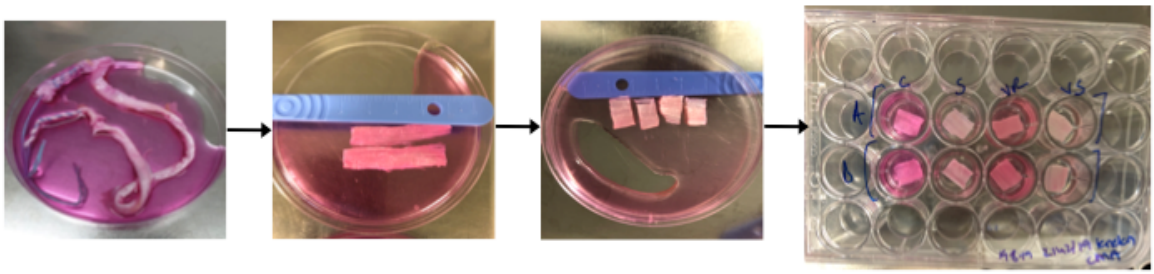

Figure 2-1 Images of the tendon ex vivo model
Tendon was cleared of surplus muscle and cut into 1cm sections then transferred to a 24-well tissue culture plate in 1ml of media with experimental conditions.

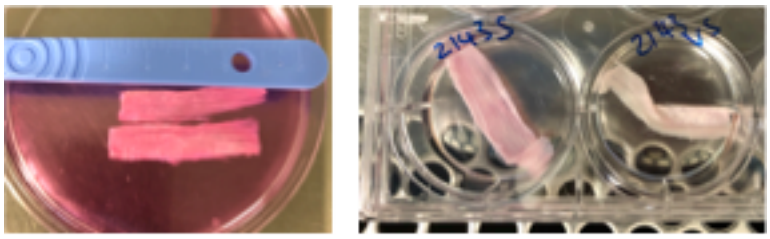

Figure 2-2 Images of tendon for biomechanical analysis
Tendon was cleared of surplus muscle and cut into 3cm sections and transferred to a 6-well tissue culture plate in 3mls of media with experimental conditions.

2.3.2 Synovial Tissue

Synovial tissue was collected from patients undergoing Orthopaedic revision arthroplasty surgery. Tissue representing synovium, was taken using a clean scalpel, and transported to the laboratory in sterile RPMI. The tissue was sectioned into approximately 2 x 1cm sections for storage in 4% buffered formalin or RNALater. Tissue in RNALater was stored at 4°C for 24 hours to allow the storage agent to penetrate the tissue, this was then stored at -20°C or proceeded directly to RNA extraction section 2.7.1, tissue in formalin was fixed at room temperature for 24 hours before transferring to 70% ethanol for paraffin embedding and analysis section 2.4.1. Laboratory synovial tissue samples were annotated as PJI (infected) or aseptic control based on routine hospital clinical assessment which referenced the MSIS guidelines see Table 1-5 & Table 1-4 and microbiology results.

2.3.3 Peripheral Blood

Peripheral blood was obtained from patients prior to undergoing Orthopaedic revision arthroplasty surgery. Blood was taken in 2.5ml Paxgene® tubes (BD Biosciences) and inverted 10 times to ensure mixing with the RNA stabilising reagent, which prevents RNAse enzymes degrading RNA. The blood was sorted at -80°C within 24 hours of collection.

2.4 Histology and immunohistochemistry

2.4.1 Synovial tissue

Synovial tissue fixed in 4% buffered formalin was processed as per section 2.3.2. The tissue was subsequently dehydrated in graded alcohol and embedded in paraffin blocks. The block was cut into to ensure the 5µm sections were representative of the whole tissue. Consecutive sections of tissue 5µm thick were cut (Leica Microsystems, Germany). The middle cut was stained with haematoxylin and eosin, re-hydrated in graded alcohol, and mounted onto a glass microscope slide with DPX mountant and a cover slip. The stained slides were imaged using a light microscope (Olympus, DP22). Un-stained sections were used in analysis by HTG molecular Diagnostics for tissue transcriptomics see section 2.7.5. All synovial tissue embedding and cutting plus assistance with

haematoxylin & eosin staining was provided by Ms Fiona McMonagle (Technician Institute of Infection, Immunity and Inflammation, University of Glasgow)

2.4.2 Tendon tissue

Treated and control tendon explant tissue section 2.3.1, fixed in 4% buffered formalin, dehydrated in graded alcohol and embedded in paraffin, were used for haematoxylin and eosin staining and Caspase 3 antigen staining (Cell Signalling Technology, UK). Sections of tissue 5µm thick were cut (Leica Microsystems, Germany), paraffin removed by xylene and rehydrated in graded alcohol. At this stage, the tissue was either stained with haematoxyxlin and eosin, re-hydrated in graded alcohol, and mounted onto glass microscope slides with DPX mountant and a cover slip or, proceeded to Immunohistochemistry staining for antigen expression as follows. Endogenous peroxidase activity was quenched with 3% (vol/vol) H2O2, and nonspecific antibody binding was blocked with 2.5% horse serum in TBST buffer for 30 minutes. Antigen retrieval was performed in 0.01 M citrate buffer for 25 minutes in a microwave. Tissues sections were incubated with primary antibody and Isotype control diluted 1:125 in 2.5% (w/v) horse serum/TBST overnight at 4°C. After two washes, slides were incubated with Vector ImmPRESS Reagent kit as per manufacturer's instructions for 30 minutes. The slides were washed and incubated with Vector ImmPACT DAB chromagen solution (1 drop per 1ml diluent) for 30 seconds, followed by extensive washing in water. Finally, the sections were counterstained with haematoxylin, dehydrated in graded alcohol and mounted in DPX with a coverslip.

2.5 MTT Cell viability assay

The MTT assay is a colorimetric assessment assay which correlates with cell viability. The yellow tetrazolium salt MTT (3-(4,5-Dimethylthiazol-2-yl)-2,5-diphenyltetrazolium bromide) is taken up by metabolizing cells and changed into a blue formazan product by reductase enzymes in the cytosol and mitochondria. The blue formazan product accumulates within viable cells, once lysed, the product can be measured and quantified by spetophotometry(Mosmann, 1983). To make a 10nM solution of MTT, 414.3mg of MTT (Sigma-Aldrich, Dorset) was dissolved in 100ml of PBS. This solution was then sterile filtered with a 0.2µm filter and stored in the dark at 4ºC until use.

2.5.1 Tenocyte viability

Tenocytes were cultured with experimental conditions in a 24 well plate, following which supernatants were aspirated, and the cells re-suspended in 250µl of MTT, incubated for 3 hours at 37ºC/5% humidified CO_2. The supernatants were removed and the cells washed with sterile RPMI and incubated with 200µl DMSO for 10 minutes to dissolve the formazan product. This was transferred into a 96 well plate (100µl per well in duplicate) and read on a MTX TC II microplate reader (Dynex Technologies) at 540nm.

2.6 Protein Quantitation

Protein quantitation in tendon supernatants was determined using enzyme linked immunosorbent assays (ELISA's) (IL-6, IL-8, MMP-3, CCL2, Cytochrome C, Pro-Colagen1α) and luminesces assays (Caspase 3) according to manufacturer's instructions, Table 2-1.

2.6.1 ELISA

All ElISA's were performed in 96 well half area high binding microplates (Corning™ Fischer Scientific) with volumes scaled accordingly. If required, plates were coated with 50µl/well of capture antibody, diluted as per instructions in PBS, sealed and incubated overnight at 4ºC. Following incubation, plates were washed once with wash buffer then blocked for 1 hour at room temperature with 150µl/well of assay buffer. During incubation, standards and samples were prepared in assay diluent. The standard curve was made as per the instructions on the Certificate of Analysis with serial 2-fold dilutions from the top standard. Following incubation with assay buffer, the wells were aspirated and 50µl of the standards and samples were pipetted into appropriate wells, followed by 25µl of detection antibody diluted as per manufacturer's instructions. Plates were sealed and incubated with continuous shaking at room temperature for 2 hours. Following this, each well was aspirated and washed 5 times with wash buffer and 50µl of Avidin-HRP diluted as per instructions added to each well. The plate was sealed and incubated as previously for 30 minutes. The wells were aspirated and washed 5 times and 50µl of TMB solution (ThermoFischer) was added to each well and incubated in the dark as above for a maximum of 15 minutes. Once the desired colour change of the standards had been achieved, 50µl of 2M H2SO4 was

added to each well to stop the reaction. Absorbance was recorded within 30 minutes of this final step on a MTX TC II microplate reader (Dynex Technologies), measured absorbance 450nm and reference absorbance 650nm.

Table 2-1 Elisa and Luminesces kits used for protein quantitation
Details of the source, buffers and assay ranges for the ELISA and Luminescence kits used. BSA-bovine serum albumin. Tween-20 and BSA (sigma Aldrich, UK), H2SO4 (Fischer scientific, UK).

Protein	Source	Coating buffer	Assay buffer	Wash buffer	Assay range pg/mL
IL-6, IL-8, MMP-3	Thermo Fischer Scientific	PBS	0.5% BSA & 0.1% Tween-20 in PBS	0.05% Tween-20, 2M H_2SO_4 in PBS	IL-6 15.6 – 1000 IL-8 12.5 – 800 MMP-3 1.25-20ng/mL
CCL2	Thermo Fischer Scientific	PBS	Provided in kit	0.05% Tween-20, 2M H_2SO_4 in PBS	7-1000
Cytochrome C	Thermo Fischer Scientific	Not required	0.5% BSA & 0.1% Tween-20 in PBS	0.05% Tween-20, 2M H_2SO_4 in PBS	0.08-5ng/mL
Pro-Collagen 1α	R&D Systems Biotechne brand	PBS	1% BSA & 0.1% Tween-20 in PBS	0.05% Tween-20, 2M H_2SO_4 in PBS	31.3-2000
Caspase 3	Caspase-GLO® 3/7, Promega	Not required	Not required	Not required	

2.6.2 Luminescence assay

Before beginning the assay, the Caspase-GLO 3/7 Buffer and lyophilized Caspase-Glo 3/7 substrate were reconstituted to form Caspase-GLO 3/7 reagent at room temperature, by transferring the buffer into the substrate and mixing by inversion. Using a white-wall 96 well plate (Corning™, Fischer Scientific) to reduce background luminesces, equal volumes (50µl) of reagent and supernatant were added to each well, along with experimental controls. The plate was sealed and incubated for 1 hour at room temperature. The luminescence was then recorded on a MicroBeta® TriLiux 1450 (Perkin Elmer life Sciences).

2.7 Quantitative polymerase chain reaction and gene expression analysis

Treated and control tendon and synovial tissue, stored in RNALater section 2.3.1 and 2.3.2 were used for gene expression analysis. If required, samples were thawed on ice prior to RNA extraction

2.7.1 RNA extraction from tissue

RNA was isolated using PureLink™ mini kit (Life Technologies) as per manufacturer's instructions. The tissue was initially disrupted and homogenised in RLT buffer. To prepare the samples, a scalpel was used to cut the tissue into <0.5cm pieces followed by metal bead homongenisation with 3 x 1 minute cycle's at 35Hz (Qiagen TissueLyer LT). Between each cycle the tubes were rested on ice for 1 minute. The supernatant was removed and incubated in a new eppendorf with protease K (10µl protease K in 690µl of nuclease free H_2O per tube) at 55oC for 15 minutes. Following this, the sample was centrifuged at 12,000rpm for 3 minutes. The supernatant was removed, combined with an equal volume of 70% (v/v) ethanol in a new Eppendorf, mixed by pipetting and spun through an RNeasy spin column by centrifuging at 12,000g for 15 seconds. The flow-through was discarded and 700µl of wash buffer I was added and the column centrifuged as before. A further wash step with 350µl of wash buffer II was performed and centrifuged as before, transferring the column to a new collection tube for DNase treatment. 10µl of DNase I mixed with 70µl RDD buffer (Qiagen) was added to each column and incubated at room temperature for 15 minutes. Following this, a further wash step with 350µl of wash buffer II

was performed, the flow-through discarded and transferred to a new 2ml collection tube. The sample was then centrifuged at 12,000g for 2 minutes with the lid open to dry the membrane. The spin column was transferred to a 1.5ml collection tube and RNA eluted using nuclease free water. RNA was quantified and purity checked using a Nanodrop 2000/200c (ThermoFischer), nuclease free water was used as a blank. Absorbance of RNA was measured at 260nM, 280nM and 230nM. The A260:280 ratio determines RNA purity, the A260:230 ratio determines the level of protein contamination. RNA was either stored at -20^{o}C until required or preceded straight to cDNA synthesis, section 2.7.2.

2.7.2 cDNA synthesis

cDNA was synthesized using High-Capacity cDNA synthesis kit (Applied Biosystems). 100ng of RNA was converted per reaction, unless there was insufficient RNA, in which case 80ng was used. The reaction was assumed to go to completion and create 100ng of cDNA. Briefly, RNA samples were diluted with nuclease free water to 10ng/µl and 10µl added to a 2 x high capacity cDNA master mix for a final volume of 20µl Table 2-2. Tubes were placed in a thermal cycler (Applied Biosystems) for the reverse transcription reaction, Table 2-3. cDNA was diluted to 1ng/µl using nuclease free water and stored at -20^{o}C.

Table 2-2 High-capacity cDNA master mix
Details of the reagents and buffers used per reaction to synthesise cDNA from RNA.

Reagent	Volume per reaction (µl)
10x RT Buffer	2
dNTP	0.8
10x RT Random Primers	2
Multiscribe™ Reverse Transcriptase	1
Nuclease free water	4.2
Total	**10**

Table 2-3 Programme settings for High-capacity cDNA synthesis

Settings	Step 1	Step 2	Step 3	Step 4
Temperature	25°C	37°C	85°C	4°C
Time (minutes)	10	120	5	∞

2.7.3 Gene expression analysis via quantitative PCR

All primers were either obtained from the previously designed stocks in the laboratory or designed specifically for this project using Integrated DNA Technologies (IDT) and the PrimerQuest tool (https://eu.idtdna.com/Primerquest/Home/Index). Details of the primers used in the project are detailed in Table 2-4. Default settings for qPCR with intercalating dyes were used e.g. an optimum melting temperature of 62°C, GC content of 50%, primer size of 22 nucleotides and amplicon of 100nts. Where possible, primers were designed to overlap exon junctions, to increase specificity for mature cDNA. Primers were tested for specificity using NCBI Blast (https://blast.ncbi.nlm.nih.gov/Blast.cgi). All qPCR primers were validated with a melt curve to ensure the presence of a single product without evidence of primer dimerization.

Transcripts were analysed by qPCR in duplicate in a 96 well plate format. The 10ul reaction was carried out using 5µl Powerup SYBR® Green (Thermo Fisher Scientific), 0.1µl of each forward and reverse primer (stock 100µM,Table 2-4) 3.8µl of nuclease free water and 1µl of cDNA. A non-template control, substituting 1µl of nuclease free water for cDNA was carried out for each primer to control for reagent contamination. The plates were sealed and centrifuged for 30 seconds prior to running on Applied Biosystems StepOne Plus System. Cycling conditions were as follows: 10 minutes at 95°C, then 40 cycles of 95°C for 15 seconds to denature, and 60°C for 1 minute to anneal and extend. Samples were normalized to GAPDH or 18s housekeeping gene and where applicable fold change calculated using the following equations:

Normalisation to housekeeping gene:

$$2^{-\Delta CT} = 2\text{-(CT gene of interest)} - \text{(CT housekeeping gene)}$$

Calculation of fold change:

$$2^{-\Delta\Delta CT} = 2\text{-}\Delta CT(\text{variable}) \,/\, 2\text{-}\Delta CT(\text{control})$$

Table 2-4 qPCR Primers
Forward and revere nucleotide sequences of the primers used in qPCR.

Primer	Forward (5’ – 3’)	Reverse (5’ – 3’)
GAPDH	TCGACAGTCAGCCGCATCTTCTTT	ACCAAATCCGTTGACTCCGACCTT
18s	GTAACCCGTTGAACCCCATT	CCATCCAATCGGTAGTAGCG
AIFM1	CAGTCAATGTTCTGGAGTGATTTG	TTGTCTTGTGCAGTTGCTTT
BCL2	AGGCTGGGATGCCTTTGT	GACTTCACTTGTGGCCCAGATA
BAX	GGAGCTGCAGAGGATGATTG	AGTTGAAGTTGCCGTCAGAA
Caspase 3	TCATTATTCAGGCCTGCCGTG	TGGATGAACCAGGAGCCATCC
CCL2	CTC AGC CAG ATG CAA TCA ATG	TGC TGC TGG TGA TTC TTC TAT
Collagen 1a	CAATGCTGCCCTTTCTGCTCCTTT	CACTTGGGTGTTTGAGCATTGCCT
Collagen 3a	TAT CGA ACA CGC AAG GCT GTG AGA	GGC CAA CGT CCA CAC CAA ATT CTT
Decorin	CGC CTC ATC TGA GGG AGC TT	TAC TGG ACC GGG TTG CTG AA
FADD	GGA AGA AGA CCT GTG TGC AG	GCA TCT TGG TGT CTG AGA CTT T
FAS	AGG GAT TGG AAT TGA GGA AGA	CTA GCT TTC CTT TCA CCT GGA
Fas Ligand	ATA GGC AAG TCC AAC TCA AGG	CAC AAG GCC ACC CTT CTT AT
HMGB1	CTC AGA GAG GTG GAA GAC CAT CT	GGG ATA TAG GTT TTC ATT TCT CTT TC
Interleukin 6	CAC TCA CCT CTT CAG AAC GAAT	GCT GCT TTC ACA CAT GTT ACT C
Interleukin 8	GTG CAT AAA GAC ATA CTC CAA ACC	GCT TTA CAA TAA TTT CTG TGT TGG C
MMP 3	ACC CAC CTT ACA TAC AGG ATT G	GTC ACC TCT TCC CAG ACT TTC
Survivin	GAA CTG GCC CTT CTT GGA G	CTT GAA GCA GAA GAA ACA GCT G
Tenascin C	GTG CCA GGA GAC CGT ACC AC	CTT TGG CTG GGT TGC TTG AC
TNFr	GAA GAA CCA GTA CCG GCA TTA T	TGC ACA CGG TGT TCT GTT

2.7.4 Prosthetic joint infection patient blood transcriptomic analysis

RNA was extracted from the blood using PAXgene® blood RNA kit following the handbook instructions for manual purification (handbook version 2 June 2015). The samples were removed from -80°C and stored overnight at 4°C to allow them to thaw. They were then brought to room temperature for 2 hours before beginning extraction to allow full lysis of the cells. Aliquots of 500μl were taken from each sample and transferred on dry ice to HTG Molecular diagnostics for analysis with their quantitative nuclease protection assay with a next generation sequencing platform. This allows quantitative analysis of a pre-defined gene panel without nucleic acid extraction. Briefly the method involves DNA nuclease protection probes flanked by universal wing sequences binding to the target RNA in the sample. These nuclease protection probes can bind the target RNA in soluble and cross-linked biological matrix (eg: formalin fixed). Universal DNA wingmen are then hybridised to the protection probe wing sequences. S1 nuclease is added which digests any non-hybridised RNA and any excess DNA wingmen. This leaves only the target RNA bound to the nuclease protection probes and flanked by the DNA wingmen in a 1:1 ratio. Heat denatures the DNA from the RNA probes, and allows for DNA amplification, quantification and sequencing Figure 2-3. The laboratory work was carried out by Mr Ihab Botros, Mr James Cooley and members of the sample logistics and development teams (HTG Molecular diagnostics, Arizona). Prior to release of data and analysis, all samples underwent three steps of quality control (QC). QC0 involved spiking the samples with a positive control, less than 25% of readouts should come from this spiked sample. Over this value and the sample was deemed to have too little RNA to proceed. QC1 analyses read depth and QC2 looks for variance, which should be present in biological samples. Data was provided as raw read counts.

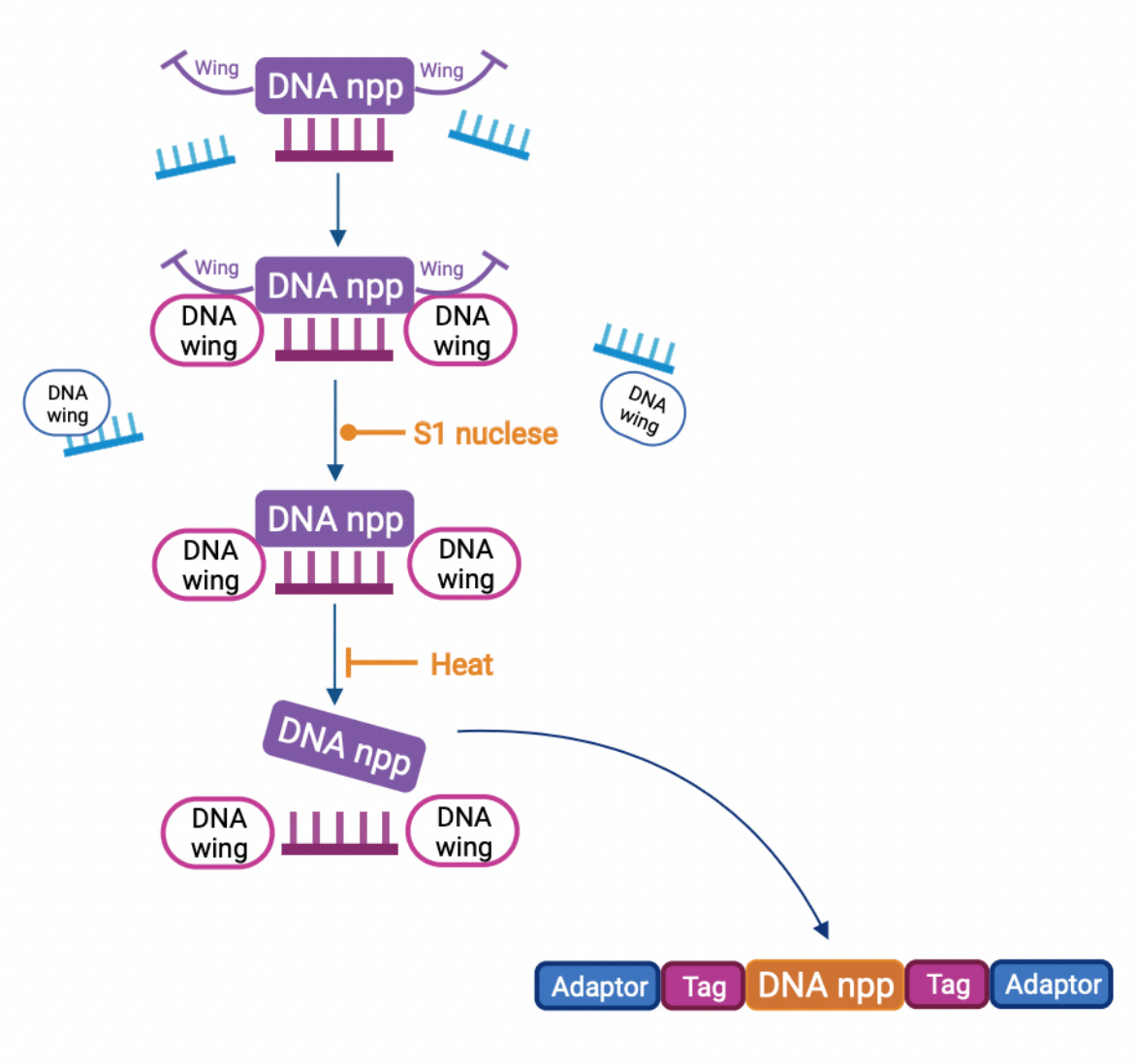

Figure 2-3 Schematic representation of HTG Molecular nuclease protection assay chemistry DNA nuclease protection probes, flanked by wingmen are hybridised to the target RNA in the biological sample. Universal DNA wingmen are then added and bind to the wingmen on the DNA nuclease protection probes. S1 nuclease is added which digests unbound RNA, excess DNA wingmen and DNA nuclease protection probe wings. Heat denatures the bond between RNA and DNA nuclease protection probe and releases the DNA nuclease protection probe. Library preparation involves adding tags – barcodes and sequencing adaptors to the DNA nuclease protection probes. The labelled DNA nuclease protection probes are concentrated and pooled ready for sequencing. DNAnpp = DNA nuclease protection probe. Image created in BioRender, adapted form HTG Molecular sample analysis report VLP00498.

RNA extraction from the remainder of the PAXgene® blood was performed in the laboratory and proceeded as follows. The samples were centrifuged at 3,000g for 10 minutes to pellet the RNA and the supernatant was discarded. The size of the pellet was noted to give an explanation should the sample have a low RNA yield. RNase-free water (4mL) was added and the pellet resuspended before another spin at 3,000g for 10 minutes. Buffer BR1 (350μL) was added and vortexed to dissolve the pellet before transferring into a fresh 1.5mL microcentrifuge tube. Buffer BR2 (300μL) and proteinase K (40μL) were added, the mixture was vortexed for 5 seconds and then incubated in a shaking incubator at 55°C for 10 minutes to remove proteins from the sample. The lysate was transferred to a PAXgene® shredder spin column and centrifuged for 3 minutes at 20,000g to homogenise the sample. The flow-through was then transferred to a fresh 1.5mL microcentrifuge tube, without disturbing the pellet, and 350μL of 100% ethanol was mixed with the sample. Thereafter, the sample was then run through the PAXgene® RNA spin column by centrifugation at 8,000g for 1 minute. The RNA from the sample was now bound to the column and the flow-through could be discarded. Buffer BR3 (350μL) was added to wash the column and spun at 8,000g for 1 minute. DNase (Qiagen) was added to the column and incubated at room temperature for 15 minutes to remove DNA contamination from the sample. The column was washed with 350μL of buffer BR3 then again with 500μL of buffer BR4, both were spun at 8,000g for 1 minute. Another 500μL of buffer BR4 was added and spun at 8,000g for 3 minutes to ensure the column was dry. The RNA was eluted from the column in 35μL buffer BR5, spun at 8,000g for 1 minute. An additional 35μL of buffer BR5 was eluted, to give a total of 70μL eluted product. The RNA sample was denatured by heating to 65°C for 5 minutes and chilled immediately on ice. RAN yield was quantified using a Qubit™ RNA high sensitivity assay kit (Thermo Fisher Scientific) following the manufacturer's protocol. Briefly, 1μL of sample was diluted in 199ul of working solution and the sample's optical density was measured using the Qubit® 3.0 Fluorometer and RNA quantity calculated. RNA samples were then stored at -80°C until required.

2.7.5 Transcriptomics of synovial tissue FFPE samples

The HTG molecular quantitative nuclease protection assay as described previously, is applicable to RNA in cross linked biological matrix eg: formalin fixed tissue samples, again using a lysis only step without RNA extraction, see section 2.7.4 and Figure 2-3. This panel of genes was analysed in the formalin fixed paraffin embedded 5µm sections of synovial tissue to identify an immune signal unique to prosthetic joint infection. The laboratory work was carried out by Mr Ihab Botros, Mr James Cooley and members of the sample logistics and development teams (HTG Molecular diagnostics, Arizona). Prior to analysis, all tissue samples underwent three steps of quality control (QC) as previously described in section 2.7.4 Data was provided as raw read counts.

2.8 **Statistical analysis**

All Statistical analysis were performed using GraphPad Prism 6 Software. On all applicable data, a test for normal distribution was carried out. When data followed a normal distribution, parametric tests were used. When data was not normally distributed or there was insufficient data to test for normality non-parametric tests were used. Specific statistical tests used and details of multiple comparisons are detailed in the relevant results section and figure legends. Significance was set at $p<0.05$.

2.9 **Bioinformatics**

Analysis of sequencing data were performed by John J Cole, Bioinformatician at University of Glasgow using in house software (Searchlight 2). Statistical significance was set at $p<0.05$.

3 Chapter 3: A novel next generation sequencing technique to identify biomarkers for prosthetic joint infection

3.1 **Introduction**

The diagnosis of PJI remains a challenge, despite international consensus meetings to update diagnostic criteria, there remains no unified diagnosis or test. Recent publications have adopted a step wise algorithm approach to diagnosis, however, the cut off values and tests included in each of these algorithms differs (McNally et al., 2020; Javad Parvizi et al., 2018). Microbiology culture identifying an infective organism remains a gold standard for diagnosis and rationalising antimicrobial treatment. This leaves a challenging 'culture negative' cohort formed of three groups; a clinically infected implant but no bacteria can be grown, usually due to prior antibiotics or biofilm bacteria not growing on traditional agar plates; a low grade PJI were clinical markers and investigations are inconclusive but clinical suspicion is high and, true culture negatives. Culture negative results can occur in around 7-15% of cases of suspected PJI (Berbari et al., 2007; Palan et al., 2019). Multiple factors such as low virulence organisms or inadequate sampling are thought to be involved, however, prior administration of antibiotics is thought to be the principle reason (Berbari et al., 2007). In clinical practice, culture negative samples are evaluated with molecular techniques in the form of broad PCR for bacterial 16s RNA. Results from previous trials analysing this method have been summarised previously Table 1-6 they show 16s RNA PCR results do not consistently out-perform standard culture methods. Possible reasons for this include sample contamination and detection coming from dead bacteria leading to a false positive result. Furthermore, the literature has reported technical challenges when poly-microbial infections are present. Other limitations include cost and availability of technology – usually only in centralised areas with samples having to be transported for analysis. Currently researched methods to improve molecular diagnostics include Multiplex PCR, cartridge systems and NGS see Appendix B Table 6-2 and Table 6-3 for a summary of the current literature.

Knowledge of the immune response to implant related infections and biofilm has led to a number of 'biomarkers' for PJI, including Leucocyte esterase and Alpha defensin, which are both included in the updated the 2018 PJI diagnostic algorithm (Javad Parvizi et al., 2018) and Interleukin-6 which has

been the subject of recent research see Appendix A Table 6-1 . Immune markers have advantages over molecular sequencing techniques, they are not susceptible to DNA contamination and can be developed into 'bedside' tests, however, at the present time, they cannot guide antimicrobial treatment as they don't provide bacterial genus level information.

In this chapter, clinical samples from revision arthroplasty surgery are sequenced using a novel technique, involving a selected immune gene panel. This technology allows RNA sequencing to be performed on formalin fixed tissue, which historically, due to issues with protein cross-linking was not available. Furthermore, the sequencing method has been developed to eliminate extraction steps; reduce analysis time and sample volume, whilst reducing possible sources of contamination and false positive results. Focusing on a specific immune gene panel aimed to eliminate spurious results seen with whole genome sequencing in PJI, whereby biologically unrelated genes can be significantly upregulated (Mohamed Omar et al., 2017). In previous research, peri-prosthetic tissue samples have shown low sensitivity when evaluated with traditional culture (Walker et al., 2020) and 16s RNA PCR techniques (Marín et al., 2012; Ryu et al., 2014). This was potentially due to small tissue sample size and spatial distribution of bacteria. We therefore analysed this sequencing technology in blood, a more easily accessible biological tissue and one that would allow us to ascertain if local tissue changes are reflected systemically. These results document the first time the immune gene response panel, developed by HTG molecular, has been evaluated in an orthopaedic cohort including PJI tissue, aseptic tissue and blood.

3.2 **Aims & Hypothesis**

- Collect and analyse patient metadata for aseptic and PJI patient cohorts.

- To use formalin fixed synovial tissue and blood collected in PAXGene® tubes, to evaluate an immune gene panel and identify a gene expression signature with PJI.

- To identify if an immune molecular signature from tissue and blood can stratify patient cohorts into aseptic control and PJI.

- To identify if an immune molecular signature from tissue and blood can stratify the PJI by bacterial strain or chronicity of infection.

To initiate infection, bacterial pathogens present unique combinations of pathogen-associated molecular patterns to specific pattern-recognition receptors expressed on immune cells. Based on this I hypothesised that an immune signature in the tissue and blood would discriminate infectious (PJI) from aseptic (control) cohorts. Furthermore, with the understanding of biofilm biology and the shielding of bacteria in mature biofilm, I hypothesised that chronicity of infection would affect this immune signature. Blood represents a reservoir and a distribution vehicle for both bacteria and cells of the immune system, therefore, it was hypothesised, that a unique immune signature would also be found from infected PJI samples in blood.

3.3 Methods

3.3.1 Patient Metadata

Clinical patient data, along with microbiology results, were collected from electronic hospital records [Glasgow University Ethics codes 14/WS/1035, IMI_2018_06_A, IMI_2018_05_S]. This was used to annotate samples as infected or aseptic and to stratify into analysis cohorts including: acute and chronic infection, age, sex and anatomical location as shown in Table 3-1. The 2014 MSIS criteria were applied to define acute and chronic infection using clinically available data Table 3-2 (Javad Parvizi & Gehrke, 2014). Hospital microbiology protocol reports the white cell count of synovial fluid from the Gram film of a centrifuged deposit and reports this as the number of cells per high-powered field as +, ++ or +++.

3.3.2 Tissue in formalin

Surplus tissue was collected from patients undergoing revision arthroplasty surgery, fixed in formalin and cut into 5µm sections as detailed in methods section 2.4.1. This tissue was analysed by HTG Molecular as described in the

methods section 2.7.5. Gene expression raw data analysis was conducted by John J. Cole (Bioinformatics, Institute of Infection, Immunity and Inflammation, University of Glasgow) and visualised using in-house RNA sequencing software Searchlight (version 2.0) Figure 3-1.

3.3.3 Peripheral blood in PaxGene® tubes

Peripheral blood was collected into PAXGene® tubes from patients prior to undergoing revision arthroplasty surgery as detailed in methods section 2.3.3. Whole blood samples (500μL) were analysed by HTG Molecular as described in methods section 2.7.4. Gene expression raw data analysis was conducted by John J. Cole (Bioinformatics, Institute of Infection, Immunity and Inflammation, University of Glasgow) and visualised using in house RNA sequencing software Searchlight (version 2.0) Figure 3-1.

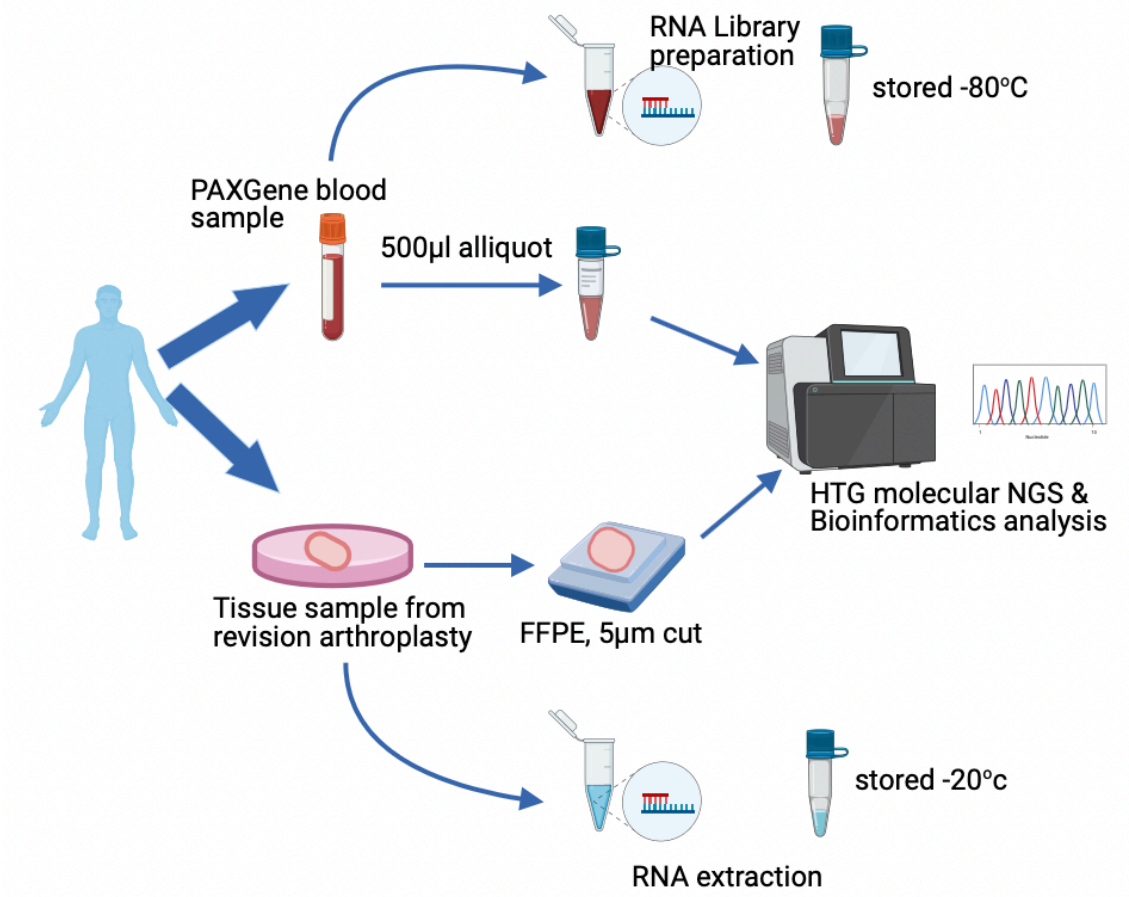

Figure 3-1 Flow diagram representing clinical sample journey from patient to results
Tissue and blood samples were collected from each patient in sterile RPMI media and PAXGene® tubes. An aliquot of blood was taken and sent to HTG molecular for analysis. RNA was extracted from the remaining PAXGene® blood sample and stored at -80°C pending validation of the immune signature. Tissue samples were fixed in formalin and then cut into 5µm sections onto a glass microscope slide. Slides were sent to HTG molecular for analysis. RNA was extracted from the remaining tissue and stored at -20°C pending validation of the immune gene signature. Due to COVID-19 the immune signature was not able to be validated in the stored tissue or blood RNA samples.

3.4 Results

3.4.1 Patient Metadata

Surplus biological samples were collected from twenty-four patients for sequencing; clinical and microbiological details of this cohort are shown in Table 3-1. There was no significant difference in age between the PJI and aseptic control cohort (66 vs 72, p=0.2), and no significant difference in male: female ratio. The majority of samples were from hip or knee revision arthroplasty, with only two samples from shoulders, however, this reflects clinical practice, with shoulder arthroplasty being less common than hip or knee. Stratification into acute and chronic infection cohorts was completed as per the 2014 MSIS guidelines (Javad Parvizi & Gehrke, 2014) using clinical history, biochemistry and microbiology results from electronic hospital records, Table 3-2. Figure 3-2 shows the pre-operative CRP (A) and white cell count values (B) for all 24 patients. The PJI cohort had significantly higher CRP and WCC compared with the aseptic cohort, however, these markers alone did not completely separate out the groups. Pre-operative values were chosen as inflammatory markers rise following surgery and it remains unclear how long post-surgery these acute phase reactants remain elevated. In the aseptic cohort, following extended microbiology culture, two tissue samples reported a positive result. In the first case (A027116), 1 out of 4 tissue samples sent to microbiology grew *bascillus simplex,* in the second case (A027118) 1 out of 5 tissue samples sent to microbiology grew *bascillus cirulans*. Both of these organisms are low virulence and were deemed by hospital microbiology multidisciplinary team review to be contaminants and were therefore not treated as PJI. Associated inflammatory markers in both of these cases were low (CRP 5 & 5.3, WCC <1 & 3.4) and therefore these samples remained assigned to the aseptic cohort.

Designated aliquots of PAXgene® blood were used for sequencing, RNA was extracted from the remaining blood as described in methods section 2.7.4. The quantity of RNA extracted from each sample is detailed in Table 3-1. This RNA was stored at -80^{o}C pending validation of a blood gene signature, however, due to COVID-19 restrictions this work could not be completed.

Table 3-1 Patient Metadata of sequencing cohort
Clinical and microbiological details of the patient cohort used by HTG Molecular for tissue and PAXGene blood sequencing. Prosthetic joint infection N=12, aseptic control N=12. No significant difference in average age, 66 years in infected cohort vs 72 years in aseptic p=0.2, analysis by t test. No significant difference in male: female ratio Fischer's exact value 1.0. One tissue sample failed QC (Quality control) and four blood samples produced insufficient library for sequencing. Strep = Streptococcus, Staph = Staphylococcus, H Influenza = haemophyllus influenza.

Tissue Sample ID	Blood Sample ID	Age	Sex	Joint	Bacteria	Acute/ Chronic	QC	RNA quantity (ng)	Blood QC	Library sequence
A027096	A028478	43	M	Hip	Strep mitis/oralis	Acute	Fail	4864	Pass	Sufficient
A027097	A028479	87	F	Hip	Staph capitis	Chronic	Pass	4864	Pass	Sufficient
A027098	A028480	74	M	Knee	Strep Group B	Acute	Pass	5312	Pass	Insufficient
A027099	A028481	86	F	Hip	Strep Group G	Acute	Pass	3744	Pass	Sufficient
A027100	A028482	54	M	Knee	Strep Group B	Acute	Pass	4704	Pass	Sufficient
A027101	A028483	47	M	Hip	Staph aureus	Acute	Pass	4016	Pass	Sufficient
A027102	A028484	74	M	Hip	Staph epidermidis	Chronic	Pass	4528	Pass	Sufficient
A027103	A028485	69	F	Knee	Pasturella	Chronic	Pass	2944	Pass	Insufficient
A027104	A028486	74	F	Knee	Strep Gallolyticus	Acute	Pass	3440	Pass	Sufficient
A027105	A028487	51	M	Hip	H. Influenza	Chronic	Pass	3424	Pass	Sufficient
A027106	A028488	70	F	Knee	Staph caprae, capitis	Chronic	Pass	2576	Pass	Sufficient
A027107	A028489	64	M	Hip	Strep mitis/oralis	Acute	Pass	4160	Pass	Sufficient
A027108	A028490	80	M	Hip	Aseptic	N/A	Pass	3504	Pass	Sufficient

Tissue Sample ID	Blood Sample ID	Age	Sex	Joint	Bacteria	Acute/ Chronic	QC	RNA quantity (ng)	Blood QC	Library sequence
A027109	A028491	62	M	knee	Aseptic	N/A	Pass	3776	Pass	Sufficient
A027110	A028492	79	F	Knee	Aseptic	N/A	Pass	2400	Pass	Sufficient
A027111	A028493	69	F	Knee	Aseptic	N/A	Pass	2944	Pass	Sufficient
A027112	A028501	79	M	Hip	Aseptic	N/A	Pass	5088	Pass	Sufficient
A027113	A028494	62	F	Shoulder	Aseptic	N/A	Pass	4384	Pass	Sufficient
A027114	A028495	67	M	Knee	Aseptic	N/A	Pass	3504	Pass	Sufficient
A027115	A028496	58	F	Knee	Aseptic	N/A	Pass	3280	Pass	Insufficient
A027116	A028497	76	F	Shoulder	Aseptic	N/A	Pass	4112	Pass	Insufficient
A027117	A028498	72	M	Hip	Aseptic	N/A	Pass	4080	Pass	Sufficient
A027118	A028499	60	F	Knee	Aseptic	N/A	Pass	3728	Pass	Sufficient
A027119	A028500	80	M	Hip	Aseptic	N/A	Pass	2496	Pass	Sufficient

Table 3-2 Microbiology and biochemistry results for infected tissue cohort
Clinical and laboratory details stratifying tissue samples into acute or chronic infection cohorts. Stratification as per 2014 MSIS guidelines (Javad Parvizi & Gehrke, 2014). CRP= C-reactive protein, LE = Leucocyte esterase, HPW = high-powered field, WCC = white cell count per HPF +<5, ++5-9, +++>10, N/A = not available.

Sample ID	Duration of symptoms	CRP	LE	Histology neuts/HPW	Synovial WCC	No. of positive tissue	No. of positive fluid
A027096_1	2 days	173	N/A	Nil	+++	4/4	3/3
A027097_1	4 months	15	N/A	+	+	3/5	1/2
A027098_1	3 days	397	N/A	Nil	N/A	1/1	1/1
A027099_1	2 days	253	N/A	++	++	1/5	1/2
A027100_1	2 days	349	N/A	++	+++	5/5	2/2
A027101_1	9 days	372	N/A	+++	N/A	6/6	0/0
A027102_1	2 years	3	N/A	++	+	2/4	0/1
A027103_1	11 months	70	N/A	+	+	4/4	1/2
A027104_1	1 days	77	N/A	+	+++	5/5	3/3
A027105_1	7 months	81	N/A	+++	++	2/5	1/2
A027106_1	18 months	54	N/A	++	+++	4/6	1/1
A027107_1	1 day	129	N/A	+	+++	4/4	1/2

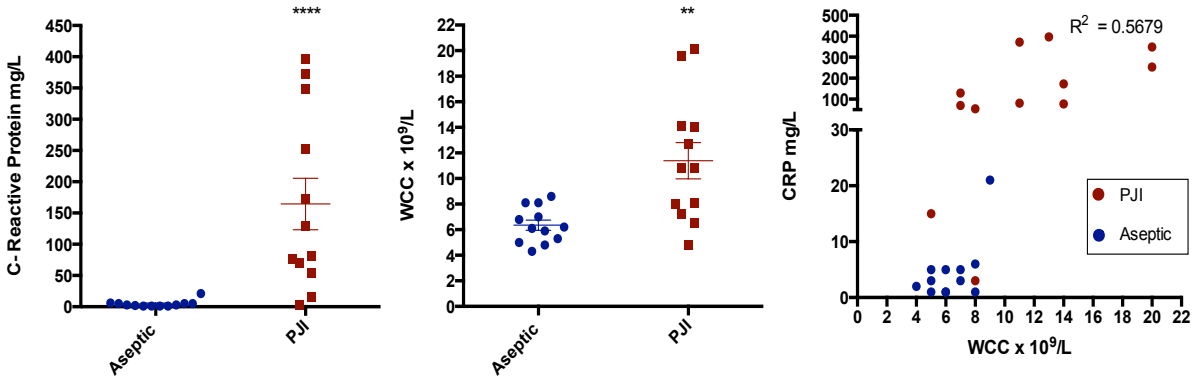

Figure 3-2 Serum and plasma inflammatory markers for aseptic and PJI sequencing cohort

(A) Serum CRP values, (B) Plasma WCC and (C) CRP plotted against WCC, aseptic shown in blue N=12, PJI shown in red N=12. Analysis by unpaired t test, **p<0.01, ****p<0.0001. WCC = white cell count (normal range 4.0-10.0 x10^9/L) (McBrearty & Moffat, 2021), CRP = C reactive protein (normal <10mg/L) (Scott & Hogg, 2019).

3.4.2 Tissue & blood sequencing quality control and bias

Sequencing results from the FFPE tissue and PAXgene blood samples underwent three levels of post sequencing quality control (QC) before data analysis.

All FFPE tissue samples passed QC1, which has a minimum read depth cut-off to identify and exclude low expressers, and QC2 which defines a minimum threshold for biological variance, as normal clinical samples should have variance between expression of genes. One tissue sample (A027096) failed QC0 quality check, Table 3-1; as the proportion of the sample (<75%) vs. spike (>25%) in positive control reads was too low, determining low sample quantity. The failed sample was re-submitted for re-evaluation, however failed QC again and was therefore excluded from future analysis.

Four of the twenty-four blood samples (two infected and two aseptic cohort) had insufficient library concentration for sequencing, therefore, PAXgene blood sample results are for the remaining 20 patient samples. All 20 PAXgene samples passed post sequencing QC metrics, Table 3-1.

The gene expression data was assessed for sources of bias that could affect the results using partition variance analysis. For the tissue samples, 'status' that is subdivided into aseptic, acute infection or chronic infection, had the largest effect on the results followed by joint location which given the anatomical and surgical differences in hip, knee and shoulder arthroplasty was not unexpected. Patient age and sex had minimal affects and therefore the data was not adjusted prior to analysis. Variance partition analysis of the blood results showed that age and sex had the biggest effect on results. This result was expected given previous research has demonstrated the effects of age and sex on gene expression results (Bongen et al., 2019), data was therefore not adjusted for these variables. Bacterial strain had an increased effect on results than status, in contrast to the FFPE tissue results and highlights an area where blood analysis may be used in this clinical scenario Figure 3-3.

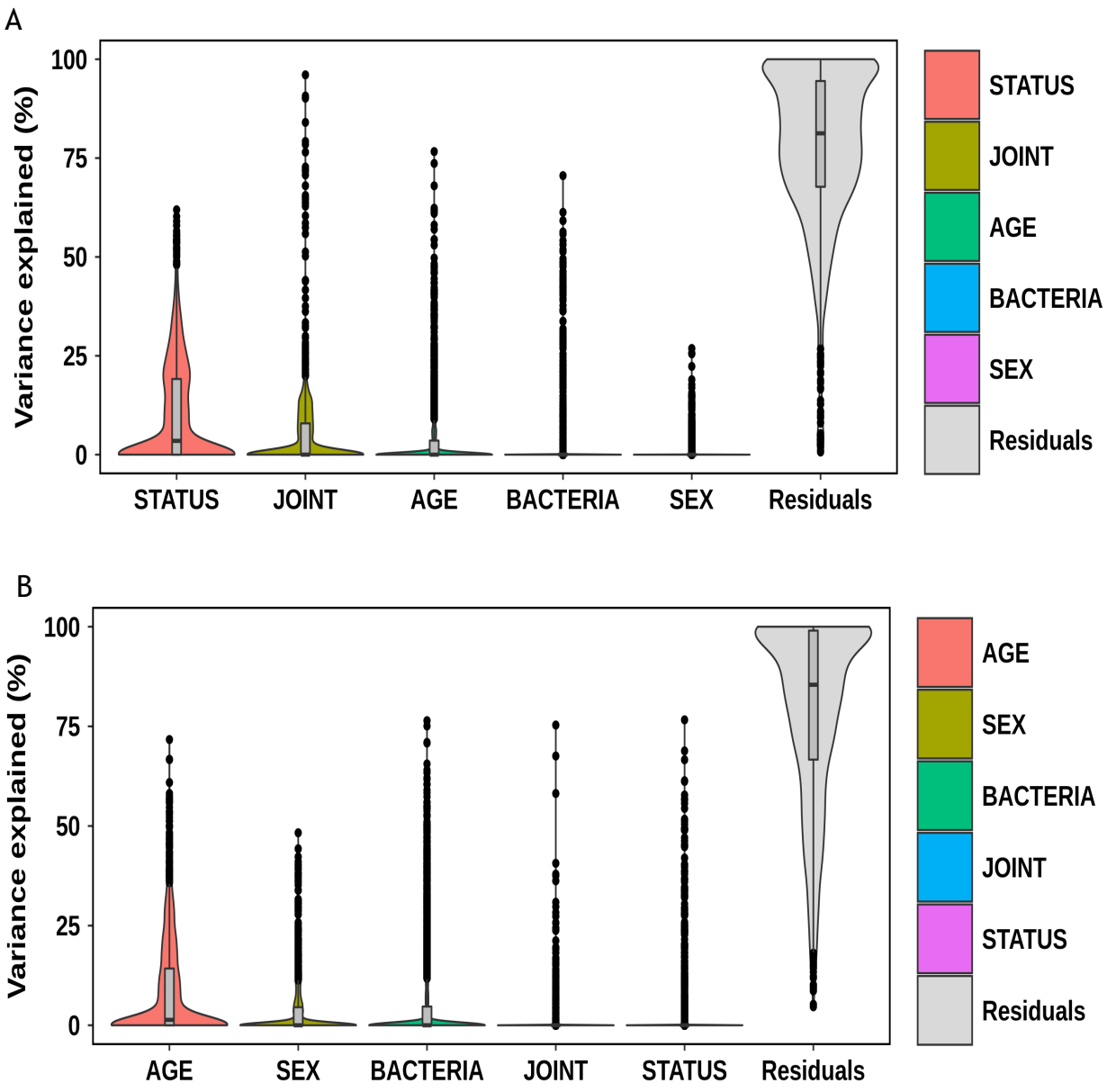

Figure 3-3 Variance partition analysis
Graphs showing the percentage of variance attributable to each factor: Age by decade, sex, bacterial strain, anatomical joint and status – acute infection, chronic infection or aseptic control for (**A**) FFPE joint tissue and (**B**) PAXgene® blood samples. Tissue shows that status - acute/chronic infection or aseptic - has the biggest effect on the results. PAXgene® blood results are more affected by age of patient.

3.4.3 FFPE Tissue sequencing: PJI vs aseptic

The comparison of aseptic vs. PJI tissue gene expression, initially using Principle Component Analysis (PCA) showed that aseptic samples were clustering separately to infected tissue Figure 3-4A. Aseptic samples in PC1 vs PC2 cluster to the left of the graph and centrally in PC3 vs PC4. The PJI samples separated and dispersed form the centre on PC3 vs PC4 in contrast to the aseptic samples and showed a separate cluster to the left of midline on PC1 vs PC2, corresponding to a potential sub group within PJI Figure 3-4A. Differential expression analysis (threshold adj. $p<0.05$ and absolute log2fold-change of >1) identified 65 genes differentially expressed between aseptic and PJI tissue. Of these 44, were significantly up-regulated and 21 significantly down regulated in PJI Figure 3-4B. Hierarchical clustering of these significantly differentially expressed genes showed the groupings which defined aseptic and PJI groups Figure 3-4C. Although the heatmap demonstrated clear clustering of the two groups, this was not uniform across all samples within a group, particularly in the PJI group, where there was a number of high expressers, shown in red. We hypothesised that this could relate to the findings from the PCA plots Figure 3-4A, that there were subdivisions of the PJI cohort. It was important to establish that the significantly differentially expressed genes in the PJI cohort vs the aseptic cohort were biologically relevant. Illustrated in Figure 3-5A, the significant genes belonged to gene sets involved in 'Cell chemotaxis' and 'Response to a molecule of bacterial origin'. A breakdown of the significant genes involved in each of these pathways is shown in Figure 3-5B. Further analysis of the significantly up-regulated genes was carried out using Area Under the Curve/Receiver Operating Characteristic curve (AUC/ROC), to establish the performance of the immune gene panel in distinguishing PJI versus aseptic. Figure 3-5C shows the AUC/POC values when all significantly differentially expressed genes between aseptic and PJI on the panel were included. This shows at a specificity of 100%, sensitivity was 85%. A machine learning algorithm was then used to identify a smaller panel of key genes which could allow clinical application, whilst optimising sensitivity and specificity. Figure 3-5D shows the results from this algorithm that identified a 4 gene panel: G0S2, CXCL5, NR1D2 and DBP, giving a specificity value of 100% and sensitivity of 82%.

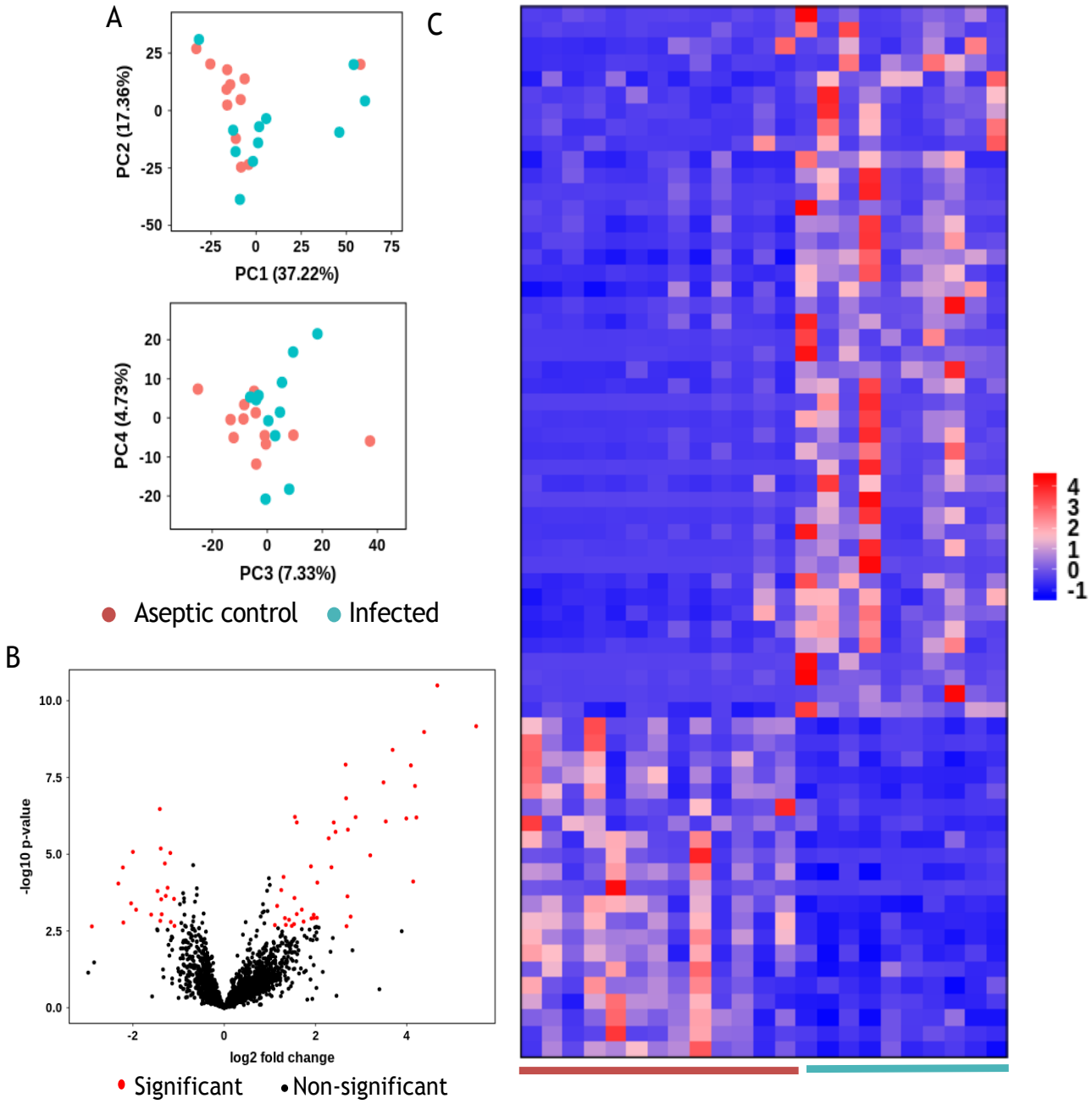

Figure 3-4 Comparison of the gene expression between aseptic control and infected FFPE tissue

(A) Gene expression data Principle component analysis (PCA) scatterplots showing PC1 vs PC2 and PC3 vs PC4. The percentage of variation explained by each component is given in the x and y-axis. **(B)** Volcano plot showing a comparison of gene expression between aseptic control and infected tissue. Significantly differential genes (adj $p<0.05$, absolute log2 fold change>1) are shown in red, non-significant genes shown in black. A positive fold change indicates up regulation in infected n=44, a negative fold change indicates down regulated in infected n=21. **(C)** Hierarchically clustered heatmap of significantly differentially expressed genes (adj, $p<0.05$, absolute log2fold >0.0) between infected and aseptic control tissue samples. Aseptic samples indicated by the red bar, infected samples by the blue bar. Colour intensity represents expression level; blue represents low expression, red high expression.

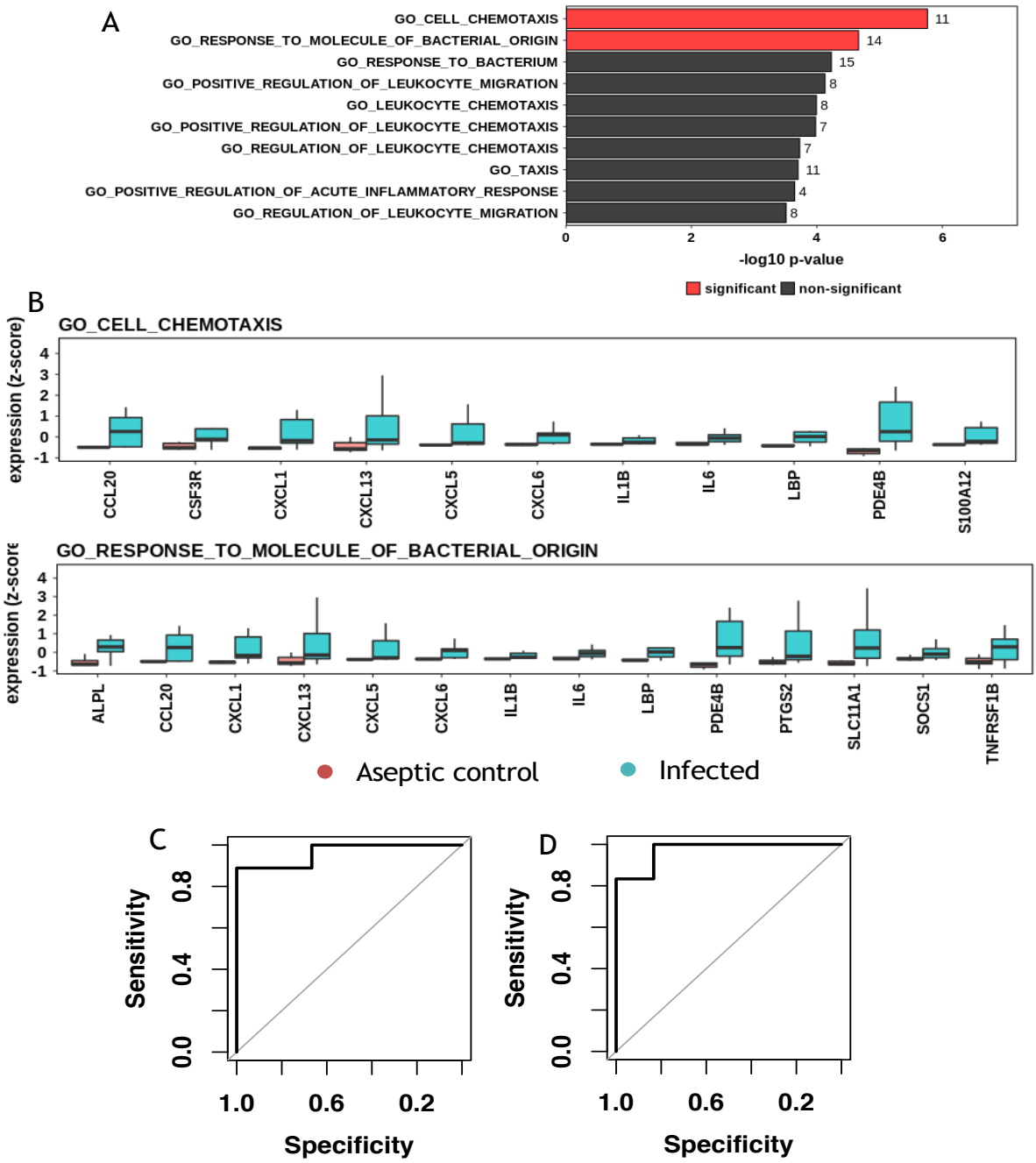

Figure 3-5 Enriched gene sets infected versus aseptic control FFPE tissue
(A) Summary bar chart showing the 10 most enriched gene sets for the significantly up regulated genes (adj p<0.05, absolute log2 fold change>1) in infected versus aseptic control tissue. The x axis shows the –log10 enrichment p value, gene set name on the y-axis. Significantly enriched gene sets are shown in red, with the number denoting how many genes in that set are significantly expressed. **(B)** Summary box plots of the two significantly differentially expressed gene sets in infected tissue. The x-axis denotes the gene, the y axis plots expression values scaled into per gene z-scores. Gene set database GO BP. **(C)** Area Under the Curve/Receiver Operator Characteristic curve (AUC/ROC) for all significantly differentially expressed genes in tissue between aseptic and PJI. **(D)** AUC/ROC curve developed with machine learning algorithm to generate specific 4-gene panel.

3.4.4 Blood sequencing: PJI vs aseptic

The blood sequencing results from the aseptic and PJI cohorts show a less clear distinction between groups. Using PCA, PC1 vs PC2 shows no clear clustering of aseptic vs PJI, however in PC3 vs PC4 there was evidence of central clustering of aseptic samples Figure 3-6A. Differential expression analysis (threshold adj. $p<0.05$ and absolute log2fold-change of >1) identified 17 significant genes, 6 significantly up-regulated in the PJI cohort Figure 3-6B & Figure 3-6C. Hierarchical clustering of these significantly differentially expressed genes does not show clear gene groupings, as seen with FFPE tissue, with the PJI cohort results driven by two high expressing samples Figure 3-6D. Of the six significantly up-regulated genes in the PJI cohort, three of these *ELANE*, *DEFA4* and *DEFA_FAMILY* are linked to Alpha defensin.

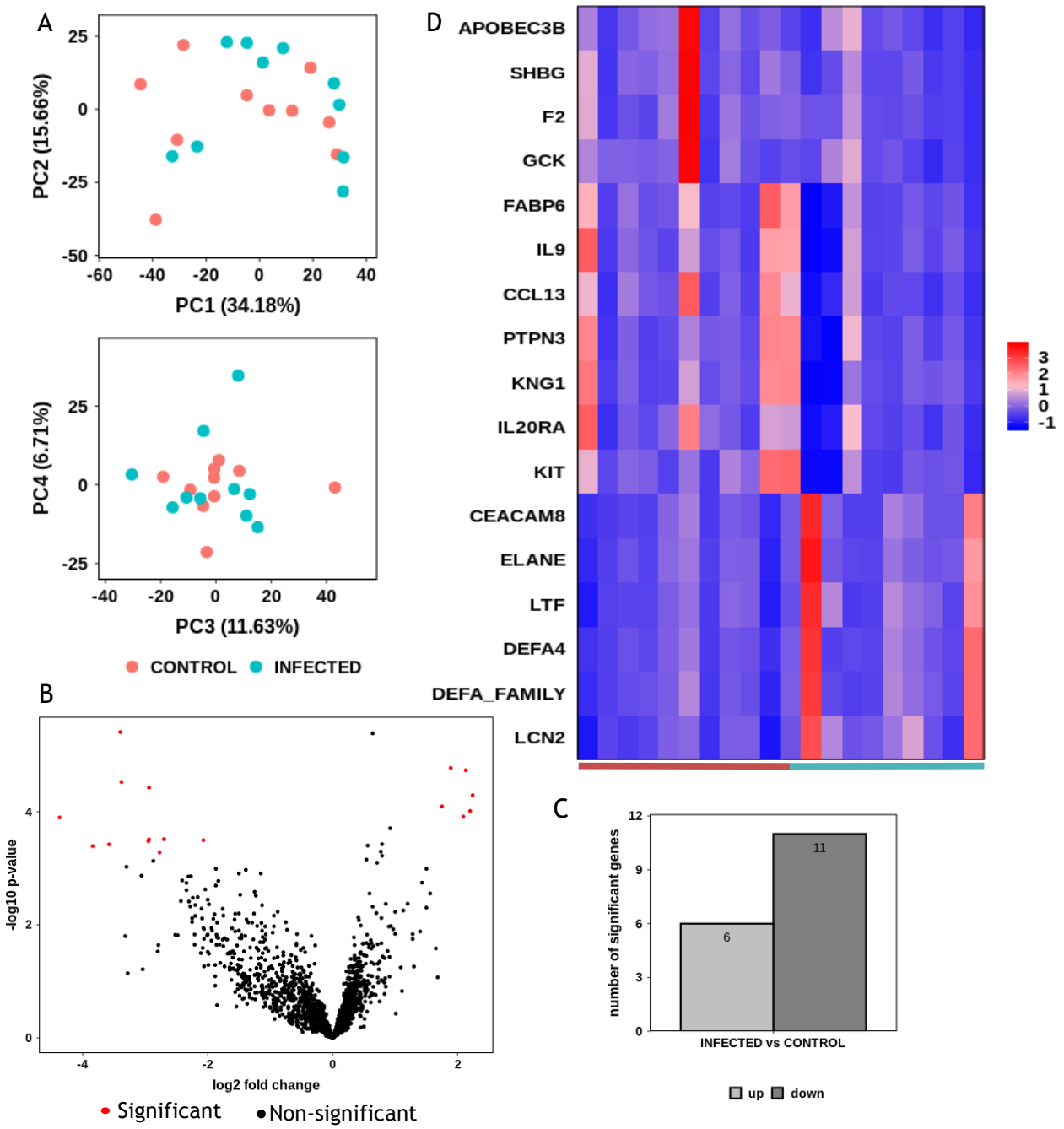

Figure 3-6 Comparison of the gene expression in blood from aseptic control and infected cases

(A) Gene expression data Principle component analysis (PCA) scatterplots showing PC1 vs PC2 and PC3 vs PC4. The percentage of variation explained by each component is given in the x and y-axis. **(B)** Volcano plot showing a comparison of gene expression between aseptic control and infected blood samples. Significantly differential genes (adj p<0.05, absolute log2 fold change>1) are shown in red, non-significant genes shown in black. A positive fold change indicates up regulation in infected. **(C)** Bar chart showing the number of significantly differentially expressed genes (p.adj < 0.05, absolute log2 fold > 1) in blood between infected and aseptic. **(D)** Heatmap of significantly differentially expressed genes (adj, p<0.05, absolute log2fold >0.0) between infected and aseptic control blood samples. Aseptic samples indicated by the red bar, infected samples by the blue bar. Colour intensity represents expression level; blue represents low expression, red high expression.

3.4.5 FFPE Tissue sequencing: Acute vs chronic PJI

Previously described clustering of the PJI results on PCA raised the hypothesis that the immune signature from tissue could distinguish sub-groups of a PJI cohort. Using the 2014 MSIS criteria (Javad Parvizi & Gehrke, 2014) the PJI cohort was divided into acute N=6 and chronic N=5 infection based on available clinical data Table 3-2. Comparing acute with chronic PJI via PCA plots showed on PC1 vs PC2 analysis that these two groups were clustering separately Figure 3-7A. Differential expression analysis (threshold adj. $P<0.05$ and absolute log2fold-change of >1) identified 45 significant genes, 28 significantly up-regulated and 17 significantly down regulated in acute infection Figure 3-7B. Hierarchical clustering of these significantly differentially expressed genes, showed how they can separate the two infection cohorts Figure 3-7C. These results suggested an underlying difference in immune signature in tissue from acutely infected and chronically infected tissue.

To further evaluate this finding the aseptic cohort was included, to look for patterns of gene expression between the 3 groups. The PCA plots showed that chronic infection had a tendency to cluster with aseptic control; PC1 vs PC2 to the left side of the plot, PC3 vs PC4 centrally Figure 3-8A. Differential expression analysis (threshold adj. $p<0.05$ and absolute log2fold-change of >1) evaluated the number of significant genes between the three groups; acute vs aseptic comparison 407 significant genes, acute vs chronic 45 significant genes and chronic vs aseptic 7 significant genes Figure 3-8B. Evaluation of the overall pattern of expression from the tissue using gene signatures showed that signature 1 identified a pattern of expression similar between the aseptic and chronically infected tissue Figure 3-8C and that associated gene sets, which identify biological activity related to these genes, did not fit clinically with response to infection Figure 3-8D. Signature 2, a pattern expressed by acutely infected tissue, Figure 3-8E, showed significantly enriched gene sets that were consistent with response to infection, ‘Response to bacterium’, ‘Response to a molecule of bacterial origin’ and ‘Defence response to other organism’, Figure 3-8F. These findings suggest that the overall gene expression of the PJI cohort was largely driven by the acutely infected tissue samples. We can also infer that chronically

infected tissue had a gene signature that trended towards aseptic tissue and did not induce an immune response consistent with a response to bacterial infection.

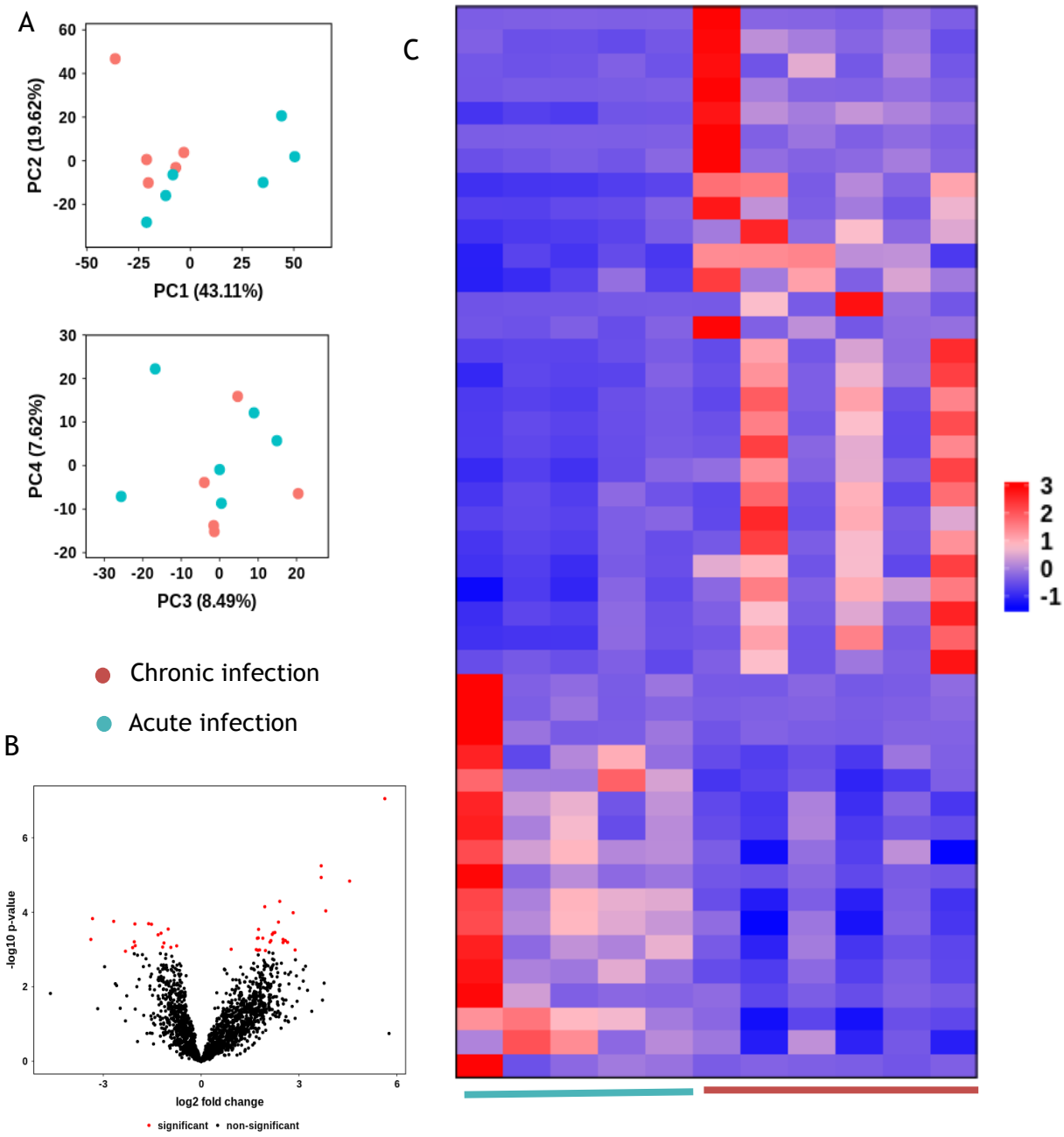

Figure 3-7 Comparison of the gene expression in synovial tissue between acute and chronic infection

(A) Gene expression data Principle component analysis (PCA) scatterplots showing PC1 vs PC2 and PC3 vs PC4. The percentage of variation explained by each component is given in the x and y-axis. **(B)** Volcano plot showing a comparison of gene expression between acute and chronically infected tissue. Significantly differential genes (adj p<0.05, absolute log2 fold change>1) are shown in red, non-significant genes shown in black. A positive fold change indicates up regulation in acute infection N=28, a negative fold change indicates down regulation in acute infection N=17. **(C)** Hierarchically clustered heatmap of significantly differentially expressed genes (adj, p<0.05, absolute log2fold >0.0) between acute and chronic infection. Acute infection shown by the red bar, chronic infection blue bar, significant genes on the y axis. Colour intensity represents expression level; blue represents low expression, red high expression.

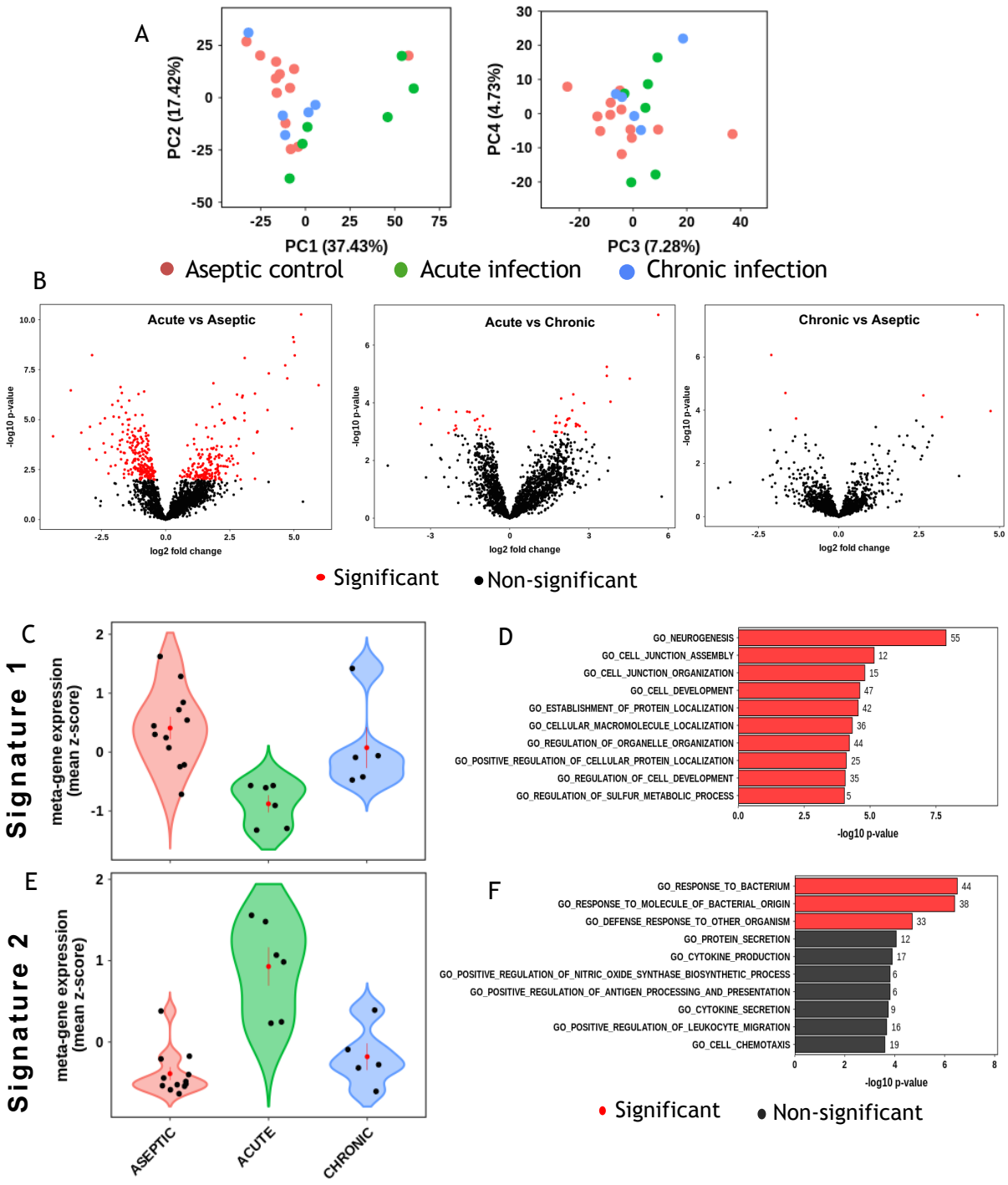

Figure 3-8 Comparison of gene expression in aseptic control, acute and chronically infected FFPE tissue

(A) Gene expression data principal component analysis (PCA) scatterplots showing PC1 vs PC2 and PC3 vs PC4. The percentage of variation explained by each component is given in the x and y-axis. **(B)** Volcano plots showing the comparison of gene expression in acute vs aseptic, acute vs chronic, chronic vs aseptic. Significantly differential genes (adj p<0.05, absolute log2 fold change>1) are shown in red, non-significant genes shown in black. A positive fold change indicates up regulation. **(C)** Violin plot showing the pattern of expression for signature 1 across the 3 sample groups: aseptic and acute and chronic infection shown on the x-axis with mean gene expression value for the signature on the y-axis. **(D)** Summary bar chart showing the 10 most enriched gene sets for Signature 1. Significantly up regulated gene sets (adj P<0.05, absolute log2fold change <1) shown in red. Signature 1 indicates biological similarity between aseptic and chronic infection. **(E)** Violin plot and **(F)** Summary bar chart showing the pattern of expression for Signature 2 which demonstrated biological difference in acute infection.

3.4.6 Blood sequencing: Acute vs chronic PJI

Analysis of the gene expression from aseptic vs PJI cohort had previously shown no clear separation in the groups Figure 3-6, identifying only 17 significantly differentially expressed genes. Further sub-analysis of this PJI cohort was therefore not carried out.

3.4.7 FFPE tissue sequencing: Bacterial strain

Tissue samples were annotated by bacterial strain as per hospital microbiology data. From published literature, around 50% of PJI cases are caused by *S.aureus* including coagulase negative staphylococcus. The remaining infections are caused by polymicrobial, *Streptococcal* or low virulence anaerobic bacteria, with a much broader range of pathogens than seen with native joint septic arthritis (Tande & Patel, 2014). In this study *Staphylococcal* (n=4) and *Streptococcal* (n=5) were the most common bacteria, there were other (n=2) bacteria present, Table 3-1. Analysing gene expression, initially by PCA plots, showed no clear clustering of bacterial groups Figure 3-9A. Focusing on *staphylococcal* and *streptococcal* bacteria again there was no distinct clustering in gene expression on PCA plot in tissue Figure 3-9B. Differential expression analysis (threshold adj. $p<0.05$ and absolute log2fold-change of >1) identified 6 genes with significantly differential expression between staphylococcal and streptococcal cohorts Figure 3-9C. From these results, FFPE tissue immune gene expression did not identify bacterial strain.

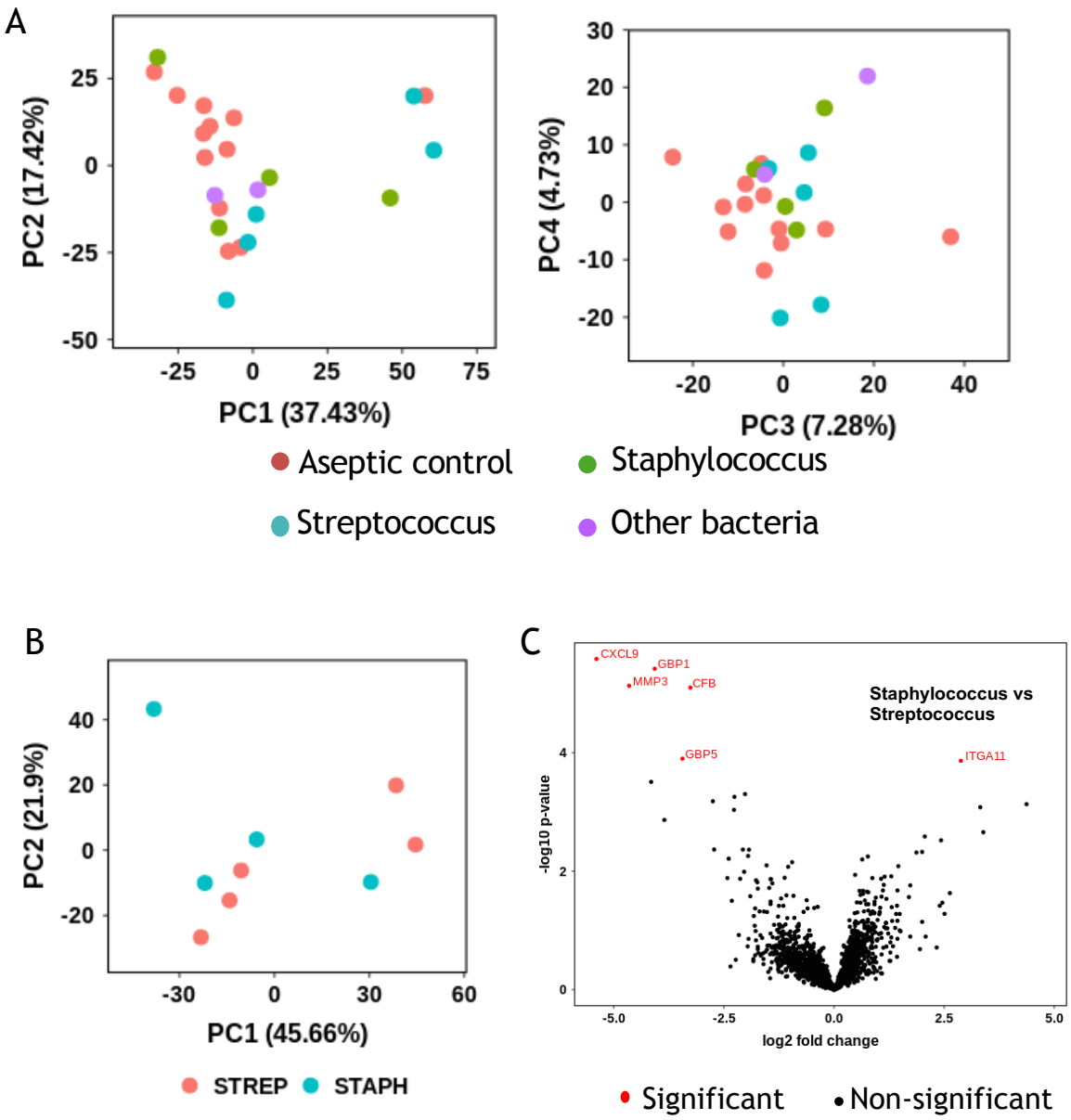

Figure 3-9 Comparison of gene expression in infected FFPE tissue by bacterial strain **(A)** Gene expression PCA scatterplots showing PC1 vs PC2 and PC3 vs PC4 for all samples, annotated by bacteria. The percentage of variation explained by each component is given in the x and y-axis. PC3 vs PC4 shows aseptic samples cluster centrally. **(B)** Gene expression PCA scatterplot showing PC1 vs PC2 for tissues samples positive for Staphylococcal n=4 and Streptococcal n=5. **(C)** Volcano plot showing the comparison of gene expression in infected tissue samples Staphylococcal vs Streptococcal. Genes are represented by dots. Significantly differential genes (adj p<0.05, absolute log2 fold change >0.0) are shown by red dots, non-significant genes are shown in black, a positive fold change represents significantly increased expression in staphylococcal.

3.4.8 Blood sequencing: Bacterial strain

Blood samples were annotated by bacterial strain using the same method as FFPE tissue. PCA analysis of staphylococcal vs streptococcal showed separation of these two groups on PC1 vs PC2, suggesting an underling difference in gene expression Figure 3-10A. Differential expression analysis (threshold adj. $p<0.05$ and absolute log2fold-change of >1) identified 98 significant genes, 55 of which were significantly up-regulated and 43 of which were significantly down regulated in *Staphylococcal* infection Figure 3-10B & Figure 3-10C. Hierarchical clustering of these significantly differentially expressed genes showed delineation into two groups displayed on the heatmap Figure 3-10D. The most significantly up-regulated genes seen with *Staphylococcal* infection CD8A and CD8B are involved in the T cell immune response, with *Streptococcal* infection, Toll like receptor 5 (TLR5) was the most significantly up-regulated gene, this is involved in recognising bacterial pathogens and activating the immune response, Figure 3-10E.

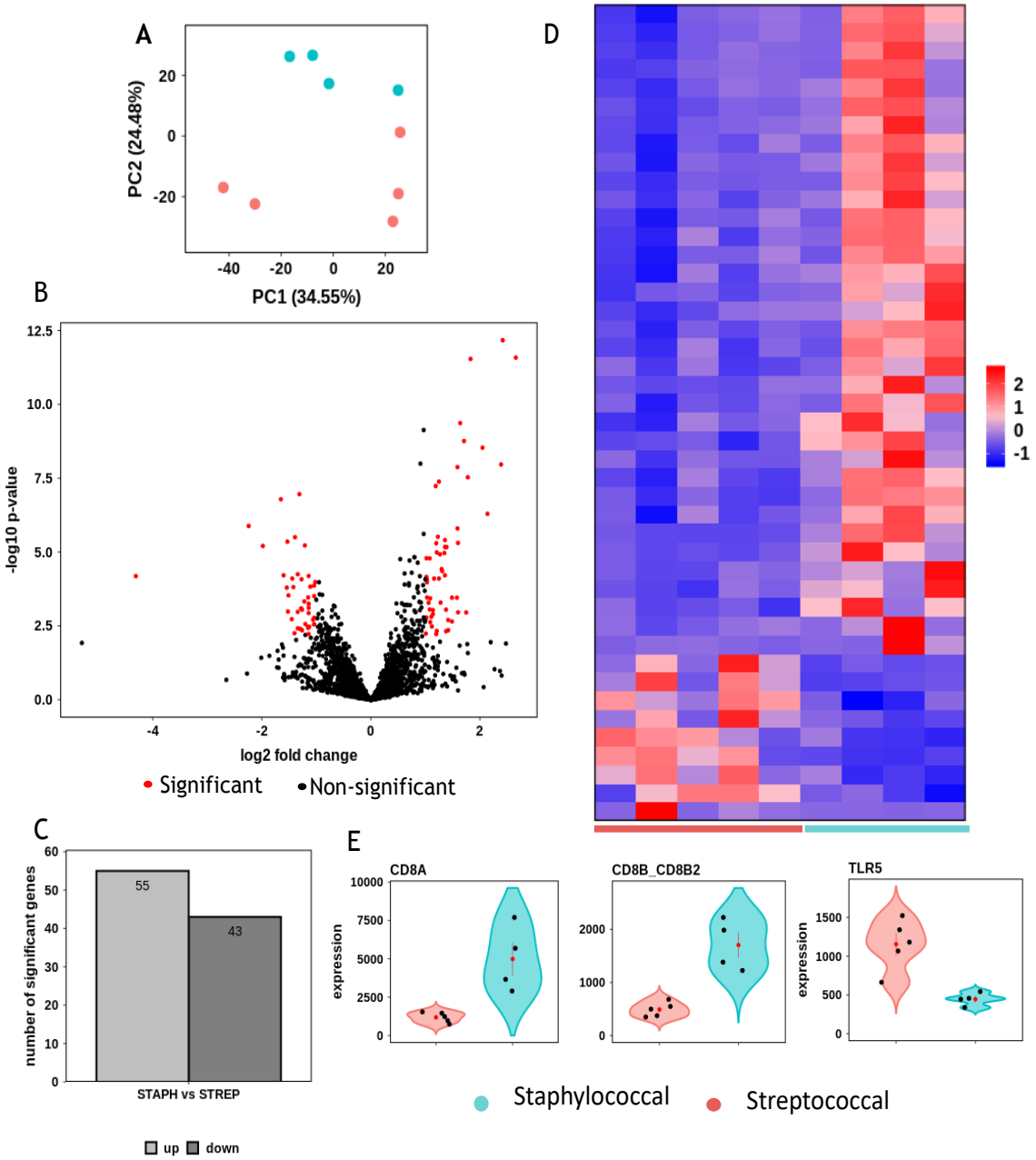

Figure 3-10 PAXgene blood staphylococcal vs streptococcal gene expression analysis (**A**) Gene expression PCA scatter plot showing PC1 vs PC2 and PC3 vs PC4. The percentage of variation explained by each component is given in the x and y-axis. PC3 vs PC4 shows central clustering of aseptic control samples. (**B**) Volcano plot showing a comparison of gene expression between staphylococcal n=4 and streptococcal n=5 infected blood samples. Significantly differential genes (adj p<0.05, absolute log2 fold change>1) are shown in red, non-significant genes shown in black. A positive fold change indicates up regulation in staphylococcal. (**C**) Bar chart showing the number of significantly differentially expressed genes (p.adj < 0.05, absolute log2 fold > 1), between staphylococcal and streptococcal. Up-regulated genes are higher in staphylococcal. (D) Heatmap of significantly differentially expressed genes (adj, p<0.05, absolute log2fold >0.0) between staphylococcal (blue bar) and streptococcal (red bar). Colour intensity represents expression level; blue represents low expression, red high expression. (**E**) Violin plots showing the most significantly up-regulated genes in staphylococcal and streptococcal infection. Group on the x-axis, gene expression on the y-axis.

3.5 **Discussion**

Research in the field of PJI has developed an understanding of biofilm biology and the immune reaction to implants, leading to the development of 'biomarkers' for use in PJI diagnostics. This work reports the first use of a novel molecular technology to sequence FFPE tissue and blood, harnessing this technology to further characterise the immune gene expression changes seen in PJI and aseptic revision arthroplasty to identify immune markers for infection.

The sequencing method, as described in methods section 2.7.4 and 2.7.5, uses NGS techniques. NGS techniques allow high through-put whole genome sequencing and are increasingly being used in PJI research, showing high levels of concordance with traditional culture methods and positive results in situations of culture negative PJI (Chen et al., 2019; Sanderson et al., 2017; Street et al., 2017; Tarabichi et al., 2018; Thoendel et al., 2018). It has also been used in other areas of medicine where pathogen identification is challenging yet crucial including culture negative meningitis and infective endocarditis (Cheng et al., 2018; Wilson et al., 2014). NGS research has noted the issue of host DNA contamination, despite steps in the method to eliminate this. In this pilot study, NGS was instead used to target the host, and sequence genes involved in the immune response to infection.

This pilot study consisted of a cohort of 24 patients, sequencing data was available for 23 of the 24 tissue samples (96%) and 20 of the 24 blood samples (83.4%). Within the cohort, there were no significant differences between PJI and aseptic groups in male to female ratio or patient age. Twenty-two of the samples came from hip or knee revision surgery, with two from shoulder revision arthroplasty. This represents clinical practice, as hip and knee surgery is more frequent. The CRP and WCC values were significantly higher in the PJI group vs the aseptic control group. These are both markers of infection and are standard clinical investigations included in all diagnostic algorithms for PJI. As this was a pilot study of a new technology it was important to have distinction in known markers for the PJI and aseptic cohorts. All PJI tissue samples were culture positive, despite this, two samples had low CRP values (3, 15) and five samples had low/normal WCC's that overlapped with values in the aseptic control group Figure 3-2. Previous studies have shown that these markers alone cannot

diagnose PJI (Akgün et al., 2018; McNally et al., 2020; Pérez-Prieto et al., 2017). Staphylococcus aureus is the most common pathogen associated with PJI however, in this infection cohort it was represented by 1 out of the 12 PJI samples. Furthermore, all samples in the infection cohort were positive for one genus of bacteria, previous literature has noted the increased incidence of polymicrobial infection in PJI. These findings may limit the conclusions of this pilot cohort. Two of the cases in the aseptic cohort had one positive sample on extended culture, deemed to be a contaminant and associated with normal CRP and WCC values. Possible sources of contamination include time of biopsy with skin or soft tissues, on transfer to the hospital laboratory and during analysis. Standardised protocols for surgical sampling and laboratory analysis are in place to try and limit these events, including the cautious reporting of one positive sample and the need for clinical correlation (Drago et al., 2019). In this scenario, both cases were treated clinically as aseptic and during 3 months follow up did not represent with infection. Furthermore, pre-operative antibiotics, if they were given, would have initiated treatment of the bacterial infection, and may potentially have affected the results. In this clinical scenario they are more likely to have been prescribed pre-hospital to patients with acute PJI infection, displaying classical symptoms of joint swelling, acute pain and erythema. The sequencing cohort were evaluated and with the available electronic clinical data, no patient received antibiotics in the 6 weeks prior to surgery.

Sequencing results from the FFPE tissue samples showed evidence of clustering into two separate groups, on PCA plot Figure 3-4S (PC3 vs PC4), aseptic samples clustered centrally, with PJI samples scattered out from midline. This demonstrated an initial proof of concept showing that there are global differences in immune gene expression between aseptic and PJI tissue, despite an implant being involved in both conditions, and, that this sequencing technology was able to detect that difference. There were 65/2002 genes significantly differentially expressed between the PJI and aseptic cohort, which belonged to clinically relevant pathways involved in cell chemotaxis and the immune response to a bacterium Figure 3-5. This initially seemed a low number, however, as noted earlier, an immune response was expected in both cohorts due to implant material. The specific genes involved in pathways up-regulated

in PJI are primarily involved in neutrophil chemotaxis and differentiation (*CXCL1, CXCL5, CXCL6, CCL20*, S100A12, CSF3R) along with bacterial cell membrane recognition (*LBP*). A previously published study analysed tissue from PJI to evaluate an immune signature, using PCR techniques and machine-learning. A 'test' cohort of samples was used to generate a 3-gene target of *DEFA1-LTF-IL1B* that identified a PJI diagnosis with an Area Under the Curve value of 97.6%. This gene combination was then validated in a new cohort of 10 samples, with a 100% concordance rate with microbiology results in the validation group (Fillerova et al., 2017). These findings are similar to our results, which identified acute neutrophil immune genes in the PJI cohort. In this study, the initial test cohort was much larger with 76 patients, N=38 PJI based on tissue microbiology and histology; the 3-gene target demonstrated 86% concordance with standard microbiology culture results, lower than the smaller validation group. The larger cohort is likely to have captured a broader time frame of infections – from acute to chronic, that may have different underlying immune signatures. A further study used tissue from revision arthroplasty and PCR techniques to evaluate the utility of Toll like receptors (TLR's) as immune biomarkers for PJI. TLR's are transmembrane receptors expressed on a variety of human cell lines, they recognise pathogens, including bacteria and viruses, and activate the immune response. This study looked specifically at TLR1 and TLR6 as these recognise bacterial lipoproteins. At optimal threshold of 0.0097, TLR 1 had sensitivity, specificity and AUC values of 95.2%, 100% and 0.995 respectively (Cipriano et al., 2014). This again links with genes found from the sequencing reported in this work, *LBP* - lipopolysaccharide-binding protein, binds to bacterial produced lipopolysaccharide and signals via TLR's to activate the immune response. TLRs can be up-regulated in periprosthetic tissue from both PJI and cases of aseptic loosening (Tamaki et al., 2009). Evaluation of TLR1 from a subsequent tissue PCR study concluded it was not a marker to classify PJI from aseptic with a specificity value of 66.6% (Fillerova et al., 2017). Therefore, *LBP* may be a more specific marker to bacterial infection than *TLR1*.

Interleukin- 6 was also identified in tissue sequencing pathway analysis, a biomarker that has been extensively studied in the literature looking at its potential for PJI diagnosis. Published studies have evaluated IL-6 in both serum and synovial fluid. The sensitivity and specificity values vary, in serum they

range from 12%-100 for sensitivity and 58%-97% for specificity. For synovial fluid the results for sensitivity range from 48.6%-89% and for specificity from 85.5%-97.6%, see Appendix A Table 6-1. Here we show that IL-6 gene expression changes are present and significantly elevated in PJI tissue (aseptic 796.6 ± 174.8 vs PJI 5233 ± 2862, mean ± SEM, normalised read count, p=0.0045). These results concur with the findings of elevated IL-6 in synovial fluid, which like tissue, is local to the implant and infection. Results from the blood sequencing show a trend towards higher IL-6 gene expression in PJI vs aseptic, however this is not significant. This result does not concur with previously published literature reporting serum IL6 protein higher in PJI (Bottner et al., 2007; Cesare et al., 2005; Ettinger et al., 2015; Gallo et al., 2018; Majors & Jagadale, 2019; T. Worthington et al., 2010), see Appendix A Table 6-1for serum sensitivities and specificities. One case in the aseptic cohort with a previously noted 1/5 tissue contaminant positive culture correlated with a high IL-6 gene expression level. A further case in PJI group received 2 days of antibiotics prior to positive microbiology samples, this case correlated with a low IL-6 gene expression level. Levels of IL-6 return to normal faster that other inflammatory markers, including CRP, therefore these two outliers may have introduced bias to this small cohort. Poor performance of serum IL-6 has previously been noted in low-grade infection, with sensitivity only 12% (Grosso et al., 2014). In this current study cohort four of the PJI cases were annotated as chronic infection, although this did not affect the FFPE tissue results, it may have limited the results seen in the PAXgene blood samples. The significantly raised IL-6 gene expression levels seen in tissue correlates with published synovial fluid results, including those evaluating a point of care lateral flow test (Wimmer et al., 2016), suggesting IL-6 may be a viable local biomarker for PJI.

To assess the diagnostic utility of the tissue sequencing, along with sensitivity and specificity of immune gene markers in PJI, Area Under the Curve Receiver Operating Characteristic (ROC) curves were calculated. Incorporating all significantly differentially expressed genes from the 2002 gene panel, resulting in a specificity of 100% and sensitivity of 85% Figure 3-5C. Using machine learning, a specific 4-gene panel was generated (*GOS2, CXCL5, NR1D2, DBP*). Using a smaller panel makes this a more practical and useable diagnostic test in clinical practice Figure 3-5D. As seen in previous work, a combination of genes

is likely to be needed given the high sensitivity of molecular methods and multiple pathway involvement from some genes. The genes used in the panel are involved in cell cycle regulation (G0S2), neutrophil activation chemokine (CXCL5), vitamin D metabolism (DBP) and (NR1D2) which has a role in transcriptional activation of IL-6. Vitamin D has been shown to be involved in the up-regulation of antimicrobial peptides.

Further analysis of tissue sequencing results from the PJI cohort, stratifying into acute and chronic infection groups using the 2014 MSIS criteria (Javad Parvizi & Gehrke, 2014) showed underlying gene expression differences between these groups Figure 3-7 & Figure 3-8. Aseptic controls and chronic infection had an underlying similar gene signature, which did not correspond to that seen with acute infection. Established biofilm, which starts at implantation and forms over 4 weeks, is present with chronic infection and can shield bacteria from the immune system, dampening immune response (Arciola et al., 2018). This may explain our results, finding only 7/2002 genes significantly differentially expressed genes between aseptic control and chronic infection. All of the PJI tissue samples included were microbiology positive as this was a pilot of the sequencing technology, however, in clinical practice culture negative results can be seen in up to 15% of PJI cases (Berbari et al., 2007; Palan et al., 2019), usually when there has been an indolent time course of clinical symptoms or prior antibiotics. Immune mediated markers therefore may be unable to diagnose infection in the setting of chronic or low grade PJI, an issue previously noted in studies evaluating CRP, ESR and IL-6 (Grosso et al., 2014; Piper et al., 2010). Further analysis identified one gene that was unique to chronic infection, *ITGB8*. This gene codes for a membrane protein avβ8 that is present on T cells and is critical for T cell immune regulation during on-going inflammation. Regulatory T cells express high amounts of avβa on their cell surface that allows them to activate TGFβ from its latent form. Activated TGFβ can then supress effector T cells (J. J. Worthington et al., 2015). Our results showed that tissue from chronic PJI had significantly lower *ITGB8* expression, than both acute infection and aseptic controls. This suggests that there may be limited on-going T cell activated inflammation in the tissue from chronic PJI compared with acute infection or aseptic controls. The majority of previous work looking at chronic bacterial infection has focused on mucosal infection – lung and gut. This has

shown that persistence of infection is a balance between the pathogens ability to modify the immune response, as discussed previously with *S.aureus* in PJI biofilm see section 1.8 and the immune regulatory mechanisms (Young et al., 2002). Previous work looking at PJI associated biofilm has suggested that chronicity of infection is driven by an immune suppressed environment, whereby immature myeloid derived suppressor cells (MDSC's) supress T cell immune function (C. E. Heim et al., 2014; Cortney E. Heim et al., 2018; Cortney E. Heim, Vidlak, & Kielian, 2015; Cortney E. Heim, Vidlak, Scherr, et al., 2015). This is an emerging area of research in implant biofilm immunology.

Sequencing results from the PAXgene® blood samples did not allow clear distinction between aseptic control and PJI cohorts. There were N=4 chronic infections in the PJI cohort, with tissue results showing an immune signature at the local level, correlating with aseptic control. For a signature to be identified in the blood, activated immune cells would have to leave the joint and enter the circulation. The number of chronic infections and the limited local response they stimulated may have limited any systemic immune repose in blood. The PJI cohort did show high expression of 3 markers, *ELANE*, *DEFA4* and *DEFA_FAMILY*, all associated with Alpha defensin which is currently included in the 2018 diagnostic algorithm as a synovial fluid test. These results suggest that AD markers can be found in the blood of PJI patients and further work may be warranted in evaluating AD in blood. Gene sequencing results from blood did show separation into two groups when the samples were annotated by bacteria, either *staphylococcal* or *streptococcal* Figure 3-10, suggesting that there is an identifiable difference in immune response to these bacteria. The cohort was too small to allow for other bacteria to be included. Previously published literature has detailed how different gene transcriptional profiles can be identified in blood from healthy individuals compared to patients diagnosed with sepsis secondary to community acquired pneumonia (Severino et al., 2014). The gene signature identified in the 10 patient sepsis cohort was also found to correlate with patient outcomes. The group reported that reduced gene expression of immune mediated markers was seen in the group with worse clinical outcomes (Severino et al., 2014). A further study evaluated blood from paediatric patients who presented to hospital with signs of infection, normal hospital microbiology samples were analysed to identify the pathogen to allow

treatment. Blood from these patients, analysed using a microarray hybridisation technique, identified a 30 gene unique transcriptional signature that differentiated *E.coli* from *S.aureus* infection. This signature was developed on a 20 patient training set and then evaluated on 40 test samples, showing 85% concordance with microbiology culture results (Ramilo et al., 2007). More recent work has come from the field of respiratory medicine, specifically separating bacterial from viral infection, to limit the overuse of antibiotics and attempt to curb antibiotic resistance. Gene transcription profiles from blood, using an RT-PCR platform diagnosed bacterial infection with 88% concordance compared with traditional pathogen based microbiological culture (Lydon et al., 2019). Individual pathogens interact with specific pattern recognition receptors on immune cells, therefore producing an individual immune response, with a unique transcriptional signature. Using this theory, these studies have switched the diagnostic strategy, from pathogen based testing to individual patient immune response. The data presented here is the first time a blood gene signature stratifying *staphylococcal* from *streptococcal* infection in a PJI cohort has been identified. Previously, genus level bacterial information has only been available following microbiology culture, and more recently from molecular methods usually employed in the culture negative setting. This process can take 48-72 hours to prove culture negative and several days for molecular 16s RNA PCR analysis. Further assessment of this finding in a larger cohort may allow earlier identification of the micro-organism from a blood test, in known PJI cases, allowing antibiotic rationalisation.

4 Chapter 4: The molecular effects of vancomycin on the anterior cruciate ligament graft

Content of this chapter has been published in the following manuscript:

Caroline M Atherton, Simon J Spencer, Kathryn McCall, Emma Garcia-Melchor, William J Leach, Michael Mullen, Brian P Rooney, Colin Walker, Prof Iain B McInnes, Neal L Millar and Moeed Akbar

Vancomycin wrap for anterior cruciate ligament surgery: Molecular insights

American Journal of Sports Medicine, January 2021 49(2) 426 - 434

4.1 Introduction

Anterior cruciate ligament reconstruction (ACLR) using patella and hamstring grafts is a routine and successful surgical procedure, with low reported levels of infection (0.14%-1.8%)(Burks et al., 2003b; Indelli et al., 2002; Torres-Claramunt et al., 2013). As with all orthopaedic surgery involving implants or grafts, it is routine to administer prophylactic antibiotics prior to the procedure in order to reduce the risk of infection and septic arthritis, potentially serious complications(Carney et al., 2018). Although, the ideal timing of administration has been debated, it is common practice to administer them prior to skin incision and tourniquet inflation(Bratzler & Houck, 2005; Bryson et al., 2016).

The most common pathogen cultured in synovial fluid following ACLR infection is coagulase negative Staphylococcus species. It is understood to be a contaminant of the graft, from either patient skin or graft preparation, coupled with the foreign body suture material inside the knee joint(Mouzopoulos et al., 2009). This suggests that targeting the graft, as a source of infection, with antimicrobials would be an efficient way to reduce post-operative infection rates.

Vancomycin is a glycopeptide antibiotic originally introduced to treat Methicillin resistant Staphylococcus aureus (MRSA) and coagulase negative Staphylococcal species with proven bactericidal activity. The minimum inhibition concentration required for Staphylococcus aureus is 0.5µg/ml, and ranges from 0.25µg/ml to 2.0µg/ml for other bacteria(Andrews, 2002). It is widely used in many forms in orthopaedic surgery; bone cement in routine arthroplasty, IV infusion to treat prosthetic joint infection and topical powder on spinal surgery wounds with results showing that it reduces infection significantly(Lemans et al., 2019; Nowinski et al., 2012). A number of other surgical specialties utilise antibiotics and antimicrobials either topically on wounds or in solution to immerse and wrap implants prior to surgery, reporting significant reductions in infection(Dhabuwala, 2010; Tarakji et al., 2016; Vander Salm et al., 1989). Cardiothoracic surgery has been at the forefront of this, applying vancomycin powder to sternotomy wounds following results of a seminal paper in 1989(Vander Salm et al., 1989) and now implanting cardiac electronic devices enveloped in a degradable antimicrobial sleeve(Tarakji et al., 2016).

The specific practice of wrapping the donor graft in a vancomycin soaked sterile swab prior to insertion in ACLR surgery has steadily increased since 2012 when the 'vancomycin wrap' was first described(Vertullo et al., 2012). Since then, there have been a number of published studies and reviews which demonstrate significantly reduced post-operative infection rates in ACLR(Figueroa et al., 2019; Jefferies et al., 2019; Pérez-Prieto et al., 2016; Phegan et al., 2016; Vertullo et al., 2012).

The molecular effects of vancomycin on human and animal peri-articular tissues, including tendon has a limited evidence base. Porcine chondrocyte death was significantly increased after exposure to vancomycin at doses of 5mg/ml or higher(Shaw et al., 2018). Human *in vitro* studies have shown vancomycin toxicity to chondrocyte and osteoblast like cells, via a reduction in cell DNA, at doses of 250µg/ml and 125µg/ml for osteoblast and chondrocytes respectively, following 48hours of treatment(Antoci et al., 2007). Two further studies have concluded that vancomycin is not toxic at doses up to 16µg/ml for 36 hours in an *ex vivo* chondrocyte model(Dogan et al., 2016) and up to 1000µg/ml for 72 hours in an *in vitro* osteoblast model(Edin et al., 1996). Porcine tendon models show that vancomycin is effective at eliminating bacterial contamination at 5mg/ml after 20 minutes of soaking, and has no effect on the biomechanical properties at doses up to 10mg/ml(Schüttler et al., 2019). Bovine studies have demonstrated that tendon can act as a reservoir for vancomycin, releasing the antibiotic for up to 24 hours into the joint, changing a source of infection, into an intra-articular prophylactic vehicle(Grayson et al., 2011).

4.2 **Aims & Hypothesis**

The current work aimed to establish whether treatment with vancomycin at 5mg/ml, the clinically used concentration, altered the structural or molecular function of the hamstring graft in anterior cruciate ligament reconstruction using human tendon in *in vitro* and *ex vivo* models. Based on published animal models of the vancomycin wrap (Schüttler et al., 2019), it was hypothesised that vancomycin at 5mg /ml would have no detrimental molecular effects on the tendon graft.

4.3 **Methods**

4.3.1 Cell viability

MTT assay, described in section 2.5 was carried out with vancomycin in both 0.9% saline and RPMI diluents, at 5mg/ml and 10mg/ml concentrations, over a time course of 30, 60 and 120 minutes.

4.3.2 Apoptosis

Induction of apoptotic pathways was analysed in tendon *ex vivo* by qPCR for apoptotic gene expression, method described in section 2.7, by ELISA for cytochrome C and caspase 3 protein quantitation, method described in section 2.6 and by IHC staining for caspase 3, method described in section 2.4. Caspase 3 stained tissue sections were imaged under a light microscope (Olympus, DP22) at x10 and x40 magnification and compared with Isotype controls. Quantification of staining was performed in two stages. Firstly, semi-quantitative staging was performed on 5 random high-powered fields, grading the percentage of positively stained cells in that filed using the Modified Bonar Score: Grade 0, no staining; grade 1,1% to 10% of cells stained positive; grade 2, 10% to 20% of cells stained positive; grade 3, more than 20% of cells stained positive). Secondly, the total number of positive and negatively stained cells in each of the 5 high-powered fields was counted to generate the mean percent positive for stained cells.

4.3.3 Matrix and Inflammation

Changes to tendon matrix and inflammatory profile as a result of vancomycin was examined by qPCR, as described in section 2.7 and ELISA, as described in section 2.6 for inflammatory and matrix gene expression and protein quantitation respectively.

4.3.4 Clinical data

Clinical data on all ACL reconstructions was collected as described in methods section 2.1 with 6-month post-operative follow up to assess for infection, re-operation or graft failure.

4.4 Results

4.4.1 Vancomycin and tenocyte viability

The viability of tenocytes following treatment with vancomycin in RPMI diluent is shown in Figure 4-1. At the clinically used concentration of 5mg/ml, tenocytes show reduced viability at all time points – 30, 60 and 120 minutes, however, this was only significant at the 60 minute time point ($p<0.05$). At the higher concentration of 10mg/ml there is no significant reduction in tenocyte viability. At this higher concentration, the results may be due to saturation, as Figure 4-2 shows the vancomycin crystallised and not all dissolved. No further experiments using the 10mg/ml were conducted as this crystallization may affect results. The MTT assay was also assessed with vancomycin in a 0.9% saline diluent, however, the tenocytes showed cell death with both saline alone and with vancomycin after 30 minutes of treatment Figure 4-2. The pH of these solutions was assessed and is shown in Table 4-1. The acidity of 0.9% saline is thought to have caused the tenocyte cell death.

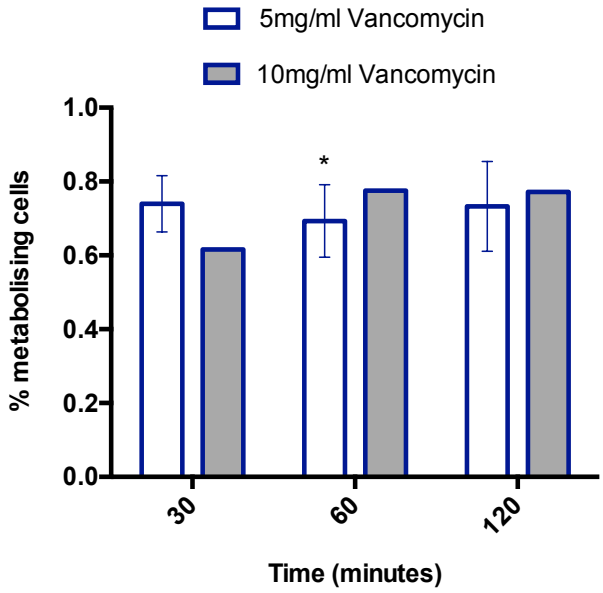

Figure 4-1 MTT assay tenocyte viability
Tenocyte viability following treatment with vancomycin in RPMI at varying concentrations at 30, 60 and 120 minutes. 100% represents untreated control cells. Results are mean ± SEM, 5mg/ml N=6, 10mg/ml N=1; *p<0.05 indicates significance vs untreated control cells, analysis by students t-test.

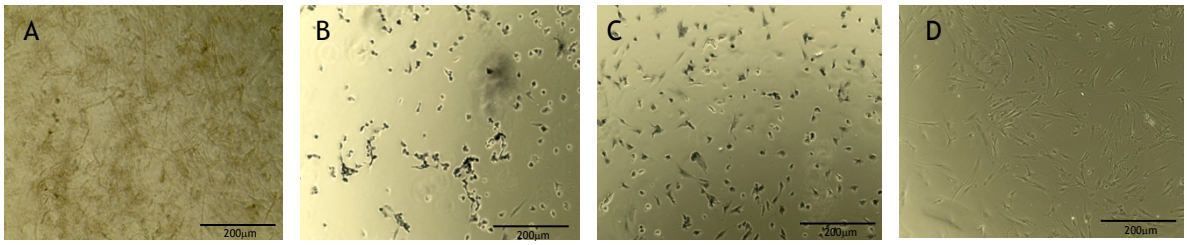

Figure 4-2 Images of treated tenocytes for MTT assay
(A) Vancomycin 10mg/ml in RPMI diluent, showing the crystals that form at the higher dose. (B) Tenocytes treated with 0.9% saline for 30 minutes and (C) Tenocytes treated with vancomycin 5mg/ml in 0.9% saline for 30 minutes, both showing that the cells have died. (D) Tenocytes treated with vancomycin 5mg/ml in RPMI.

Table 4-1 pH of vancomycin in solution
Vancomycin maintains neutral pH in RPMI diluent at 5 and 10mg/ml. Dissolved in acidic 0.9% saline, it reduces the pH further. RPMI = Roswell Park Memorial Institute 1640 Medium. PBS = Phosphate buffered saline

	Vancomcyin mg/ml		
	0	5	10
RPMI	7.5	7.46	7.42
PBS	7.4		
0.9% saline	5.5	3.75	3.63

4.4.2 Vancomycin and tendon apoptosis

The expression of nine apoptotic genes, following vancomycin treatment of tendon explant in RPMI and 0.9% saline diluent is shown in Figure 4-3. Tendon cultured in RPMI and 0.9% saline showed a trend towards increased expression of apoptotic genes when compared with fresh untreated tendon, however this was not significant. There was also no significant difference in apoptotic gene expression seen between tendon cultured in RPMI *vs* 0.9% saline. This finding is important, as RPMI is a laboratory solution used for cell and tissue culture and is not used or available in clinical practice. Furthermore, the data shows that there is no significant difference in apoptotic gene expression between 0.9% saline, the current standard in clinical practice, and vancomycin in 0.9% saline. BAX and AIFM 1 show significant increased expression in vancomycin 0.9% saline compared to RPMI control. BAX is a pro-apoptotic gene which results in cytochrome c release from mitochondria whilst AIFM1 is part of the caspase dependent apoptotic pathway.

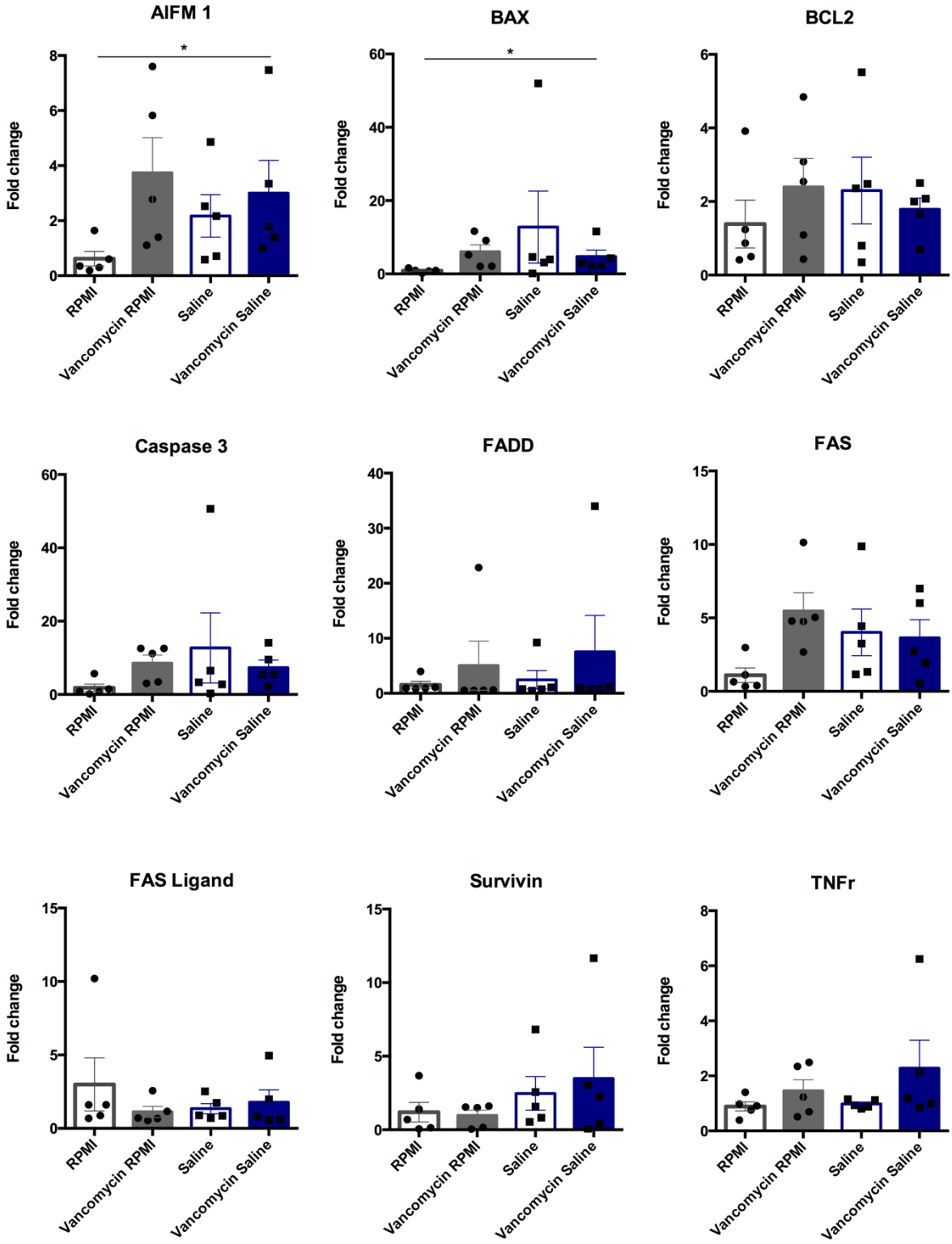

Figure 4-3 Apoptotic gene expression in control and vancomycin treated tendon
Apoptotic gene expression in control and treated tendon explants. AIFM1, BAX, TNFr, caspase 3, FADD, FAS, FAS ligand, survivin, BCL2 gene expression in tendon explant at 16 hours following 1 hour vancomycin treatment. Data are mean ±SEM, normalised to untreated tendon, relative to housekeeping gene, N=5. Analysis via ANOVA on ΔCT values, multiple comparisons: untreated *vs* RPMI, untreated *vs* saline, RPMI *vs* saline, saline *vs* vancomycin saline, RPMI *vs* vancomycin saline.

The effect on apoptosis was further explored by caspase 3 and cytochrome C protein quantitation in treated and control tendon explant tissue and supernatants. Cytochrome C is mitochondrial signalling protein involved in the intrinsic apoptotic pathway (Garrido et al., 2006). Figure 4-4 shows the results of Cytochrome C quantitation in 1-hour and 16-hour supernatants. Saline and vancomycin saline treatment conditions are associated with a trend towards increased protein levels in supernatant, consistent with the BAX gene expression data, however, the results are not significant compared with RPMI control. There was no significant difference between saline alone and following the addition of vancomycin.

Caspase 3, an enzyme common to both intrinsic and extrinsic apoptotic pathways was measured in supernatants by luminescence assay and by immunohistochemistry staining of tendon tissue. Protein levels measured in tendon explant supernatant at 1-hour show reduced levels in both vancomycin treatment conditions compared with RPMI control and 0.9% saline alone. At 16 hours post treatment, caspase 3 protein levels increased in all conditions and there remained a trend towards reduced levels in supernatants from vancomycin saline treated tendon Figure 4-5. At the 1-hour time point, there may have been interference in the assay by vancomycin, as both conditions showed low results. At 16 hours this would not be expected as the vancomycin solution is replaced with RPMI; these results concur with previously presented gene expression data for caspase 3.

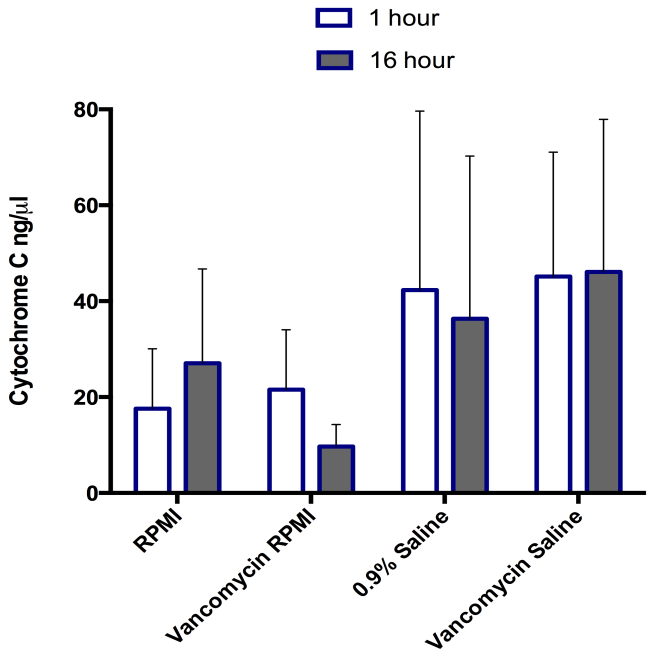

Figure 4-4 Cytochrome C in control and treated tendon supernatants
Tendon treated with vancomycin 5mg/m in RPMI or saline diluent for 1 hour. Cytochrome C measured in 1 hour and 16 hour supernatants. Data are mean ± SEM, N=3. Analysis via ANOVA, multiple comparisons: RPMI *vs* saline, RPMI *vs* vancomycin saline, saline *vs* vancomycin saline.

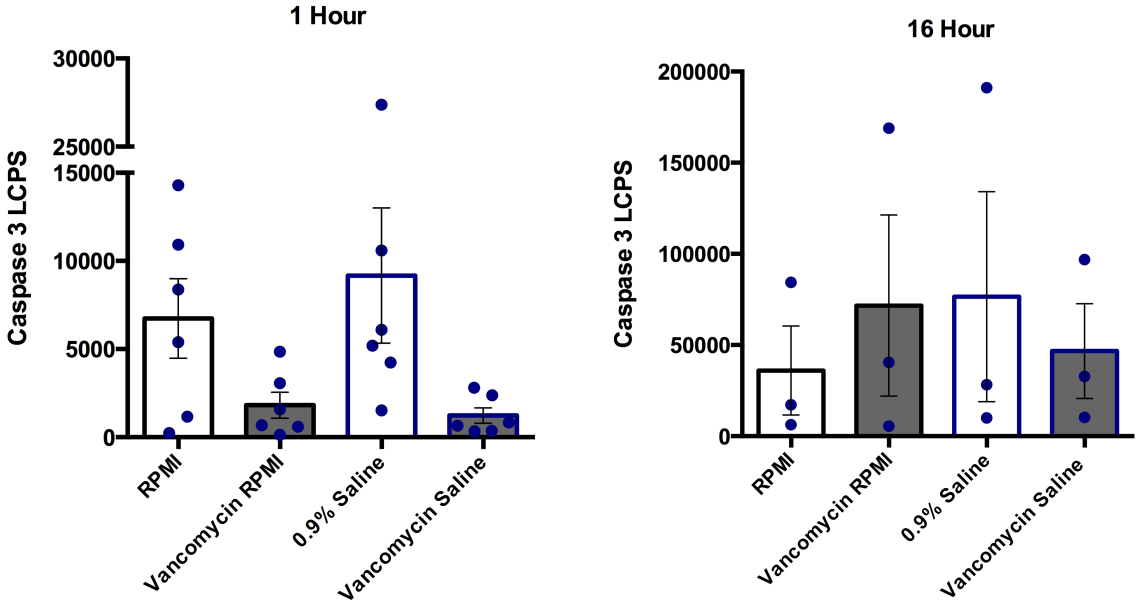

Figure 4-5 Caspase 3 in control and treated tendon supernatants
Tendon treated with vancomycin 5mg/m in RPMI or saline diluent for 1 hour. Caspase 3 measured by luminescence assay in 1-hour and 16-hour supernatants. Data are mean ± SEM, N=6 for 1 hour, N=3 for 16-hour. Analysis via ANOVA, multiple comparisons: RPMI *vs* saline, RPMI *vs* vancomycin saline, saline *vs* vancomycin saline.

Caspase 3 antigen immunohistochemistry staining results are shown in Figure 4-6. The results show that treatment with vancomycin does not cause disruption to the uniform collagen tendon structure, however, it is associated with a trend towards more positive staining for caspase 3 compared with untreated or control tissue in RPMI and 0.9% saline. Images from two different donors are shown in Figure 4-6C and show the variability in clinical samples. Donor 1977 has areas of increased cellularity, vascularity and loss of polarisation of collages fibres across control and treated tendon. These features are in keeping with pre-existing tendinopathy and tendon degeneration(Fearon et al., 2014).

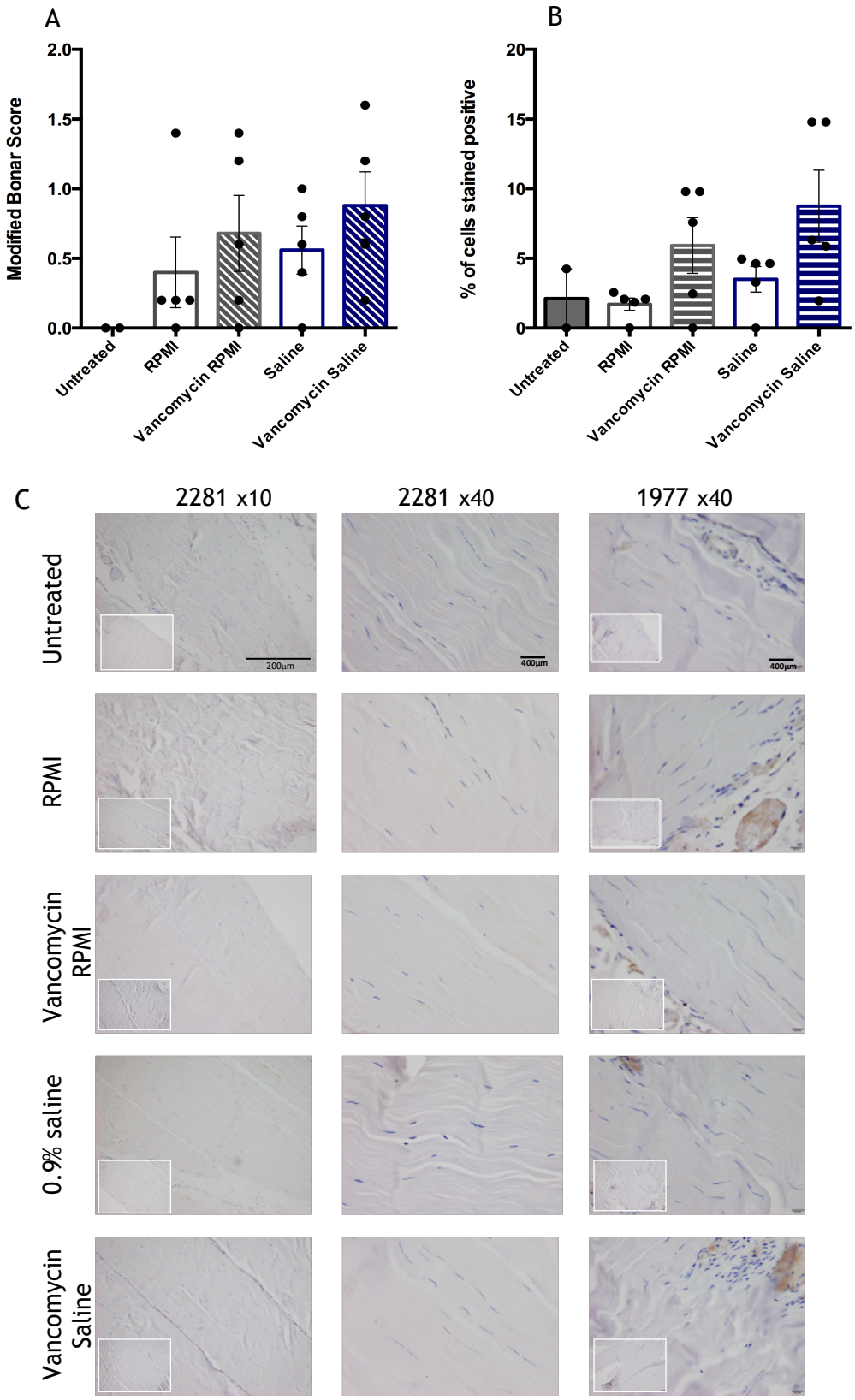

Figure 4-6 Caspase 3 Immunohistochemistry staining of control and treated tendon explant (**A**) Graph illustrating modified Bonar scores from tendon explant tissue stained for cleaved caspase 3, N=5. Modified Bonar score depicts number of positively stained cells per 5 high-powered field (x40) per sample, 0=no staining, 1=1-10%, 2=10-20%, 3>20%, mean +/- SEM, analysis by ANOVA, multiple comparisons: RPMI *vs* saline, RPMI *vs* vancomycin saline, saline *vs* vancomycin saline. (**B**) Quantitative expression of caspase 3, mean % cells positive per treatment condition based on 5 high-power fields, N=5, analysis by ANOVA, multiple comparisons untreated vs RPMI/saline, RPMI *vs* saline, RPMI *vs* vancomycin saline, saline *vs* vancomycin saline. (**C**) Caspase 3 IHC staining of human tendon explant, treated with experimental conditions for 1 hour, isotype rabbit IgG bottom left corner. Two donors represented 2281 and 1977, x10 and x40 magnification.

4.4.3 Vancomycin and tendon matrix

Tendon matrix gene expression results are shown in Figure 4-7. There was no significant difference in RPMI, 0.9% saline or vancomycin treated tendon compared with fresh untreated tendon. Additionally, vancomycin treated tendon showed no significant increase in matrix gene expression compared with the laboratory control RPMI or clinical control 0.9% saline, however, it was associated with a trend towards increased expression of collagen 3α. This protein is associated with tendon damage and may be a reflection of explant model preparation as described in methods, or evidence of pre-existing tendinopathy in clinical samples. Quantitation of collagen 1α in tendon explant supernatants showed a non-significant trend towards reduced protein in saline and vancomycin saline treated tendon.

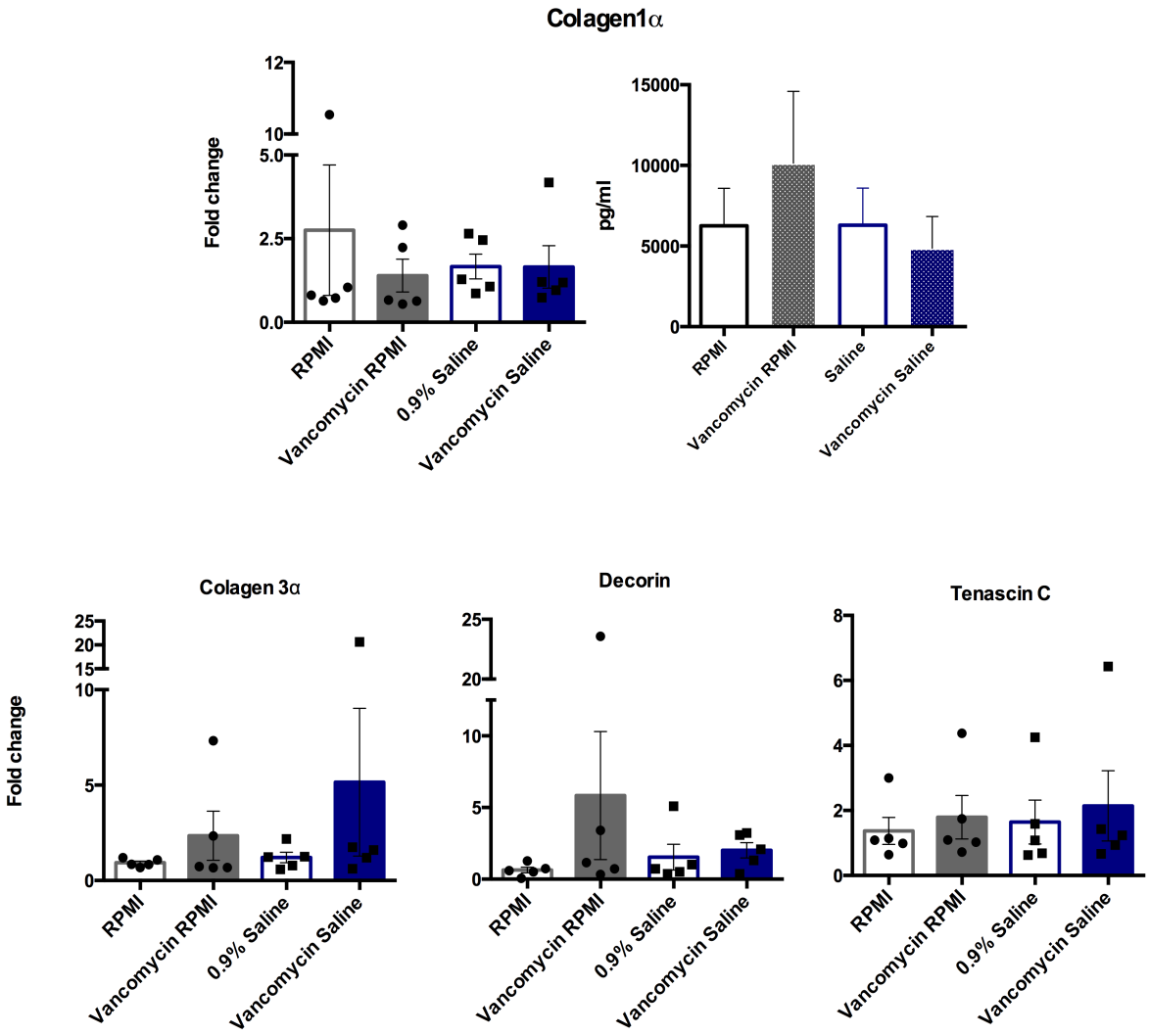

Figure 4-7 Tendon matrix gene and protein expression in control and vancomycin treated tendon

Vancomycin effect on matrix gene and protein expression in tendon. Collagen 1α, Collagen 3α, Decorin and Tenascin C gene expression in tendon explant at 16 hours following 1 hour vancomycin treatment. Data are mean ±SEM, normalised to untreated tendon, relative to housekeeping gene, N=5, analysis by ANOVA, multiple untreated vs RPMI, untreated vs saline, RPMI vs saline, saline vs vancomycin saline, RPMI vs vancomycin saline. Collagen 1α protein measured by quantitative ELISA assay. Tendon treated for 1 hour, incubated for 16 hours, data represent mean ±SEM, N=10. Analysis via ANOVA, multiple comparisons: RPMI vs saline, saline vs vancomycin saline, RPMI vs vancomycin saline.

4.4.4 Vancomycin and tendon inflammation

Tendon inflammatory gene expression and cytokine results are shown in Figure 4-8. There are significant increased gene expression values for IL-6 and MMP3 in RPMI vs untreated tendon and for IL-8 gene expression for saline treated vs untreated tendon. This shows that culturing tendon ex vivo, even in RPMI can lead to an inflammatory profile within the tissue. From multiple comparison analysis, there were no significant increases in tendon inflammatory cytokine gene expression when saline and vancomycin in saline were compared with RPMI. Although not significant, the cytokine data demonstrate a consistent trend towards reduced inflammatory protein release with vancomycin in saline treatment compared with both saline alone and vancomycin in RPMI diluent.

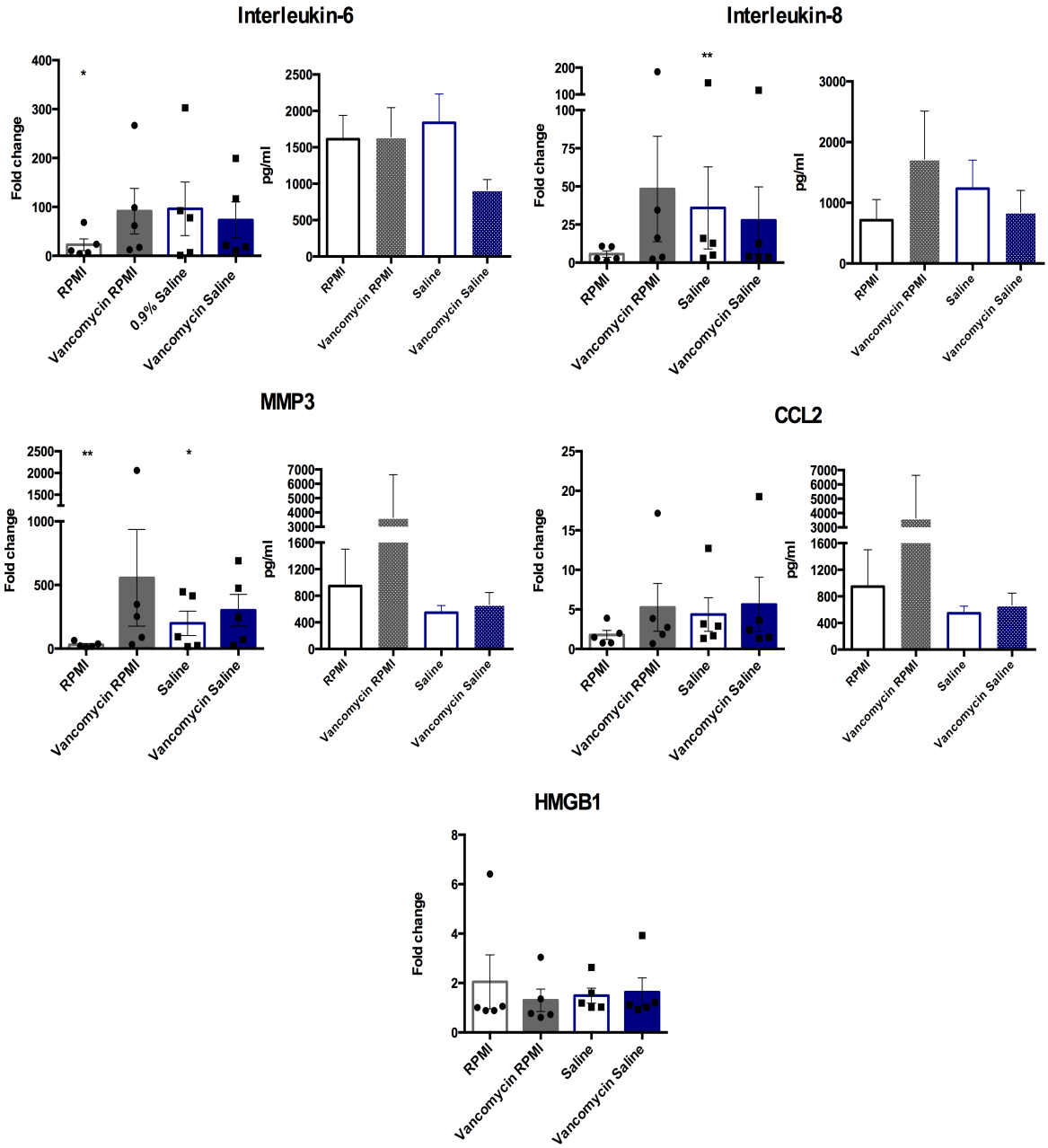

Figure 4-8 Tendon inflammatory gene and protein expression in control and vancomycin treated tendon

The effect of vancomycin on inflammatory gene and protein expression in tendon. IL-6, IL-8, MMP3, CCL2 and HMBG1 gene expression in tendon explant at 16 hours following 1 hour vancomycin treatment. Data are mean ±SEM, normalised to untreated tendon, relative to housekeeping gene, N=5, *p<0.05 **p<0.01 relative to untreated tendon. IL6, IL8, MMP3 and CCL2 protein measured by quantitative ELISA assay. Tendon treated for 1 hour, incubated for 16 hours, data represent mean ±SEM, IL6, MMP3, CCL2 N=11, IL8 N=10, analysis via ANOVA, multiple comparisons: untreated vs RPMI, untreated vs saline, RPMI vs saline, saline vs vancomycin saline, RPMI vs vancomycin saline.

4.4.5 Vancomycin and tendon biomechanics

Tendon explant was collected and cut into 3cm sections, as described in methods section 2.3.1. Due to the process involved in biomechanical analysis, a minimum size of 2.5cm of tendon was required for each treatment condition, therefore, due to sample availability only 0.9% saline and vancomycin 5mg/ml in saline were assessed, as these are the clinically relevant conditions. N=5 donors have been treated with experimental conditions and stored at -20^{o}C. These samples were unable to be analysed in the time period due to restrictions in place following the Covid-19 pandemic.

4.4.6 Vancomycin wrap clinical data

Over a 12-month period there were 142 ACL reconstructions performed, in 38 of these the use of vancomycin wrap was documented on the operation notes, data presented in Table 4-2. All patients in both treatment groups received prophylactic antibiotics in accordance with hospital protocol and there were no significant differences in patient age, ASA grade or type of graft used. There was one documented case of septic arthritis in the vancomycin wrap group and five other cases of superficial wound infection, two in the vancomycin wrap group. The deep infection case was a hamstring ACL graft, ASA grade 1 patient. The infection started with breakdown of the tibial wound and development of a sinus. Theatre tissue samples grew MSSA and E.coli. The patient was treated with surgical washout & debridement, plastic surgery input for rotational flap to cover the tibial skin defect and an extended course of antibiotics. The prosthetic endobutton securing the graft was removed at debridement, with subsequent follow up lachmans test was documented as having a firm endpoint. Of the five documented superficial wound infections, two required surgical washout, both documented as not communicating with the joint. All required oral antibiotics for duration of 1-2 weeks. There was no significant difference in infection rates between the two treatment groups. There were no documented graft failures at 6 months follow up.

Table 4-2 Clinical data from ACL reconstructions
All ACL reconstructions undertaken in a 12-month period July 2018-July 2019 in a single centre, operating across two clinical sites. Follow up at 6 months for details of infection. Analysis by students t test.

	Vancomycin wrap 5mg/ml	No Vancomycin wrap	*P* value
Number of patients	38	104	
Prophylactic antibiotics %	100	100	
Age, mean (range)	29.7 (19-49)	26.8 (13-56)	0.62
Sex Male, n (%)	33 (86.8)	86 (82.7)	
ASA Grade			
• **ASA1**	28	86	0.24
• **ASA2**	10	18	
Graft (revision surgery)			
• **Hamstring**	32 (0)	80 (4)	0.49 (0.39)
• **Patella**	6 (3)	24 (11)	
Infection: 6 month follow up	3	3	0.34
• **Septic arthritis**	1	0	
• **Superficial wound**	2	3	

4.5 **Discussion**

The first description of the "vancomycin wrap" for ACLR was in 2012; since then a number of studies have demonstrated its effectiveness in combination with usual IV antibiotic prophylaxis at reducing post-operative infection rates to almost 0%(Baron et al., 2019; Figueroa et al., 2019; Jefferies et al., 2019; Offerhaus et al., 2019; Pérez-Prieto et al., 2016; Phegan et al., 2016; Vertullo et al., 2012). One study reported infection rates in the control group, treated with prophylactic IV antibiotics alone as 1.4% (N=285) compared to 0% in patients who were treated with prophylactic IV antibiotics in combination with vancomycin wrap (N=870)(Vertullo et al., 2012). A further study which conducted post-operative follow up of 1300 consecutive ACL reconstructions using the vancomycin wrap in combination with standard IV antibiotic prophylaxis, reported zero post-operative infections against a retrospective control group (N=240) who reported infections in 2.4% of patients(Phegan et al., 2016). A more recent study which looked at 1640 patients, found the use of vancomycin wrap during ACL reconstruction was associated with a 10-fold reduction in post-operative infection (0.1% vs 1.2%)(Baron et al., 2019).

This work is the first to evaluate the molecular and structural effects that vancomycin has on a human hamstring graft for ACLR. The results of the current work indicate that vancomycin appears safe and has no detrimental effects on the cellular or molecular structure of the tendon graft used for ACLR.

The addition of vancomycin at the commonly used clinical dose of 5mg/ml did result in a reduction in tenocyte viability at 60 minutes. It is common in an in vitro model to experience biological variability and we did not see this reduction sustained following 30 or 120 minutes of treatment Figure 4-1. Previously published literature that used the same assay to assess chondrocyte viability found vancomycin safe at doses up to 16µg/ml over 36hours of treatment, which is above the minimum inhibitory concentration for staphylococcus aureus, the most commonly culture pathogen in ACLR infection (Dogan et al., 2016). At higher doses of 10mg/ml, the antibiotic crystallised in solution Figure 4-2. This dose was therefore no longer used as it could interfere with results and is not used in clinical practice.

There were many variables to consider when setting up the tendon explant model, which was used for apoptotic, matrix, inflammatory and biomechanical analysis. It remains unclear from published literature how much of the antibiotic is absorbed both by the sterile swab and by the tendon itself and therefore what concentration the tenocytes are exposed to. In one study it is reported that the sterile swab absorbed on average 7ml of the 100ml solution containing vancomycin at 5mg/ml(Vertullo et al., 2012). Bovine studies specifically looking at absorbance and elution of vancomycin from tendon have demonstrated that both of these characteristics are affected by graft size and rinsing(Grayson et al., 2011), which occurs in clinical practice once implanted, with arthroscopic washout of the joint. It is challenging to develop a model that accounts for all of these variables. We therefore submerged uniform size tendon explant pieces in vancomycin or saline for 1 hour. This eliminated any effect drying may have had on the tendon and was long enough to encompass reported average times from graft harvest to implantation, 30 minutes (range 28 - 43 minutes)(M E Hantes et al., 2008). The graft was washed twice with RPMI and then cultured for 16 hours post 1 hour treatment. We used this as our 'surgical scenario' model and feel this accurately reflects current practice and gives confidence that our molecular findings translate to everyday clinical practice. Changes in gene expression and protein release into supernatant are not instant reactions therefore, allowing 16 hours of tissue culture ensured our results reflected changes in the tendon molecular environment. Washing of the tendon following treatment was employed which replicates clinical practice and studies show that after 12 hours, elution rates between rinsed and un-rinsed tendon are no longer significantly different and have both reached a steady state(Grayson et al., 2011).

Tendon explant cultured in RPMI showed a small increase in apoptotic gene expression compared with fresh untreated tendon, however this was not significant. Clinically relevant was the finding that tendon cultured in 0.9% saline showed no significant difference compared with both fresh untreated tendon and tendon cultured in RPMI. RPMI is deemed ideal culture media, it is not available in clinical practice, therefore 0.9% saline was used as the clinical control. Prior to the introduction of the vancomycin wrap and in centres that do not use this practice, the ACL graft is wrapped in 0.9% saline. There was a

consistent trend towards increased apoptotic gene expression in all conditions (saline, vancomycin RPMI and vancomycin saline) compared with RPMI alone, however, the results were only significant for two apoptotic genes, BAX and AIFM1, when vancomycin saline was compared to RPMI Figure 4-3. BAX and AIFM1, associated with the cytochrome C and caspase 3 apoptotic pathways. Cytochrome C protein data at 1 and 16 hours concur with the BAX gene expression data, showing a trend towards increased levels with vancomycin saline, however, the protein release was not significantly different to control RPMI Figure 4-4. Caspase 3 protein data analysed by luminescence assay at 1 hour showed potentially spurious results, with marked reductions in caspase 3 in both vancomycin treatment groups Figure 4-5. The 1 hour supernatant contains dissolved vancomycin, it is possible the antibiotic may interfere with the luminesce readings. At 16 hours, following incubation with RPMI alone, this was not the case and the results are in line with gene expression data, showing a slight trend towards reduction in caspase 3 with vancomycin in saline.

Further caspase 3 analysis was performed with IHC staining. The representative images form donor 2281 show that vancomycin treatment caused no disruption to the uniform tendon structure Figure 4-6C. The semi quantitative scoring shows that there was a trend towards more positive staining with vancomycin treatment, however, this was not significant when compared with untreated or control tendon. Images from donor 1977 highlight the variability in clinical samples. The images show tendon with areas of increased cellularity, vascularity and loss of polarisation of collages fibres across both control and treated tendon. These findings are in keeping with tendinopathy and are not thought to be caused by tendon culture or vancomycin treatment(Fearon et al., 2014).

Exploration of the effect of vancomycin treatment on the matrix component of the graft post treatment demonstrated no significant difference in matrix gene expression compared to untreated tendon, control RPMI treated tendon, or tendon in saline alone. Vancomycin in saline was associated with an increase in collagen 3α gene expression, although not significant. This result comes from one outlier. As seen with the immunohistochemistry images in Figure 4-6C, this may reflect pre-existing tendinopathy changes in that donor tendon and highlights the issue of variability in clinical samples. The results show a

reduction in Collagen 1α protein release in vancomycin saline treated tendon supernatants compared with all 3 other treatment conditions. This finding may be as a result of lower Collagen 1α protein breakdown from the tissue explant into the supernatant following vancomycin treatment and thus may reflect a positive effect of vancomycin treatment.

The primary functions of the tendon graft in ALCR are transfer mechanical load and mechanical stability. Although the current study did not directly measure the biomechanical properties of the tendon graft following vancomycin treatment, histological data indicates vancomycin treatment does not affect the integrity of the graft structure. This is further inferred by the matrix gene and protein results noted above. The preparation of samples for biomechanical analysis has been completed and it is hoped that this work can be finalised in the coming months. Recent published literature has evaluated the biomechanical properties of bovine patella tendon following saline and vancomycin 5mg/ml in saline treatment. The results showed no difference in Young's modulus or elongation strain between the treatment groups concluding that vancomycin at 5mg/ml did not alter the material properties of the tendon(Lamplot et al., 2021).

Vancomycin, as well as being antimicrobial has also been shown to have immune modulating potential. In inflammatory mediated conditions, it has been shown to act via alterations in the host T cell population which leads to reduced inflammation(Abarbanel et al., 2013). In a sepsis model however, vancomycin was found to have pro-inflammatory effects on the innate immune system(Bode et al., 2015). We therefore investigated the inflammatory effect vancomycin had on tendon. Our results show that vancomycin in saline showed a consistent trend towards reduced inflammatory cytokine release, compared with 0.9% saline and RPMI alone and vancomycin in RPMI diluent. Previous work has shown that inflammation has a negative effect on the health of a tendon and IL-6 is involved in the development of tendinopathy(Millar et al., 2009).

These results suggest vancomycin treatment is not detrimental to the cellular viability of the tendon graft but may have small beneficial effects pointing towards a homeostatic, molecular environment to encourage graft viability. The reduction in collagen 1α release and inflammatory cytokine release indicate

reduced cellular stress and may be linked with the reduction seen in apoptotic gene expression of caspase. A recent retrospective cohort study reviewed 1779 patients who underwent ACLR, with vancomycin soaking of the hamstring graft employed in 853 of these cases. Over a 5 year period, whereby 100 patients were randomly selected for follow-up each year, graft failure and re-rupture rates were reported to be significant lower in the vancomycin wrap group; 8 failures out of 257 vs 16 failures out of 167 patients in the control group $p<0.01$(Offerhaus et al., 2019).

The clinical data presented in this study represents small numbers from a single unit covering two hospital sites. Using the operation note to establish the use of the vancomycin wrap may underestimate the numbers in this group as there is no option to select "vancomycin 5mg/ml wrap' from the pre-populated choices on the currently used software programme. The one deep infection with MSSA and E.coli was from a patient who received a vancomycin wrap, and whilst vancomycin is active against these pathogens, it is not the first line choice for E.coli. Risk factors and prevention strategies for post-operative infection in ACLR are multifactorial, with longer surgical times and higher BMI both shown to be independent predictors(Baron et al., 2019). When infection rates are already low, one intervention alone may not consistently alter outcomes. This was the conclusion in one study assessing the efficacy of local vancomycin to spinal surgery wounds who reported no difference in infection rates vs usual IV antibiotic prophylaxis (1.61% vs 1.68%)(Tubaki et al., 2013). Furthermore, infection in ACLR can be caused by multiple pathogens, which may not be susceptible to vancomycin and the increasing use of one antibiotic as local prophylaxis may begin to select out for non-staphylococcal infections, which doesn't constitute resistance, but may have implications for clinical treatment protocols should infection occur (Heller et al., 2015).

Antibiotic resistance is an important consideration as an increasing number of antibiotics are being used in the peri-operative period as prophylaxis. Data from cardiothoracic surgery, using vancomycin paste in sternotomy wounds has not found antibiotic resistance to be an issue given that topical use does not lead to therapeutic serum levels of the drug(Lazar et al., 2011). Animal studies have demonstrated that once wrapped in a vancomycin solution, the ACL graft can act as a reservoir, continuing to release the drug over 24 hours, at gradually

decreasing levels, below a dose considered toxic to cells(Grayson et al., 2011). Exposing tissues to prolonged subtherapeutic levels of a drug is a known way to establish resistance(Andersson & Hughes, 2014). Future evaluation on the safety of the vancomycin wrap in ACLR could include serum and synovial drugs levels following surgery to investigate this.

There are limitations to this work, primarily with the tendon explant model. There are many variables involved in the vancomycin wrap during surgery, the volume of antibiotic absorbed by the swab and by the graft, both influenced by the volume of tissue and rinsing during the arthroscopic procedure and the effect of drying of the graft prior to implantation, under the lamina flow. It is challenging to create a model that encompasses all of these variables. We believe the model we used accurately reflects the effect of the antibiotic alone on the graft. Further *ex vivo* work and clinical follow up are recommended to investigate the biomechanical properties of human tendon graft post treatment, if there is any association with reduced graft failure and any indications of antibiotic resistance.

5 Summary and future work

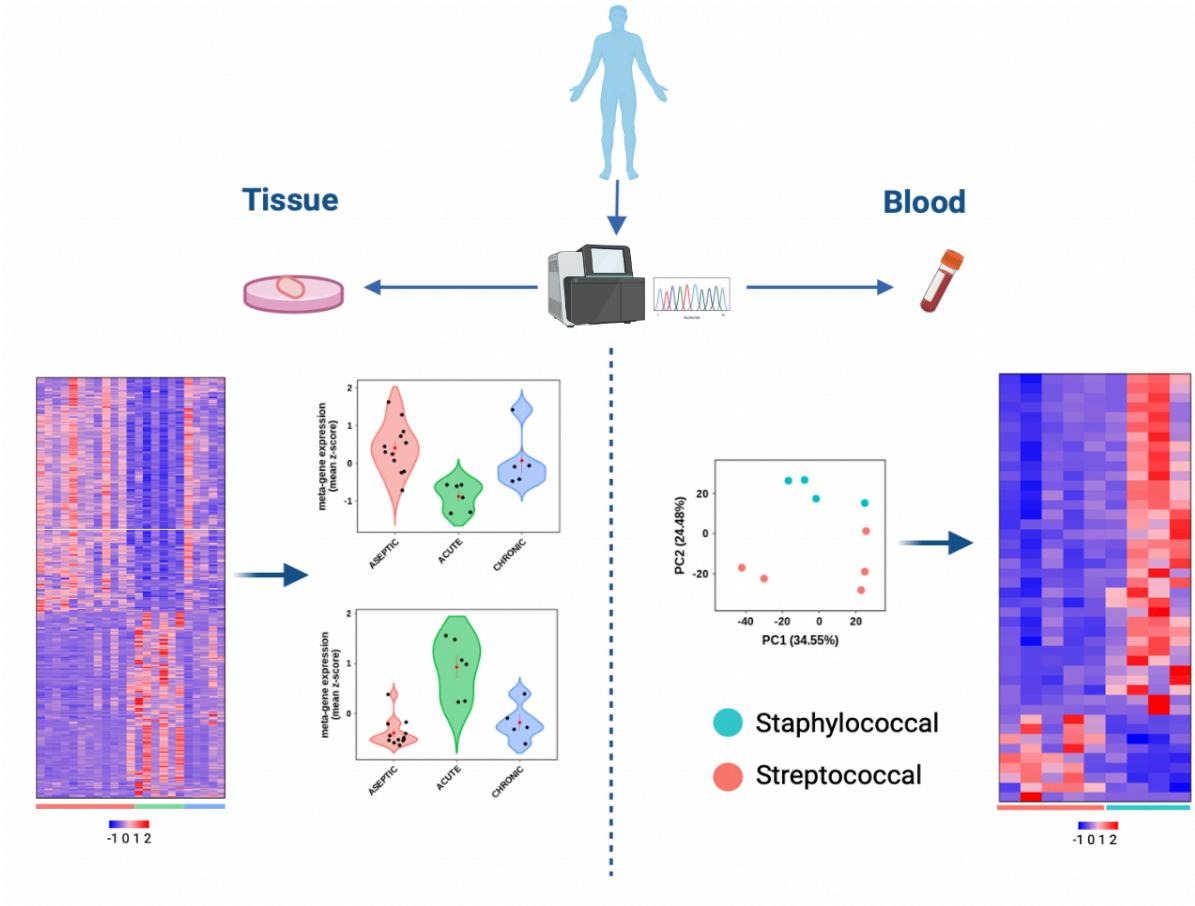

Figure 5-1 Summary of findings from Chapter 3
A diagram summarising the key finding from the sequencing of tissue and blood from orthopaedic revision surgery using an immune gene response panel. Tissue sequencing results demonstrated transcriptional signatures which allowed discrimination between aseptic, chronic and acute infection. Furthermore, metagenomic signatures highlighted the similarity between the immune signature form chronic infection and aseptic control tissue, indicating an attenuated immune response seem with chronic infection, potentially due to bacteria embedded in biofilm matrix. Blood sequencing results demonstrated a unique transcriptional signature that identified staphylococcal from streptococcal infection.

5.1 Gene expression signature from PJI tissue

Synovial tissue was collected from patients undergoing orthopaedic revision arthroplasty. This tissue was fixed in formalin and sections were analysed for gene expression using a 2002 immune response gene panel. This work represents the first time the immune gene response panel, developed by HTG molecular, has been analysed on PJI and aseptic tissue from orthopaedic revision arthroplasty patients. It is also the first sequencing work to investigate the host immune response as a potential diagnostic test in PJI. The data showed that status – aseptic, acute or chronic infection had the largest effect on the gene sequencing results from synovial tissue. Tissue from the PJI cohort had significantly higher expression of genes involved in immune 'cell chemotaxis' and 'response to a molecule of bacterial origin' which are clinically relevant pathways in infection. Further analysis of the data allowed us to develop AUC/ROC curves to assess the diagnostic ability of the immune response gene panel and use machine learning to optimise a 4 gene panel for PJI: *G0S2, CXCL5, NR1D2 and DBP*, with sensitivity and specificity of 82% and 100%% respectively. In addition, data analysis identified sub-groups within the PJI cohort relating to time frame of infection, those cases deemed as 'acute' infection as per MSIS 2018 guidelines showed a different pattern of gene expression to 'chronic' infection and aseptic control. We concluded that the PJI transcriptomic response was largely driven by the 'acute' infection cohort, with the chronic infection cohort sharing a gene expression pattern with aseptic control Figure 5-1. From this we inferred that the immune response in chronic implant related infection is attenuated, linking with known biofilm biology, where bacteria are shielded from the immune system. This may have implications for the use of known and future immune mediated biomarkers including alpha defensin and leucocyte esterase in chronic PJI diagnosis.

5.2 Gene expression signature from PJI blood

Peripheral blood was collected preoperatively from patients undergoing orthopaedic revision arthroplasty for gene expression analysis on a 2002 gene immune response panel. This work represents the first time the immune gene panel developed by HTG molecular, has been analysed in blood using a revision arthroplasty cohort – including PJI and aseptic cases. Furthermore, this work is

novel in its evaluation of the immune repose as a potential diagnostic test in PJI. Variance partition analysis showed that bacterial strain was a factor that had one of the biggest effects on sequencing results. Annotating blood samples by bacterial strain identified a significant difference in immune gene signature between *Staphylococcal* and *Streptococcal* infections. The current diagnostic algorithms rely on microbiological tissue or fluid analysis for bacterial identification and diagnosis, however, as previously noted, identification of tissue planes can be unreliable in revision surgery and may miss areas of infection and biofilm clusters. Blood is a more uniform biological sample, avoiding the need for surgery to obtain sterile peri-articular samples. Identification of bacterial infection from blood is an area of evolving research, particularly in paediatric infection and respiratory medicine.

5.3 **Limitations of PJI sequencing work**

This was a pilot study to demonstrate the use of a novel sequencing technology. The numbers of patients included (n=24) was low and sequencing data was not able to be generated for n=1 patient in the tissue analysis due to low sample quality and n=4 in the blood analysis due to insufficient library concentration for sequencing.

During revision arthroplasty surgery, defining specific tissue planes/orientation can be challenging, therefore, there was wide variability in the tissue samples received. Furthermore, sequencing analysis was performed on one 5μm section of tissue from each patient, previous literature has noted variation in spatial distribution of bacteria in PJI (Walker et al., 2020). Both factors may have affected tissue sequencing results. Insufficient library concentration from n=4 blood samples may have been the result of inadequate mixing with the stabilising agent at the time of sample collection, or an issue with binding of the DNA nuclease protection probes/wingmen to the target RNA, meaning target RNA was digested by the S1 nuclease. Gene expression analysis was available for two bacterial strains *Staphylococcal* and *Streptococcal*. In PJI multiple pathogens are commonly involved, in some cases polymicrobial infection. This pilot study didn't include polymicrobial infections with different bacterial genus strains, however, did include multiple species eg: *streptococcus mitis/oralis*

grouped as '*Streptococcal*'. Due to COVID-19 planned validation of the gene signature in synovial tissue and blood could not be carried out.

5.4 PJI sequencing future work

Laboratory and larger patient cohort validation of the results from this pilot study are now required. The identification of a gene signature that identifies *Staphylococcal* versus *Streptococcal* in blood is an encouraging finding for PJI diagnosis in the future, as it would allow gene level information without the need for extended microbiological tissue culture. A larger cohort will also identify more bacterial strains and assess if they too produce a unique immune signature. Next generation gene sequencing techniques are now routinely being evaluated in research focusing on PJI. Common pitfalls with regards to human DNA contamination of the sample are reported. This pilot study reports the use of a novel sequencing technique switching the diagnostic method – instead looking for the host immune repose to a pathogen. These sequencing methods have the potential to take PJI diagnosis into the era of personalise medicine.

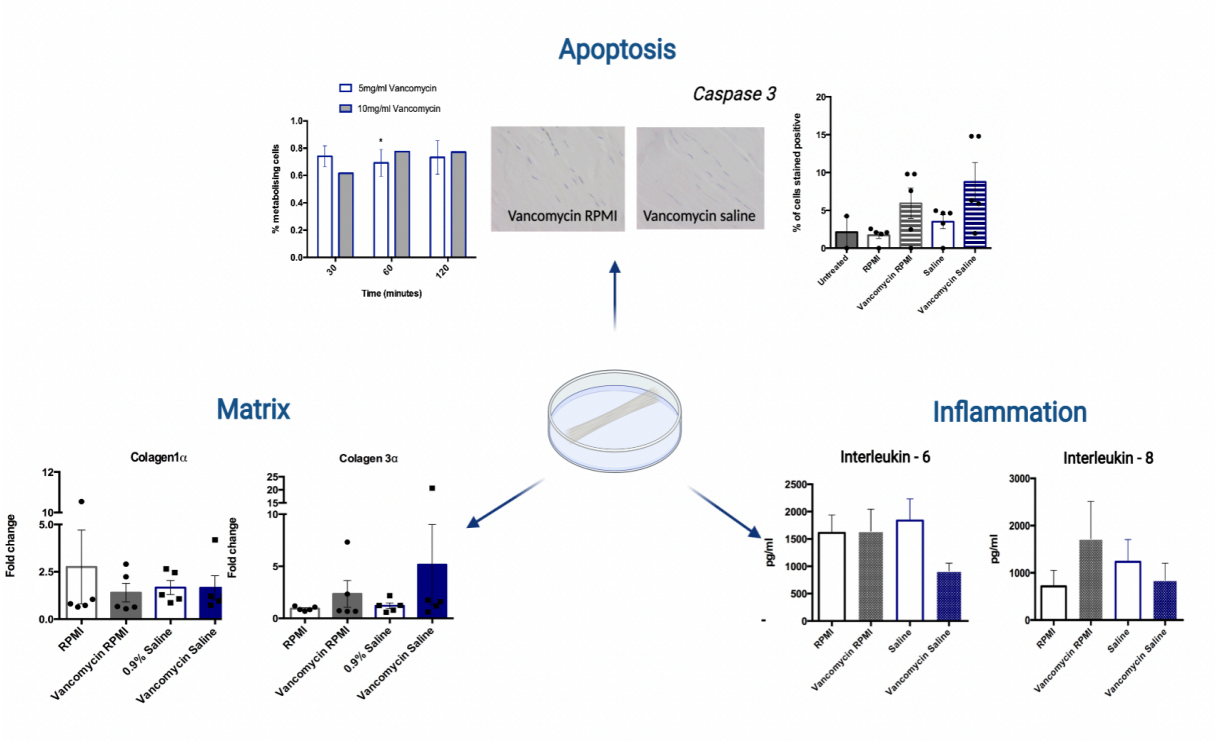

Figure 5-2 Summary of findings from Chapter 4
A diagram summarising the main findings from the working assessing the molecular effects of vancomycin on tendon. Apoptosis: *In vitro* work demonstrated a reduction in tenocyte viability following treatment of cells with vancomycin at 60 minutes. This reduction was not seen at the 30- or 120-minute time point and could therefore represent biological variability in the assay. It is unclear how much of the vancomycin the tenocytes are directly exposed to. Therefore, further apoptosis assays used the tendon explant model and showed no significant or consistent increase in Caspase 3 protein, suggesting vancomycin did not induce tenocyte apoptosis. Matrix: After treatment with vancomycin in the tendon explant model, gene expression of *collagen1*α and *collagen3*α were not significantly increased indicating no aberrant change to tendon matrix composition. Inflammation: Vancomycin treatment in the tendon explant model was associated with a trend towards reduced inflammatory cytokine release which may represent a role for vancomycin inducing a homeostatic molecular environment and could be implicated in the increased graft survival seen in clinical practice (Offerhaus et al., 2019) .

5.5 **Molecular effects of vancomycin *in vitro***

Tenocytes were cultured from surplus human hamstring tendon following ACLR and used to assess cell viability following treatment with vancomycin antibiotic. We found a reduced tenocyte viability after 60 minutes, however this finding was not seen at 30 or 120 minutes. This may be due to biological variability in the assay, however, all time points showed an overall trend towards reduced cell viability. These experiments used 5mg/ml of vancomycin and as explained in the *ex vivo* model, variance in antibiotic absorbance along with interposition of matrix proteins make it challenging to know the concentration tenocytes *in vivo* are exposed to. It is also unclear if a reduction in tenocyte viability translates into a clinical difference in outcomes following ACLR as the process of graft integration following ACL 'ligamentisation' is known to include a period of cell avascular necrosis.

5.6 **Molecular effect of vancomycin *ex vivo***

Surplus tendon tissue following surgery for ACLR was used to set up a tendon *ex vivo* model to investigate the molecular effect of vancomycin on human tendon. We found that treatment of the tendon with 5mg/ml of vancomycin solution up to 1 hour was not associated with a significant or consentient increase in the expression of apoptotic markers. Gene expression of two apoptotic proteins AIFM 1 and BAX was increased following vancomycin treatment, however, protein analysis of the associated cytochrome C and caspase 3 pathways did not find a significant increase with vancomycin compared with control conditions. Vancomycin treatment was not found to significantly alter tendon matrix proteins but was associated with a significant reduction in the release of inflammatory cytokines. Previous work has discussed the negative effect inflammation can have on tendon and the development of tendinopathy (Millar et al., 2009). These findings suggest that vancomycin may have a homeostatic and beneficial effect on the health of the tendon graft. In line with this finding, recent evidence has pointed towards prolonged graft integrity following ACLR with vancomycin treatment of the graft (Offerhaus et al., 2019).

5.7 Limitations of tendon vancomycin work

The *in vitro* tendon model used RPMI as the control solution, in clinical practice 0.9% saline is used, however this lowered pH and altered the osmotic environment causing tenocyte cell death. When whole tendon sections were used in the *ex vivo* model, 0.9% saline was able to be used at the control, suggesting a level of protection when the cells are embedded in matrix. Obtaining high quality human tendon samples from ACL surgery is challenging, defining when the sample was taken – before or after graft preparation is crucial as it may have already been affected by drying or damaged during stitching or passing through the bone tunnels. However, using human tissue enabled better translation of laboratory results to clinical practice. There were several challenges outlined in setting up the tendon *ex vivo* explant model including the volume of antibiotic absorbed by the graft influenced by the size of graft and rinsing during the arthroscopic procedure along with the effect of drying during graft preparation in the lamina flow theatre. It was additionally challenging to create a model that considered all these variables to allow conclusions to be draw on vancomycin effect only. We believe the model we established was consistent, with uniform size tendon sections being immersed in antibiotic solution, eliminating drying and therefore accurately reflecting the effects of vancomycin on tendon.

5.8 Vancomycin tendon future work

Biomechanical analysis of *ex vivo* tendon treated with vancomycin was planned for this project with tendon tissue collected, treated and stored ready for analysis. Due to COVID 19 these experiments could not be carried out. Recent publications have shown that vancomycin has no detrimental effects on tendon biomechanical properties, however, these papers used animal tissue with bovine and porcine tendon models (Lamplot et al., 2021; Schüttler et al., 2019). Vancomycin treatment of the ACL grafts is becoming more common in clinical practice and it is important to establish the risks of antibiotic resistance. It remains unclear how much, if any, of the vancomycin is absorbed into the systemic circulation following surgery. This level should be established as repeated exposure of bacteria to subtherapeutic levels of an antibiotic is a known method for the development of antibiotic resistance.

6 Appendices

6.1 **Appendix A**

Table 6-1 Studies evaluating Interleukin - 6 in Prosthetic Joint Infection
Details of the studies which evaluated IL-6 as a biomarker for PJI in serum and synovial fluid. ELISA = Enzyme Linked Immunosorbent Assay.

Author/Year	No. of Patients	Cut off value	Method	Sensitivity	Specificity
Di Caseare 2005	Aseptic 41 PJI 17	10 pg/ml	Serum ELISA	100%	95%
Bottner 2007	Aseptic 57 PJI 21	12pg/mL	Serum ELISA	95%	87%
Nilsdotter-Augustinsson 2007	Aseptic 60 PJI 25	10,000pg/mL	Synovial fluid ELISA	69%	93%
Worthington 2010	Aseptic 30 PJI 16	9pg/mL	Serum ELISA	81%	77%
Grosso 2014	Aseptic 45 PJI 24	5pg/ml	Serum Florescent multiplex bead assay	12%	93%
Deirmengian 2014 (b)	Aseptic 66 PJI 29	2300pg/ml	Synovial fluid Bead Immunoassay	89%	97%
Randeau 2014	Aseptic 72 PJI 48	Serum 2.6pg/ml Synovial fluid 2100pg/ml & 9000pg/ml	Serum & synovial fluid ELISA	Serum 79.4% Synovial fluid 2100pg/ml 62.5% Synovial fluid 9000pg/ml 46.8%	Serum 58.3% Synovial fluid 2100pg/ml 85.7% Synovial fluid 9000pg/ml 97.6%
Ettinger 2015	Aseptic 57 PJI 41	5.12pg/mL	Serum ELISA	80%	87.7%
Wimmer 2016	Aseptic 20 PJI 6	10,000pg/ml	Synovial fluid Lateral flow vs ELISA	Not reported	Not reported
Gallo 2018	Aseptic 147 PJI 93	Serum 12.55ng/L Synovial 20,988 ng/L	Serum & synovial fluid ELISA	Serum 86.7% Synovial 68%	Serum 89.5% Synovial 95.4%
Majors 2019	Aseptic 27 PJI 32	9.14pg/ml	Serum ELISA	81%	63%

6.2 **Appendix B**

Table 6-2 Studies evaluating Multiplex PCR in Prosthetic joint infection
Multiplex PCR allows multiple primer templates in one reaction

Author/ year	No. of patients	Sample	Method	Sensitivity	Specificity
Achermann 2010	PJI 37 Aseptic 0	Sonicated fluid PCR vs sonicated fluid & tissue culture	Stepifast® Multiplex PCR Roche®, tissue/fluid culture	Sonicate fluid PCR: 78% Socnicate fluid culture:62% Tissue culture: 65%	Not reported
Portillo 2012	PJI24 Aseptic 62	Sonicated fluid PCR vs sonicated fluid & tissue culture	Stepifast® Multiplex PCR Roche®, tissue/fluid culture	Sonicated fluid PCR: 96% Sonicated fluid culture: 71% Tissue culture: 67%	Sonicated fluid PCR: 100% Sonicated fluid culture: 100% Tissue culture: 98%
Estenban 2012	PJI 31 Aseptic 44	Sonicated fluid PCR vs Sonicate fluid culture	Multiplex panel 16s rRNA (Hain Lifescience)	Sonicate fluid PCR: 83.9% Sonicated fluid culture: 77.4%	68.2% 88.6%
Cazanave 2013	PJI 144 Aseptic 290	Sonicated fluid PCR and culture, Tissue + Synovial fluid culture	Multiplex PCR (16s rRNA + bacteria specific genes) Roche, Culture	Sonicate fluid PCR: 77.1% Sonicate fluid culture: 72.9% Tissue culture: 70.1% Synovial fluid culture: 66.3%	Sonicate fluid PCR: 97.9% Sonicate fluid culture: 98.3% Tissue culture: 97.9% Synovial fluid culture: 96.9%
Ryu 2014	PJI 64 Aseptic 31	Sonicated fluid + tissue PCR, Sonicated fluid, tissue synovial fluid culture	Multiplex PCR 16s rRNA + bacteria specific genes (Roche), culture	Sonicate fluid PCR: 78% Sonicate fluid culture: 76.7% Tissue PCR:15.6% Tissue culture: 68.9% Synovial fluid culture:72%	Sonicate fluid PCR: 100% Sonicate fluid culture: 100% Tissue PCR: 96.8% Tissue culture: 70% Synovial fluid culture:96%
Kawamura 2017	PJI 23 Aseptic 64	Synovial fluid & Tissue	LightCycler Nano® Multiplex RT-qPCR 16s rRNA (28 bacteria)	91%	88%

Table 6-3 Studies evaluating Multiplex Cartridge Systems in the diagnosis of Prosthetic joint Infection

All studies evaluated the Unyvero i60 Implant and tissue infection ITI cartridge that includes 102 pathogens along with antimicrobial resistance markers

Author/ year	No. of patients	Sample	Method	Sensitivity	Specificity
Borde 2015	Aseptic 47 PJI 7	Tissue PCR	Unyvero i60 implant and tissue infection ITI mPCR system, Curetis ® and 16s rRNA PCR	Univero i60 mPCR:42.8% 16s rRNA PCR: 85.7%	Univero i60 mPCR:95.2% 16s rRNA PCR: 97.8%
Hischeb eth 2016	PJI 18 Aseptic 13	Synovial fluid, Sonicate fluid	Unyvero i60 implant and tissue infection ITI mPCR system, Curetis ®	66.7%	100%
Lausma nn 2017	PJI 34 Aseptic 26	Synovial fluid	Unyvero i60 implant and tissue infection ITI mPCR system, Curetis ®	78.8%	100%
Suda 2017	PJI 13 Aseptic 17	Tissue PCR, Synovasure®	Uniyero i60 implant and tissue ITI mPCR system, Curetis ® and Synovasure	Univero i60 mPCR: 30.8% Synovasure: 76.9%	Univero i60 mPCR: 100% Synovasure: 82.4%
Malandi an 2018	PJI 276 Aseptic 164	Tissue PCR	Unyvero i60 implant and tissue ITI mPCR system, Curetis ®	Univero i60 mPCR PCR: 47.4%	Univero i60 mPCR: 93.9%

References

Abarbanel, D. N., Seki, S. M., Davies, Y., Marlen, N., Benavides, J. A., Cox, K., Nadeau, K. C., & Cox, K. L. (2013). Immunomodulatory effect of vancomycin on Treg in pediatric inflammatory bowel disease and primary sclerosing cholangitis. *Journal of Clinical Immunology*, *33*(2), 397–406.

Akgün, D., Müller, M., Perka, C., & Winkler, T. (2018). The serum level of C-reactive protein alone cannot be used for the diagnosis of prosthetic joint infections, especially in those caused by organisms of low virulence. *Bone and Joint Journal*, *100B*(11), 1482–1486. https://doi.org/10.1302/0301-620X.100B11.BJJ-2018-0514.R1

Alamanda, V. K., & Springer, B. D. (2019). The prevention of infection 12: Modifiable risk factors. *Bone and Joint Journal*, *101B*(1), 3–9. https://doi.org/10.1302/0301-620X.101B1.BJJ-2018-0233.R1

Anderson, J. M. (2001). Biological responses to materials. *Annual Review of Materials Science*, *31*, 81–110. https://doi.org/10.1146/annurev.matsci.31.1.81

Andersson, D. I., & Hughes, D. (2014). Microbiological effects of sublethal levels of antibiotics. *Nature Reviews Microbiology*, *12*(7), 465–478. https://doi.org/10.1038/nrmicro3270

Andrews, J. M. (2002). Determination of minimum inhibitory concentrations. *Journal of Antimicrobial Chemotherapy*, *49*(6), 1049–1049. https://doi.org/10.1093/jac/dkf083

Antoci, V., Adams, C. S., Hickok, N. J., Shapiro, I. M., & Parvizi, J. (2007). Antibiotics for local delivery systems cause skeletal cell toxicity in vitro. *Clinical Orthopaedics and Related Research*, *462*, 200–206. https://doi.org/10.1097/BLO.0b013e31811ff866

Arciola, C. R., Campoccia, D., & Montanaro, L. (2018). Implant infections: Adhesion, biofilm formation and immune evasion. *Nature Reviews*

Microbiology, *16*(7), 397–409. https://doi.org/10.1038/s41579-018-0019-y

Atkins, B. L., Athanasou, N., Deeks, J., Crook, D. W. M., Simpson, H., Peto, T., Mclardy-Smith, P., Berendt, A. R., Benson, M., Carr, A., Collopy, D., Cooke, P., Kenwright, J., McClardy-Smith, P., Simpson, H., De Steiger, R., Gundle, R., Willett, K., Atkins, B., … Athanasou, N. (1998). Prospective evaluation of criteria for microbiological diagnosis of prosthetic-joint infection at revision arthroplasty. *Journal of Clinical Microbiology*, *36*(10), 2932–2939. https://doi.org/10.1128/jcm.36.10.2932-2939.1998

Baron, J., Shamrock, A., Cates, W., Cates, R., An, Q., Wolf, B., Bollier, M., Duchman, K., & Westermann, R. (2019). Graft Preparation with Intraoperative Vancomycin Decreases Infection After ACL Reconstruction: A Review of 1,640 Cases. *Journal of Bone and Joint Surgery Am*, *101*(24), 2187–2193.

Bejon, P., Byren, I., Atkins, B. L., Scarborough, M., Woodhouse, A., McLardy-Smith, P., Gundle, R., & Berendt, A. R. (2011). Serial measurement of the C-reactive protein is a poor predictor of treatment outcome in prosthetic joint infection. *Journal of Antimicrobial Chemotherapy*, *66*(7), 1590–1593. https://doi.org/10.1093/jac/dkr182

Bémer, P., Léger, J., Tandé, D., Plouzeau, C., Valentin, S., Jolivet-gougeon, A., Lemarié, C., Kempf, M., Héry-arnaud, G., Bret, L., Juvin, E., Giraudeau, B., & Corvec, S. (2016). How Many Samples and How Many Culture Media To Diagnose a Prosthetic Joint Infection : a Clinical and Microbiological Prospective Multicenter Study. *Journal of Clinical Microbiology*, *54*(2), 385–391. https://doi.org/10.1128/JCM.02497-15.Editor

Berbari, E. F., Marculescu, C., Sia, I., Lahr, B. D., Hanssen, A. D., Steckelberg, J. M., Gullerud, R., & Osmon, D. R. (2007). Culture-negative prosthetic joint infection. *Clinical Infectious Diseases*, *45*(9), 1113–1119. https://doi.org/10.1086/522184

Bingham, J., Clarke, H., Spangehl, M., Schwartz, A., Beauchamp, C., & Rn, B. G. (2014). The Alpha Defensin-1 Biomarker Assay can be Used to Evaluate the

Potentially Infected Total Joint Arthroplasty. *Clinical Orthopaedics and Related Research*, *472*(12), 4006–4009. https://doi.org/10.1007/s11999-014-3900-7

Bode, C., Muenster, S., Diedrich, B., Jahnert, S., Weisheit, C., Steinhagen, F., Boehm, O., Hoeft, A., Meyer, R., & Baumgarten, G. (2015). Linezolid, vancomycin and daptomycin modulate cytokine production, Toll-like receptors and phagocytosis in a human in vitro model of sepsis. *The Journal of Antibiotics*, *68*, 485–490.

Bongen, E., Lucian, H., Khatri, A., Fragiadakis, G. K., Bjornson, Z. B., Nolan, G. P., Utz, P. J., & Khatri, P. (2019). Sex Differences in the Blood Transcriptome Identify Robust Changes in Immune Cell Proportions with Aging and Influenza Infection. *Cell Reports*, *29*(7), 1961-1973.e4. https://doi.org/10.1016/j.celrep.2019.10.019

Bori, G. (2018). *Histopathology in Periprosthetic Joint Infection : When Will the Morphomolecular Diagnosis Be a Reality ? 2018*. https://doi.org/10.1155/2018/1412701

Bottner, F., Wegner, A., Winkelmann, W., Becker, K., Erren, M., & Gotze, C. (2007). Interleukin-6, procalcitonin and TNF- : MARKERS OF PERI-PROSTHETIC INFECTION FOLLOWING TOTAL JOINT REPLACEMENT. *Journal of Bone and Joint Surgery - British Volume*, *89-B*(1), 94–99. https://doi.org/10.1302/0301-620X.89B1.17485

Bratzler, D. W., & Houck, P. M. (2005). Antimicrobial prophylaxis for surgery: An advisory statement from the National Surgical Infection Prevention Project. *American Journal of Surgery*, *189*(4), 395–404. https://doi.org/10.1016/j.amjsurg.2005.01.015

Bryson, D. J., Morris, D. L. J., Shivji, F. S., Rollins, K. R., Snape, S., & Ollivere, B. J. (2016). Antibiotic prophylaxis in orthopaedic surgery: Difficult decisions in an era of evolving antibiotic resistance. *Bone and Joint Journal*, *98-B*(8), 1014–1019. https://doi.org/10.1302/0301-620X.98B8.37359

Burks, R. T., Friederichs, M. G., Fink, B., Luker, M. G., West, H. S., & Greis, P. E. (2003a). Treatment of postoperative anterior cruciate ligament infections with graft removal and early reimplantation. *American Journal of Sports Medicine*, *31*(3), 414–418. https://doi.org/10.1177/03635465030310031501

Burks, R. T., Friederichs, M. G., Fink, B., Luker, M. G., West, H. S., & Greis, P. E. (2003b). Treatment of postoperative anterior cruciate ligament infections with graft removal and early reimplantation. *American Journal of Sports Medicine*, *31*(3), 414–418. https://doi.org/10.1177/03635465030310031501

Carney, J., Heckmann, N., Mayer, E. N., Alluri, R. K., Vangsness, C. T., Hatch, G. F., & Weber, A. E. (2018). Should antibiotics be administered before arthroscopic knee surgery? A systematic review of the literature. *World Journal of Orthopaedics*, *9*(11), 262–270. https://doi.org/10.5312/wjo.v9.i11.262

Cazanave, C., Greenwood-Quaintance, K. E., Hanssen, A. D., Karau, M. J., Schmidt, S. M., Urena, E. O. G., Mandrekar, J. N., Osmon, D. R., Lough, L. E., Pritt, B. S., Steckelberg, J. M., & Patel, R. (2013). Rapid molecular microbiologic diagnosis of prosthetic joint infection. *Journal of Clinical Microbiology*, *51*(7), 2280–2287. https://doi.org/10.1128/JCM.00335-13

Cesare, D. P., E, C., C, P., & Liu, C. (2005). Serum Interleukin-6 as a marker of periprosthetic infection following total hip and knee arthroplasty. *Journal of Bone and Joint Surgery Am*, *87*(9), 1921–1927.

Chen, M. F., Chang, C. H., Chiang-Ni, C., Hsieh, P. H., Shih, H. N., Ueng, S. W. N., & Chang, Y. (2019). Rapid analysis of bacterial composition in prosthetic joint infection by 16s rRnA metagenomic sequencing. *Bone and Joint Research*, *8*(8), 367–377. https://doi.org/10.1302/2046-3758.88.BJR-2019-0003.R2

Cheng, J., Hu, H., Kang, Y., Chen, W., Fang, W., Wang, K., Zhang, Q., Fu, A., Zhou, S., Cheng, C., Cao, Q., Wang, F., Lee, S., & Zhou, Z. (2018). Identification of pathogens in culture-negative infective endocarditis cases by metagenomic analysis. *Annals of Clinical Microbiology and*

Antimicrobials, *17*(1), 43. https://doi.org/10.1186/s12941-018-0294-5

Cipriano, C., Maiti, A., Hale, G., & Jiranek, W. (2014). The Host Response: Toll-Like Receptor Expression in Periprosthetic Tissues as a Biomarker for Deep Joint Infection. *The Journal of Bone and Joint Surgery Am*, *96*, 1682–1688.

Dale, H., Fenstad, A. M., Hallan, G., Havelin, L. I., Furnes, O., Overgaard, S., Pedersen, A. B., Kärrholm, J., Garellick, G., Pulkkinen, P., Eskelinen, A., Mäkelä, K., & Engesæter, L. B. (2012). Increasing risk of prosthetic joint infection after total hip arthroplasty. *Acta Orthopaedica*, *83*(5), 449–458. https://doi.org/10.3109/17453674.2012.733918

Deehan, D. J., & Cawston, T. E. (2005). The biology of integration of the anterior cruciate ligament. *The Journal of Bone and Joint Surgery. British Volume*, *87-B*(7), 889–895. https://doi.org/10.1302/0301-620X.87B7.16038

Deirmengian, C., Kardos, K., Kilmartin, P., Cameron, A., Schiller, K., Booth, R. jr, & Parvizi, J. (2015). The alpha-defensin test for periprosthetic joint infection outperforms the leukocyte esterase test strip. *Clinical Orthopaedics and Related Research*, *473*(1), 198–203.

Deirmengian, C., Kardos, K., Kilmartin, P., Cameron, A., Schiller, K., & Parvizi, J. (2014a). Combined measurement of synovial fluid alpha-defensin and c-reactive protein levels: Highly accurate for diagnosing periprosthetic joint injection. *The Journal of Bone and Joint Surgey Am*, *96*(17), 1439–1445.

Deirmengian, C., Kardos, K., Kilmartin, P., Cameron, A., Schiller, K., & Parvizi, J. (2014b). Diagnosing Periprosthetic Joint Infection: Has the era of the biomarker arrived? *Clinical Orthopaedics and Related Research*, *472*, 3254–3262. https://doi.org/10.1007/s11999-014-3543-8

Dhabuwala, C. (2010). In Vitro Assessment of Antimicrobial Properties of Rifampin-Coated Titan® Coloplast Penile Implants and Comparison with Inhibizone®. *Journal of Sexual Medicine*, *7*(10), 3516–3519.

Dogan, M., Isyar, M., Yilmaz, I., Bilir, B., Sirin, D. Y., Cakmak, S., &

Mahirogullari, M. (2016). Are the leading drugs against Staphylococcus aureus really toxic to cartilage? *Journal of Infection and Public Health*, *9*(3), 251–258. https://doi.org/10.1016/j.jiph.2015.10.004

Drago, Clerici, Morelli, Ashok, Benzakour, Bozhkova, Alizadeh, del Sel, Sharma, Peel, Mattina, & Romanò. (2019). The World Association against Infection in Orthopaedics and Trauma (WAIOT) procedures for Microbiological Sampling and Processing for Periprosthetic Joint Infections (PJIs) and other Implant-Related Infections. *Journal of Clinical Medicine*, *8*(7), 933. https://doi.org/10.3390/jcm8070933

Drago, L., & De Vecchi Elena. (2017). Microbiological diagnosis of implant related infections: Scientific evidence and cost/benefit analysis of routine antibiofilm processing. *Medical Biology Advances in Microbiology, Infectious Diseases and Public Health*, *5*, 51–67.

Edin, M. L., Miclau, T., Lester, G. E., Lindsey, R. W., & Dahners, L. E. (1996). Effect of Cefazolin and Vancomycin on osteoblasts in vitro. *Clinical Orthopaedics and Related Research*, *333*, 245–251.

Ettinger, M., Calliess, T., Kielstein, J. T., Sibai, J., Brückner, T., Lichtinghagen, R., Windhagen, H., & Lukasz, A. (2015). Circulating Biomarkers for Discrimination between Aseptic Joint Failure, Low-Grade Infection, and High-Grade Septic Failure. *Clinical Infectious Diseases*, *61*(3), 332–341. https://doi.org/10.1093/cid/civ286

Fearon, A., Dahlstrom, J. E., Twin, J., Cook, J., & Scott, A. (2014). The Bonar score revisited: Region of evaluation significantly influences the standardized assessment of tendon degeneration. *Journal of Science and Medicine in Sport*, *17*(4), 346–350. https://doi.org/10.1016/j.jsams.2013.07.008

Figueroa, D., Figueroa, F., Calvo, R., Lopez, M., & Goñi, I. (2019). Presoaking of Hamstring Autografts in Vancomycin Decreases the Occurrence of Infection Following Primary Anterior Cruciate Ligament Reconstruction. *Orthopaedic Journal of Sports Medicine*, *7*(9), 4–7.

https://doi.org/10.1177/2325967119871038

Fillerova, R., Gallo, J., Radvansky, M., Kraiczova, V., Kudelka, M., & Kriegova, E. (2017). Excellent Diagnostic Characteristics for Ultrafast Gene Profiling of DEFA1-IL1B-LTF in detection of prosthetic joint infections. *Journal of Clinical Microbiology*, *55*(9), 2686–2697.

Fink, B., Makowiak, C., Fuerst, M., Berger, I., Schafer, P., & Frommelt, L. (2008). The value of synovial biopsy, joint aspiration and C-reactive protein in the diagnosis of late peri-prosthetic infection of total knee replacements. *Journal of Bone and Joint Surgery - British Volume*, *90-B*(7), 874–878. https://doi.org/10.1302/0301-620X.90B7.20417

Gallo, J., Svoboda, M., Zapletalova, J., Proskova, J., & Juranova, J. (2018). Serum IL-6 in combination with synovial IL-6/ CRP shows excellent diagnostic power to detect hip and knee prosthetic joint infection. *PLoS ONE*, *13*(6), 1–16. https://doi.org/10.1371/journal.pone.0199226

Garrido, C., Galluzzi, L., Brunet, M., Puig, P. E., Didelot, C., & Kroemer, G. (2006). Mechanisms of cytochrome c release from mitochondria. *Cell Death and Differentiation*, *13*(9), 1423–1433. https://doi.org/10.1038/sj.cdd.4401950

Gbejuade, H. O., Lovering, A. M., & Webb, J. C. (2015). The role of microbial biofilms in prosthetic joint infections: A review. *Acta Orthopaedica*, *86*(2), 147–158. https://doi.org/10.3109/17453674.2014.966290

Gehrke, T., Lausmann, C., Citak, M., Bonanzinga, T., Frommelt, L., & Zahar, A. (2018). The accuracy of the alpha defensin lateral flow device for diagnosis of periprosthetic joint infection. *Journal of Bone and Joint Surgery - American Volume*, *100*(1), 42–48. https://doi.org/10.2106/JBJS.16.01522

Gibon, E., Córdova, L. A., Lu, L., Lin, T., Yao, Z., Hamadouche, M., & Goodman, S. B. (2017). The biological response to orthopedic implants for joint replacement. II: Polyethylene, ceramics, PMMA, and the foreign body reaction. *J Biomed Mater Res B Appl Biomater*, *105*(6), 1–15.

https://doi.org/10.1002/jbm.b.33676.The

Grayson, J. E., Grant, G. D., Dukie, S., & Vertullo, C. J. (2011). The in vitro elution characteristics of vancomycin from tendons. *Clinical Orthopaedics and Related Research*, *469*(10), 2948–2952. https://doi.org/10.1007/s11999-011-1768-3

Gries, C. M., & Kielian, T. (2017). Staphyloccal biofilms and immune polarization in during prosthetic joint infection. *Journal of American Academy of Orthopaedic Surgery*, *25*(Supp1 1), S20–S24.

Grosso, M., Frangiamore, S., Saleh, A., Kovac, M., Hayashi, R., Ricchetti, E., Bauer, T., & Iannotti, J. (2014). Poor utility of serum Interleukin-6 levels to predict indolent periprosthetic shoulder infections. *Journal of Shoulder and Elbow Surgery*, *23*(9), 1277–1281.

Gulotta, L. V, & Rodeo, S. A. (2007). Biology of Autograft and Allograft Healing in Anterior Cruciate Ligament Reconstruction. *Clinics in Sports Medicine*, *26*(4), 509–524. https://doi.org/10.1016/j.csm.2007.06.007

Gundtoft, P. H., Overgaard, S., Schonheyder, H. C., Moller, J. K., Kjærsgaard-Andersen, P., & Pedersen, A. B. (2015). The “true” incidence of surgically treated deep prosthetic joint infection after 32,896 primary total hip arthroplasties. *Acta Orthopaedica*, *86*(3), 326–334. https://doi.org/10.3109/17453674.2015.1011983

Haddad, F. S. (2014). Editorial: Have we reached the era of the bespoke anterior cruciate ligament reconstruction? *The Bone & Joint Journal*, *96-B*(6), 709–710. https://doi.org/10.1302/0301-620X.96B6.34312

Hantes, M E, K, B. G., Varitimidis, E. S., Giotikas, D., Petinaki, E., & Malizos, K. N. (2008). Autograft Contamination During Preparation for Anterior Cruciate Ligament Reconstruction. *Journal of Bone and Joint Surgery -*, *90*(4), 760–764.

Hantes, Michael E., Raoulis, V. A., Doxariotis, N., Drakos, A., Karachalios, T., &

Malizos, K. N. (2017). Management of septic arthritis after arthroscopic anterior cruciate ligament reconstruction using a standard surgical protocol. *Knee*, *24*(3), 588–593. https://doi.org/10.1016/j.knee.2017.02.007

Hasegawa, A., Nakahara, H., Kinoshita, M., Asahara, H., Koziol, J., & Lotz, M. K. (2013). Cellular and extracellular matrix changes in anterior cruciate ligaments during human knee aging and osteoarthritis. *Arthritis Research & Therapy*, *15*(1), R29–R29. https://doi.org/10.1186/ar4165

Heim, C. E., Vidlak, D., Scherr, T. D., Kozel, J. A., Holzapfel, M., Muirhead, D. E., & Kielian, T. (2014). Myeloid-Derived Suppressor Cells Contribute to Staphylococcus aureus Orthopedic Biofilm Infection. *The Journal of Immunology*, *192*(8), 3778–3792. https://doi.org/10.4049/jimmunol.1303408

Heim, Cortney E., Vidlak, D., & Kielian, T. (2015). Interleukin-10 production by myeloid-derived suppressor cells contributes to bacterial persistence during Staphylococcus aureus orthopedic biofilm infection . *Journal of Leukocyte Biology*, *98*(6), 1003–1013. https://doi.org/10.1189/jlb.4vma0315-125rr

Heim, Cortney E., Vidlak, D., Odvody, J., Hartman, C. W., Garvin, K. L., & Kielian, T. (2018). Human prosthetic joint infections are associated with myeloid-derived suppressor cells (MDSCs): Implications for infection persistence. *Journal of Orthopaedic Research*, *36*(6), 1605–1613. https://doi.org/10.1002/jor.23806

Heim, Cortney E., Vidlak, D., Scherr, T. D., Hartman, C. W., Garvin, K. L., & Kielian, T. (2015). IL-12 Promotes Myeloid-Derived Suppressor Cell Recruitment and Bacterial Persistence during Staphylococcus aureus Orthopedic Implant Infection . *The Journal of Immunology*, *194*(8), 3861–3872. https://doi.org/10.4049/jimmunol.1402689

Heller, A., McIff, T. E., Lai, S.-M., & Burton, D. C. (2015). Intrawound vancomycin powder decreases staphylococcal surgical site infections following posterior instrumented spinal arthrodesis. *Journal of Spinal Disorders Tech*, *28*(10).

Hexter, A. T., Hislop, S. M., & Blunn, G. W. (2018). The effect of bearing surface on risk of periprosthetic joint infection in total hip arthroplasty. *The Bone and Joint Journal*, *100-B*(2), 134–142. https://doi.org/10.1302/0301-620X.100B2.BJJ-2017-0575.R1

Hexter, A. T., Thangarajah, T., Blunn, G., & Haddad, F. S. (2018). Biological augmentation of graft healing in anterior cruciate ligament reconstruction. *The Bone & Joint Journal*, *100-B*(3), 271–284. https://doi.org/10.1302/0301-620X.100B3.BJJ-2017-0733.R2

Indelli, P. F., Dillingham, M., Fanton, G., & Schurman, D. J. (2002). Septic arthritis in postoperative anterior cruciate ligament reconstruction. *Clinical Orthopaedics and Related Research*, *398*, 182–188. https://doi.org/10.1097/00003086-200205000-00026

Jefferies, J. G., Aithie, J. M. S., & Spencer, S. J. (2019). Vancomycin-soaked wrapping of harvested hamstring tendons during anterior cruciate ligament reconstruction. A review of the 'vancomycin wrap.' *Knee*, *26*(3), 524–529. https://doi.org/10.1016/j.knee.2019.04.008

Kallala, R. F., Vanhegan, I. S., Ibrahim, M. S., Sarmah, S., & Haddad, F. S. (2015). Financial analysis of revision knee surgery based on NHS tariffs and hospital costs. *The Bone & Joint Journal*, *97-B*(2), 197–201. https://doi.org/10.1302/0301-620X.97B2.33707

Kasparek, M. F., Kasparek, M., Boettner, F., Faschingbauer, M., Hahne, J., & Dominkus, M. (2016). Intraoperative Diagnosis of Periprosthetic Joint Infection Using a Novel Alpha-Defensin Lateral Flow Assay. *Journal of Arthroplasty*, *31*(12), 2871–2874. https://doi.org/10.1016/j.arth.2016.05.033

Kim, S.-J., Postigo, R., Koo, S., & Kim, J. H. (2014). Infection After Arthroscopic Anterior Cruciate Ligament Reconstruction. *Orthopedics*, *37*(7), 477–484. https://doi.org/10.3928/01477447-20140626-06

Kleiss, S., Jandl, N. M., Novo de Oliveira, A., Rüther, W., & Niemeier, A. (2019).

Diagnostic accuracy of alpha-defensin enzyme-linked immunosorbent assay in the clinical evaluation of painful hip and knee arthroplasty with possible prosthetic joint infection: A prospective study of 202 cases. *Bone and Joint Journal*, *101 B*(8), 970–977. https://doi.org/10.1302/0301-620X.101B8.BJJ-2018-1390.R2

Knight, S. R., Aujla, R., & Biswas, S. P. (2011). 100 Years of Operative History Er Ci Us E on Er Al. *Orthopaedic Reviews*, *3*, 2–4. https://doi.org/10.4081/or.2011.16

Kunutsor, S. K., Barrett, M. C., Whitehouse, M. R., Craig, R. S., Lenguerrand, E., Beswick, A. D., & Blom, A. W. (2020). Incidence, temporal trends and potential risk factors for prosthetic joint infection after primary total shoulder and elbow replacement: Systematic review and meta-analysis. *Journal of Infection*, *80*(4), 426–436. https://doi.org/10.1016/j.jinf.2020.01.008

Lamagni, T. (2014). Epidemiology and burden of prosthetic joint infections. *Journal of Antimicrobial Chemotherapy*, *69*(SUPPL1), 5–10. https://doi.org/10.1093/jac/dku247

Lamplot, J. D., Liu, J. N., Hutchinson, I. D., Chen, T., Wang, H., Wach, A., Rodeo, S. A., & Warren, R. F. (2021). Effect of Vancomycin Soaking on Anterior Cruciate Ligament Graft Biomechanics. *Arthroscopy: The Journal of Arthroscopic & Related Surgery*, *37*(3), 953–960. https://doi.org/10.1016/j.arthro.2020.10.040

Lazar, H. L., Barlam, T., & Cabral, H. (2011). The Effect of Topical Vancomycin Applied to Sternotomy Incisions on Postoperative Serum Vancomycin Levels. *Journal of Cardiac Surgery*, *26*(5), 461–465.

Lemans, J. V. C., Öner, F. C., Wijdicks, S. P. J., Ekkelenkamp, M. B., Vogely, H. C., & Kruyt, M. C. (2019). The efficacy of intrawound vancomycin powder and povidone-iodine irrigation to prevent surgical site infections in complex instrumented spine surgery. *Spine Journal*, *19*(10), 1648–1656. https://doi.org/10.1016/j.spinee.2019.05.592

Lin, T. W., Cardenas, L., & Soslowsky, L. J. (2004). Biomechanics of tendon injury and repair. *Journal of Biomechanics*, *37*(6), 865–877. https://doi.org/https://doi.org/10.1016/j.jbiomech.2003.11.005

Little, D., Thompson, J. W., Dubois, L. G., Ruch, D. S., Moseley, M. A., & Guilak, F. (2014). Proteomic differences between male and female anterior cruciate ligament and patellar tendon. *PLoS ONE*, *9*(5). https://doi.org/10.1371/journal.pone.0096526

Lum, Z. C., Natsuhara, K. M., Shelton, T. J., Giordani, M., Pereira, G. C., & Meehan, J. P. (2018). Mortality During Total Knee Periprosthetic Joint Infection. *The Journal of Arthroplasty*, *33*(12), 3783–3788. https://doi.org/10.1016/j.arth.2018.08.021

Lydon, E. C., Henao, R., Burke, T. W., Aydin, M., Nicholson, B. P., Glickman, S. W., Fowler, V. G., Quackenbush, E. B., Cairns, C. B., Kingsmore, S. F., Jaehne, A. K., Rivers, E. P., Langley, R. J., Petzold, E., Ko, E. R., McClain, M. T., Ginsburg, G. S., Woods, C. W., & Tsalik, E. L. (2019). Validation of a host response test to distinguish bacterial and viral respiratory infection. *EBioMedicine*, *48*, 453–461. https://doi.org/https://doi.org/10.1016/j.ebiom.2019.09.040

Madanat, R., Laaksonen, I., Graves, S. E., Lorimer, M., Muratoglu, O., & Malchau, H. (2018). Ceramic bearings for total hip arthroplasty are associated with a reduced risk of revision for infection. *Hip International*, *28*(3), 222–226. https://doi.org/10.1177/1120700018776464

Majors, I., & Jagadale, V. S. (2019). Serum interleukin 6 could be a valuable initial diagnostic tool in prosthetic knee joint infections. *European Journal of Orthopaedic Surgery and Traumatology*, *29*(8), 1781–1788. https://doi.org/10.1007/s00590-019-02519-y

Maletis, G. B., Inacio, M. C. S., Desmond, J. L., & Funahashi, T. T. (2013). Reconstruction of the anterior cruciate ligament. *The Bone & Joint Journal*, *95-B*(5), 623–628. https://doi.org/10.1302/0301-620X.95B5.30872

Marazzi, M. G., Randelli, F., Brioschi, M., Drago, L., Romanò, C. L., Banfi, G., Massaccesi, L., Crapanzano, C., Morelli, F., Corsi Romanelli, M. M., & Galliera, E. (2018). Presepsin: A potential biomarker of PJI? A comparative analysis with known and new infection biomarkers. *International Journal of Immunopathology and Pharmacology*, *31*, 1–10. https://doi.org/10.1177/0394632017749356

Marín, M., Garcia-Lechuz, J. M., Alonso, P., Villanueva, M., Alcalá, L., Gimeno, M., Cercenado, E., Sánchez-Somolinos, M., Radice, C., & Bouza, E. (2012). Role of universal 16S rRNA gene PCR and sequencing in diagnosis of prosthetic joint infection. *Journal of Clinical Microbiology*, *50*(3), 583–589. https://doi.org/10.1128/JCM.00170-11

Marrale, J., Morrissey, M. C., & Haddad, F. S. (2007). A literature review of autograft and allograft anterior cruciate ligament reconstruction. *Knee Surgery, Sports Traumatology, Arthroscopy*, *15*(6), 690–704. https://doi.org/10.1007/s00167-006-0236-1

Matava, M., Evans, T., Wright, R., & Shively, R. (1998). Septic arthritis of the knee following anterior cruciate ligament reconstruction: results of a survey of sports medicine fellowship directors. *Arthroscopy: The Journal of Arthroscopic & Related Surgery*, *14*(7), 717–725. https://doi.org/10.1016/S0749-8063(98)70098-2

McBrearty, M., & Moffat, T. (2021). *South Glasgow Hospitals Haematology Handbook, Diagnostics Directorate, South Glasghow*.

McNally, M., Sousa, R., Wouthuyzen-Bakker, M., Chen, A. F., Soriano, A., Vogely, H. C., Clauss, M., Higuera, C. A., & Trebše, R. (2020). The EBJIS definition of periprosthetic joint infection. *The Bone & Joint Journal*, *103-B*(1), 18–25. https://doi.org/10.1302/0301-620X.103B1.BJJ-2020-1381.R1

Millar, N. L., Wei, A. Q., Molloy, T. J., Bonar, F., & Murrell, G. A. C. (2009). Cytokines and apoptosis in supraspinatus tendinopathy. *Journal of Bone and Joint Surgery - Series B*, *91*(3), 417–424. https://doi.org/10.1302/0301-620X.91B3.21652

Miller, M. D., Thompson, S. R., & Hart, J. A. (2016). *Review of Orthopaedics* (6th ed.). Elsevier Ltd.

Monk, A. P., Davies, L. J., Hopewell, S., Harris, K., Beard, D. J., Price, A. J., & Monk, A. P. (2016). Surgical versus conservative interventions for treating anterior cruciate ligament injuries . In *Cochrane library U6 - ctx_ver=Z39.88-2004&ctx_enc=info%3Aofi%2Fenc%3AUTF-8&rfr_id=info%3Asid%2Fsummon.serialssolutions.com&rft_val_fmt=info%3Aofi%2Ffmt%3Akev%3Amtx%3Ajournal&rft.genre=article&rft.atitle=Surgical+versus+conservative+interventions+for+tre* (Vol. 2016, Issue 4, p. CD011166). John Wiley & Sons, Ltd . https://doi.org/10.1002/14651858.CD011166.pub2

Mosmann, T. (1983). Rapid colorimetric assay for cellular growth and survival: Application to proliferation and cytotoxicity assays. *Journal of Immunological Methods*, *65*(1–2), 55–63. https://doi.org/10.1016/0022-1759(83)90303-4

Mouzopoulos, G., Fotopoulos, V. C., & Tzurbakis, M. (2009). Septic knee arthritis following ACL reconstruction: A systematic review. *Knee Surgery, Sports Traumatology, Arthroscopy*, *17*(9), 1033–1042. https://doi.org/10.1007/s00167-009-0793-1

Murray, M. M., Martin, S. D., Martin, T. L., & Spector, M. (2000). Histological changes in the human anterior cruciate ligament after rupture. In *Journal of bone and joint surgery. American volume* (Vol. 82, Issue 10, p. 1387).

Naendrup, J. H., Marche, B., de Sa, D., Koenen, P., Otchwemah, R., Wafaisade, A., & Pfeiffer, T. R. (2019). Vancomycin-soaking of the graft reduces the incidence of septic arthritis following ACL reconstruction: results of a systematic review and meta-analysis. *Knee Surgery, Sports Traumatology, Arthroscopy*, *0*(0), 0. https://doi.org/10.1007/s00167-019-05353-1

Namba, R. S., Inacio, M. C. S., & Paxton, E. W. (2013). Risk factors associated with deep surgical site infections after primary total knee arthroplasty: an analysis of 56,216 knees. *Journal of Bone and Joint Surgery Am*, *95*(9), 775.

NHS Digital, & Analytical Team PROMS. (2020). *Finalised Patient Reported Outcome Measures (PROMs) in England for Hip & Knee Replacements, April 2018 – March 2019*. https://digital.nhs.uk/data-and-information/publications/statistical/patient-reported-outcome-measures-proms/finalised-hip--knee-replacements-april-2018---march-2019

NJR Editorial Board. (2019). *The National Joint Registry of England, Wales and Northern Ireland, 16th Annual Report 2019*.

Nowinski, R. J., Gillespie, R. J., Shishani, Y., Cohen, B., Walch, G., & Gobezie, R. (2012). Antibiotic-loaded bone cement reduces deep infection rates for primary reverse total shoulder arthroplasty: A retrospective, cohort study of 501 shoulders. *Journal of Shoulder and Elbow Surgery*, *21*(3), 324–328. https://doi.org/10.1016/j.jse.2011.08.072

Offerhaus, C., Balke, M., Hente, J., Gehling, M., Blendl, S., & Höher, J. (2019). Vancomycin pre-soaking of the graft reduces postoperative infection rate without increasing risk of graft failure and arthrofibrosis in ACL reconstruction. *Knee Surgery, Sports Traumatology, Arthroscopy*, *27*(9), 3014–3021. https://doi.org/10.1007/s00167-018-5323-6

Omar, M., Ettinger, M., Reichling, M., Petri, M., Guenther, D., Gehrke, T., Krettek, C., & Mommsen, P. (2015). Synovial C-reactive protein as a marker for chronic periprosthetic infection in total hip arthroplasty. *Bone and Joint Journal*, *97-B*(2), 173–176. https://doi.org/10.1302/0301-620X.97B2.34550

Omar, Mohamed, Klawonn, F., Brand, S., Stiesch, M., Krettek, C., & Eberhard, J. (2017). Transcriptome-Wide High-Density Microarray Analysis Reveals Differential Gene Transcription in Periprosthetic Tissue From Hips With Chronic Periprosthetic Joint Infection vs Aseptic Loosening. *Journal of Arthroplasty*, *32*(1), 234–240. https://doi.org/10.1016/j.arth.2016.06.036

Ong, K. L., Kurtz, S. M., Lau, E., Bozic, K. J., Berry, D. J., & Parvizi, J. (2009). Prosthetic Joint Infection Risk After Total Hip Arthroplasty in the Medicare Population. *Journal of Arthroplasty*, *24*(6 SUPPL.), 105–109. https://doi.org/10.1016/j.arth.2009.04.027

Palan, J., Nolan, C., Sarantos, K., Westerman, R., King, R., & Foguet, P. (2019). Culture-negative periprosthetic joint infections. *EFORT Open Reviews*, *4*(10), 585–594. https://doi.org/10.1302/2058-5241.4.180067

Parvizi, J, Jacovides, C., Antoci, V., & Ghanem, E. (2011). Diagnosis of periprosthetic joint infection: the utility of a simple yet unappreciated enzyme. *Journal of Bone and Joint Surgery Am*, *93*(4), 2242–2248.

Parvizi, Javad, & Gehrke, T. (2014). Definition of periprosthetic joint infection. *Journal of Arthroplasty*, *29*(7), 1331. https://doi.org/10.1016/j.arth.2014.03.009

Parvizi, Javad, Tan, T. L., Goswami, K., Higuera, C., Della Valle, C., Chen, A. F., & Shohat, N. (2018). The 2018 Definition of Periprosthetic Hip and Knee Infection: An Evidence-Based and Validated Criteria. *Journal of Arthroplasty*, *33*(5), 1309-1314.e2. https://doi.org/10.1016/j.arth.2018.02.078

Parvizi, Javad, Zmistowski, B., Berbari, E. F., Bauer, T. W., Springer, B. D., Della Valle, C. J., Garvin, K. L., Mont, M. A., Wongworawat, M. D., & Zalavras, C. G. (2011). New definition for periprosthetic joint infection: From the workgroup of the musculoskeletal infection society. *Clinical Orthopaedics and Related Research*, *469*(11), 2992–2994. https://doi.org/10.1007/s11999-011-2102-9

Pepys, M. B. (1981). C-REACTIVE PROTEIN FIFTY YEARS ON. *The Lancet*, *317*(8221), 653–657. https://doi.org/https://doi.org/10.1016/S0140-6736(81)91565-8

Pérez-Prieto, D., Portillo, M. E., Puig-Verdié, L., Alier, A., Martínez, S., Sorlí, L., Horcajada, J. P., & Monllau, J. C. (2017). C-reactive protein may misdiagnose prosthetic joint infections, particularly chronic and low-grade infections. *International Orthopaedics*, *41*(7), 1315–1319. https://doi.org/10.1007/s00264-017-3430-5

Pérez-Prieto, D., Torres-Claramunt, R., Gelber, P. E., Shehata, T. M. A., Pelfort,

X., & Monllau, J. C. (2016). Autograft soaking in vancomycin reduces the risk of infection after anterior cruciate ligament reconstruction. *Knee Surgery, Sports Traumatology, Arthroscopy*, *24*(9), 2724–2728. https://doi.org/10.1007/s00167-014-3438-y

Phegan, M., Grayson, J. E., & Vertullo, C. J. (2016). No infections in 1300 anterior cruciate ligament reconstructions with vancomycin pre-soaking of hamstring grafts. *Knee Surgery, Sports Traumatology, Arthroscopy*, *24*(9), 2729–2735. https://doi.org/10.1007/s00167-015-3558-z

Piper, K. E., Fernandez-Sampedro, M., Steckelberg, K. E., Mandrekar, J. N., Karau, M. J., Steckelberg, J. M., Berbari, E. F., Osmon, D. R., Hanssen, A. D., Lewallen, D. G., Cofield, R. H., Sperling, J. W., Sanchez-Sotelo, J., Huddleston, P. M., Dekutoski, M. B., Yaszemski, M., Currier, B., & Patel, R. (2010). C-Reactive Protein, Erythrocyte Sedimentation Rate and Orthopedic Implant Infection. *PLoS ONE*, *5*(2), e9358. https://doi.org/10.1371/journal.pone.0009358

Portillo, M. E., Salvadó, M., Sorli, L., Alier, A., Martínez, S., Trampuz, A., Gómez, J., Puig, L., & Horcajada, J. P. (2012). Multiplex PCR of sonication fluid accurately differentiates between prosthetic joint infection and aseptic failure. *Journal of Infection*, *65*(6), 541–548. https://doi.org/10.1016/j.jinf.2012.08.018

Qu, X., Zhai, Z., Wu, C., Jin, F., Li, H., Wang, L., Liu, G., Liu, X., Wang, W., Li, H., Zhang, X., Zhu, Z., & Dai, K. (2013). Preoperative aspiration culture for preoperative diagnosis of infection in total hip or knee arthroplasty. *Journal of Clinical Microbiology*, *51*(11), 3830–3834. https://doi.org/10.1128/JCM.01467-13

Ramachandran, M. (2006). *Basci Orthopaedic Sciences: The Stanmore Guide*.

Ramilo, O., Allman, W., Chung, W., Mejias, A., Ardura, M., Glaser, C., Wittkowski, K. M., Piqueras, B., Banchereau, J., Palucka, A. K., & Chaussabel, D. (2007). Gene expression patterns in blood leukocytes discriminate patients with acute infections. *Blood*, *109*(5), 2066–2077.

https://doi.org/https://doi.org/10.1182/blood-2006-02-002477

Randau, T. M., Friedrich, M. J., Wimmer, M. D., Reichert, B., Kuberra, D., Stoffel-Wagner, B., Limmer, A., Wirtz, D. C., & Gravius, S. (2014). Interleukin-6 in serum and in synovial fluid enhances the differentiation between periprosthetic joint infection and aseptic loosening. *PLoS ONE*, *9*(2), 1–6. https://doi.org/10.1371/journal.pone.0089045

Renstrom, P., Ljungqvist, A., Arendt, E., Beynnon, B., Fukubayashi, T., Garrett, W., Georgoulis, T., Hewett, T. E., Johnson, R., Krosshaug, T., Mandelbaum, B., Micheli, L., Myklebust, G., Roos, E., Roos, H., Schamasch, P., Shultz, S., Werner, S., Wojtys, E., & Engebretsen, L. (2008). Non-contact ACL injuries in female athletes: An International Olympic Committee current concepts statement. *British Journal of Sports Medicine*, *42*(6), 394–412. https://doi.org/10.1136/bjsm.2008.048934

Ryu, S. Y., Greenwood-Quaintance, K. E., Hanssen, A. D., Mandrekar, J. N., & Patel, R. (2014). Low sensitivity of periprosthetic tissue PCR for prosthetic knee infection diagnosis. *Diagnostic Microbiology and Infectious Disease*, *79*(4), 448–453. https://doi.org/10.1016/j.diagmicrobio.2014.03.021

Saeed, K., Dryden, M., Sitjar, A., & White, G. (2013). Measuring synovial fluid procalcitonin levels in distinguishing cases of septic arthritis, including prosthetic joints, from other causes of arthritis and aseptic loosening. *Infection*, *41*(4), 845–849. https://doi.org/10.1007/s15010-013-0467-2

Sakamoto, K., Arkawa, H., Mita, S., Ishiko, T., Ikei, S., Egami, H., Hisano, S., & Ogawa, M. (1994). Elevation of circulating interleukin 6 after surgery: factors influencing the serum level. *Cytokine*, *6*(2), 181–186.

Sanderson, N. D., Street, T. L., Foster, D., Swann, J., Atkins, B. L., Brent, A. J., McNally, M. A., Oakley, S., Taylor, A., Peto, T. E. A., Crook, D., & Eyre, D. W. (2017). Real-time analysis of nanopore-based metagenomic sequencing from orthopaedic device infection. *BioRxiv*, *2018*, 1–11. https://doi.org/10.1101/220616

Schüttler, K. F., Scharm, A., Stein, T., Heyse, T. J., Lohoff, M., Sommer, F., Spiess-Naumann, A., & Efe, T. (2019). Biomechanical and microbiological effects of local vancomycin in anterior cruciate ligament (ACL) reconstruction: a porcine tendon model. *Archives of Orthopaedic and Trauma Surgery*, *139*(1), 73–78. https://doi.org/10.1007/s00402-018-3006-x

Scott, L. J., & Hogg, J. (2019). *SOUTH GLASGOW BIOCHEMISTRY LABORATORY HANDBOOK FOR SERVICE USERS*.

Scottish arthroplasty project steering group. (2020). *Scottish Arthroplasty Project Report 2020*. https://www.arthro.scot.nhs.uk/Reports/Dashboard-2020.html

Selders, G. S., Fetz, A. E., Radic, M. Z., & Bowlin, G. L. (2017). An overview of the role of neutrophils in innate immunity, inflammation and host-biomaterial integration. *Regenerative Biomaterials*, *4*(1), 55–68. https://doi.org/10.1093/rb/rbw041

Severino, P., Silva, E., Baggio-Zappia, G. L., Brunialti, M. K. C., Nucci, L. A., Rigato Jr., O., da Silva, I. D. C. G., Machado, F. R., & Salomao, R. (2014). Patterns of Gene Expression in Peripheral Blood Mononuclear Cells and Outcomes from Patients with Sepsis Secondary to Community Acquired Pneumonia. *PLOS ONE*, *9*(3), 1–8. https://doi.org/10.1371/journal.pone.0091886

Shafafy, R., McClatchie, W., Chettiar, K., Gill, K., Hargrove, R., Sturridge, S., & Guyot, A. (2015). Use of leucocyte esterase reagent strips in the diagnosis or exclusion of prosthetic joint infection. *Bone and Joint Journal*, *97-B*(9), 1232–1236. https://doi.org/10.1302/0301-620X.97B9.34910

Shaw, K. A., Eichinger, J. K., Nadig, N., & Parada, S. A. (2018). In Vitro Effect of Vancomycin on the Viability of Articular Chondrocytes. *Journal of Orthopaedic Trauma*, *32*(3), 148–153. https://doi.org/10.1097/BOT.0000000000001040

Sigmund, I. K., Yermak, K., Perka, C., Trampuz, A., & Renz, N. (2018). Is the

Enzyme-linked Immunosorbent Assay More Accurate Than the Lateral Flow Alpha Defensin Test for Diagnosing Periprosthetic Joint Infection? *Clinical Orthopaedics and Related Research*, *476*(8), 1645–1654. https://doi.org/10.1097/CORR.0000000000000336

Sophia Fox, A. J., Bedi, A., & Rodeo, S. A. (2009). The basic science of articular cartilage: Structure, composition, and function. *Sports Health*, *1*(6), 461–468. https://doi.org/10.1177/1941738109350438

Sousa, R., Serrano, P., Gomes Dias, J., Oliveira, J. C., & Oliveira, A. (2017). Improving the accuracy of synovial fluid analysis in the diagnosis of prosthetic joint infection with simple and inexpensive biomarkers. *Bone and Joint Journal*, *99-B*(3), 351–357.

Southwood, R. T., Rice, J. L., McDonald, P. J., Hakendorf, P. H., & Rozenbilds, M. A. (1985). Infection in experimental hip arthroplasties. *The Journal of Bone and Joint Surgery (Br)*, *67*(2), 229–231.

Street, T. L., Sanderson, N. D., Atkins, B. L., Brent, A. J., Cole, K., Foster, D., McNally, M. A., Oakley, S., Peto, L., Taylor, A., Peto, T. E. A., Crook, D. W., & Eyre, D. W. (2017). Molecular diagnosis of orthopedic-device-related infection directly from sonication fluid by metagenomic sequencing. *Journal of Clinical Microbiology*, *55*(8), 2334–2347. https://doi.org/10.1128/JCM.00462-17

Tamaki, Y., Takakubo, Y., Goto, K., Hirayama, T., Sasaki, K., Konttinen, Y. T., Goodman, S. B., & Takagi, M. (2009). Increased expression of toll-like receptors in aseptic loose periprosthetic tissues and septic synovial membranes around total hip implants. *Journal of Rheumatology*, *36*(3), 598–608. https://doi.org/10.3899/jrheum.080390

Tande, A. J., & Patel, R. (2014). Prosthetic joint infection. *Clinical Microbiology Reviews*, *27*(2), 302–345. https://doi.org/10.1128/CMR.00111-13

Tarabichi, M., Shohat, N., Goswami, K., & Parvizi, J. (2018). Can next generation sequencing play a role in detecting pathogens in synovial fluid?

Bone and Joint Journal, *100B*(2), 127–133. https://doi.org/10.1302/0301-620X.100B2.BJJ-2017-0531.R2

Tarakji, K. G., Mittal, S., Kennergren, C., Corey, R., Poole, J., Stromberg, K., Lexcen, D. R., & Wilkoff, B. L. (2016). Worldwide Randomized Antibiotic EnveloPe Infection PrevenTion Trial (WRAP-IT). *American Heart Journal*, *180*, 12–21. https://doi.org/10.1016/j.ahj.2016.06.010

Thoendel, M. J., Jeraldo, P. R., Greenwood-Quaintance, K. E., Yao, J. Z., Chia, N., Hanssen, A. D., Abdel, M. P., & Patel, R. (2018). Identification of prosthetic joint infection pathogens using a shotgun metagenomics approach. *Clinical Infectious Diseases*, *67*(9), 1333–1338. https://doi.org/10.1093/cid/ciy303

Thorpe, C. T., Birch, H. L., Clegg, P. D., & Screen, H. R. C. (2013). The role of the non-collagenous matrix in tendon function. *International Journal of Experimental Pathology*, *94*(4), 248–259. https://doi.org/10.1111/iep.12027

Torres-Claramunt, R., Pelfort, X., Erquicia, J., Gil-González, S., Gelber, P. E., Puig, L., & Monllau, J. C. (2013). Knee joint infection after ACL reconstruction: Prevalence, management and functional outcomes. *Knee Surgery, Sports Traumatology, Arthroscopy*, *21*(12), 2844–2849. https://doi.org/10.1007/s00167-012-2264-3

Trampuz, A., Piper, K. E., Jacobson, M. J., Hanssen, A. D., Unni, K. K., Osmon, D. R., Mandrekar, J. N., Cockerill, F. R., Steckelberg, J. M., Greenleaf, J. F., & Patel, R. (2007). Sonication of removed hip and knee prostheses for diagnosis of infection. *New England Journal of Medicine*, *357*(7), 654–663. https://doi.org/10.1056/NEJMoa061588

Tsaras, G., Osmon, D. R., Mabry, T., Lahr, B., Sauveur, J. St., Yawn, B., Kurland, R., & Berbari, E. F. (2012). Incidence, Secular Trends, and Outcomes of Prosthetic Joint Infection: A Population-Based Study, Olmsted County, Minnesota, 1969–2007. *Infection Control & Hospital Epidemiology*, *33*(12), 1207–1212. https://doi.org/10.1086/668421

Tubaki, V. R., Rajasekaran, S., & Shetty, A. P. (2013). Effects of using intravenous antibiotic only versus local intrawound vancomycin antibiotic powder application in addition to intravenous antibiotics on postoperative infection in spine surgery in 907 patients. *Spine*, *38*(25), 2149–2155. https://doi.org/10.1097/BRS.0000000000000015

Vander Salm, T., Okike, O. N., & Pasque, M. K. (1989). Reduction of sternal infection by application of topical vancomycin.e. *Journal of Thoracic Cardiovascualr Srugery*, *98*, 618–622.

Vertullo, C. J., Quick, M., Jones, A., & Grayson, J. E. (2012). A surgical technique using presoaked vancomycin hamstring grafts to decrease the risk of infection after anterior cruciate ligament reconstruction. *Arthroscopy*, *28*(3).

Walker, L. C., Clement, N. D., Wilson, I., Hashmi, M., Samuel, J., & Deehan, D. J. (2020). The Importance Of Multi-site Intra-operative Tissue Sampling In The Diagnosis Of Hip And Knee Periprosthetic Joint Infection - Results From A Single Centre Study. *Journal of Bone and Joint Infection*, *5*(3), 151–159. https://doi.org/10.7150/jbji.39499

Wang, G. (2014). Human antimicrobial peptides and proteins. *Pharmaceuticals*, *7*(5), 545–594. https://doi.org/10.3390/ph7050545

Wetters, N. G., Berend, K. R., Lombardi, A. V, Morris, M. J., Tucker, T. L., & Valle, C. J. Della. (2012). Winner of the Rand Award Leukocyte Esterase Reagent Strips for the Rapid Diagnosis of Periprosthetic Joint Infection. *Journal of Arthroplasty*, *27*(8), 8–11. https://doi.org/10.1016/j.arth.2012.03.037

Wilson, M. R., Naccache, S. N., Samayoa, E., Biagtan, M., Bashir, H., Yu, G., Salamat, S. M., Somasekar, S., Federman, S., Miller, S., Sokolic, R., Garabedian, E., Candotti, F., Buckley, R. H., Reed, K. D., Meyer, T. L., Seroogy, C. M., Galloway, R., Henderson, S. L., … Chiu, C. Y. (2014). Actionable Diagnosis of Neuroleptospirosis by Next-Generation Sequencing. *New England Journal of Medicine*, *370*(25), 2408–2417.

https://doi.org/10.1056/nejmoa1401268

Wimmer, M. D., Ploeger, M. M., Friedrich, M. J., Bornemann, R., Roessler, P. P., Gravius, S., & Randau, T. M. (2016). The QuickLine IL-6 lateral flow immunoassay improves the rapid intraoperative diagnosis of suspected periprosthetic joint infections. *Technology and Health Care*, *24*(6), 927–932. https://doi.org/10.3233/THC-161247

Windisch, C., Brodt, S., Roehner, E., & Matziolis, G. (2017). C-reactive protein course during the first 5 days after total knee arthroplasty cannot predict early prosthetic joint infection. *Archives of Orthopaedic and Trauma Surgery*, *137*(8), 1115–1119. https://doi.org/10.1007/s00402-017-2709-8

Worthington, J. J., Kelly, A., Smedley, C., Bauché, D., Campbell, S., Marie, J. C., & Travis, M. A. (2015). Integrin αvβ8-Mediated TGF-β Activation by Effector Regulatory T Cells Is Essential for Suppression of T-Cell-Mediated Inflammation. *Immunity*, *42*(5), 903–915. https://doi.org/10.1016/j.immuni.2015.04.012

Worthington, T., Dunlop, D., Casey, A., Lambert, P., Luscombe, J., & Elliott, T. (2010). Serum procalcitonin, interleukin-6, soluble intercellular adhesin molecule-1 and IgG to short-chain exocellular lipoteichoic acid as predictors of infection in total joint prosthesis revision. *British Journal of Biomedical Science*, *67*(2), 71–76. https://doi.org/10.1080/09674845.2010.11730294

Wouthuyzen-Bakker, M., Ploegmakers, J. J. W., Ottink, K., Kampinga, G. A., Wagenmakers-Huizenga, L., Jutte, P. C., & Kobold, A. C. M. (2018). Synovial Calprotectin: An Inexpensive Biomarker to Exclude a Chronic Prosthetic Joint Infection. *Journal of Arthroplasty*, *33*(4), 1149–1153. https://doi.org/10.1016/j.arth.2017.11.006

Young, D., Hussell, T., & Dougan, G. (2002). Chronic bacterial infections: Living with unwanted guests. *Nature Immunology*, *3*(11), 1026–1032. https://doi.org/10.1038/ni1102-1026

Zimmerli, W., & Sendi, P. (2011). Pathogenesis of implant-associated infection:

The role of the host. *Seminars in Immunopathology*, *33*(3), 295–306. https://doi.org/10.1007/s00281-011-0275-7